Politecnico di Torino

Department of Energy and Electrical Engineering

Master of Science in Nuclear and Energy Engineering: Energy Innovation

Master Thesis

Techno-economic assessment of a pulverized coal plant with CO2 capture, based on novels composite Pebax membranes

Candidate: Scaffidi Argentina Gabriele 265489

Supervisors: Prof. Andrea Lanzini
Prof. Massimo Santarelli
Dott. Salvatore Cannone

March 2021

Acknowledgements

My warmest thanks go to Andrea Lanzini that with patience and passion introduced me to this challenging but fascinating world, and support me with their knowledge during the writing of the thesis.

My warmest thanks to Salvatore Cannone for all the advice and the willingness to help me with the best choice.

Other thanks go to my family for emotional and economic support. Thanks to other people that helped me a lot from all points of view, and among them, a special thanks go to Francesca and all my friends, always present in my life.

Contents

List of Tables

1 Introduction

1.1 Background

The global energy consumption is increasing, due to population and civilization. The increase in energy demand is strictly related to the growth of energy production, causing the increase of greenhouse gases (GHG) emission in the atmosphere. The energy production is guided by fossil fuels like natural gas and coal, with a rise of 5.0% and 3.3%, respectively [1], with respect the previous year. It is noticeable an important growth into Asian countries. Despite the fact that fossil fuels are one of the causes of climate change, they have an important role in the global economy. Global energy consumption is evaluated with the index, TES (Total Energy Supply). TES is a function of production, import/export, and sea stacks and it is doubled between 1971 and 2018. Despite the energy transition should be based on renewable energy sources and natural gas, coal (27%) and oil (32%) has important portions in the energy mix. It is visible, in the graph in figure 1.1, the small fraction related to intermittent renewable energy sources (2%), like solar and wind[1]. It is possible to analyze the consumption in different sectors. Figure 1.2 shows that during the years, the industrial sector has high energy demand (38%), followed by transport (29%). The residential sector has had a non-negligible request (21%), but it is decreased due to energy-efficient measurements in buildings [1].

The growing energy demand involves an increase of primary sources for energy production. Fossil fuels are necessary to guarantee system stability and base-load. The exclusive use of renewable energy sources does not guarantee security for the load, due to their intermittent nature. Fossil fuels produce energy through combustion reaction. The exhaust gases are composed by nitrogen oxides (NOx), sulfur oxides (SOx), secondary gases, and carbon dioxide (CO2). Carbon dioxide is one of the main factors that contribute to climate change, due to its GHG nature.

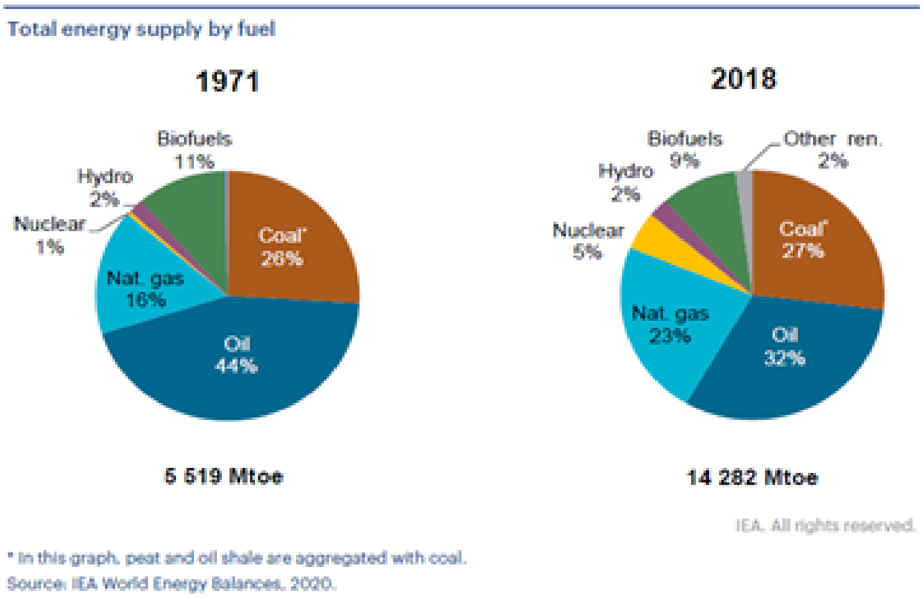

* In this graph, peat and oil shale are aggregated with coal.
Source: IEA World Energy Balances, 2020.

Figure 1.1: Total energy supply by fuel for 1971 and 2018 [1]

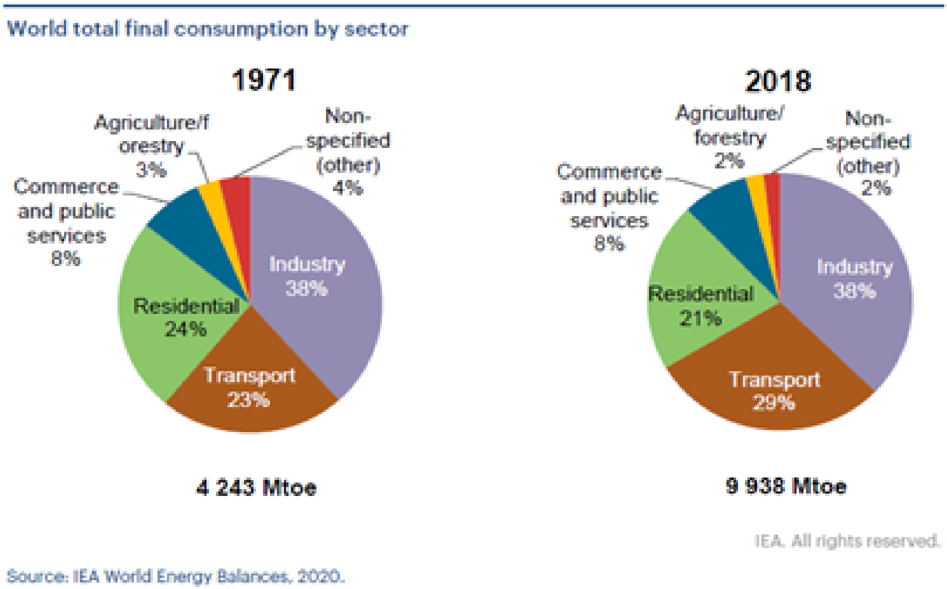

Source: IEA World Energy Balances, 2020.

Figure 1.2: World total final consumption by sector for 1971 and 2018 [1]

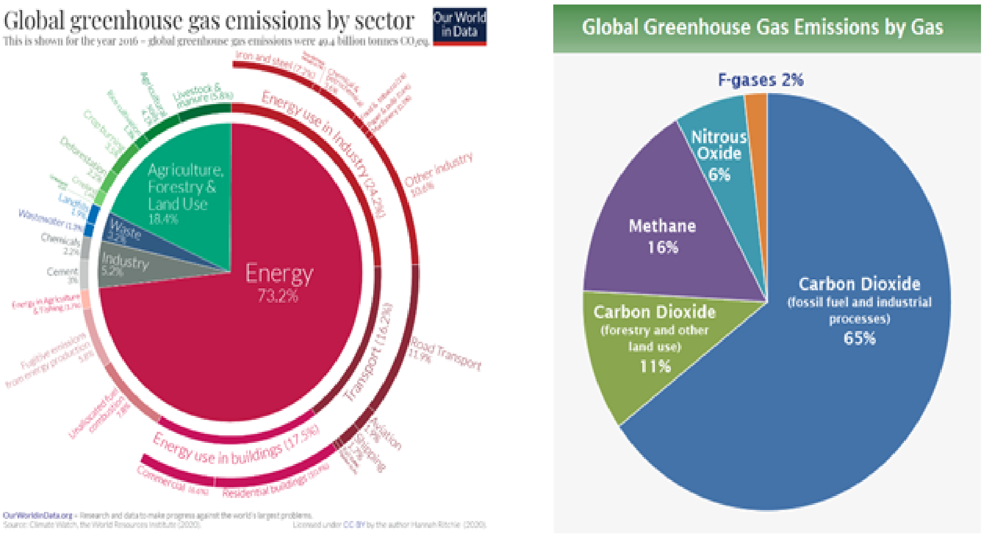

Figure 1.3: (a) GHG emissions by sector [2], (b) GHG gases emissions in atmosphere[3]

GHG emissions, human activities, and energy-intensive processes damage our planet, causing a rise in average surface earth temperature. The rise of temperature affects human health, biodiversity, and lifestyle. The aim of the Paris Agreement is to limit the increase of the average temperature to 2 °C, and pursue efforts toward a 1,5 °C limit, compared with preindustrial temperatures, to avoid dangerous levels of climate change. In the graph in figure 1.3 (a) are shown fractions of GHG emission by sector. It is noticeable that 3/4 of the emissions are related to the energy sector, with different contributes (transport, industry, residential) [2]. To reduce the GHG emissions, energy solutions as CO2 capture technologies and efficiency improve, could be a driving force to obtain Paris agreement objectives. Greenhouse gases are CO2, CH4, N2O, HFC, SF6. In figure 1.3 (b) is shown the important role of carbon dioxide emission in atmosphere, related to industrial processes and fossil sources. It is fundamental to implement measures to reduce atmospheric CO2 emissions.

The amount of carbon dioxide in the atmosphere still rises day by day. The biggest release is related to the decade 2000-2010 , in which 49 Gt of CO2 are released in the atmosphere. Scripps Institute of Oceanography reports that carbon dioxide in the atmosphere increases from 315 ppm in 1958, to 415 ppm into 2020 [4]. In 2050, it is estimated that CO2 reaches the value of 500 ppm. It is fundamental to have a natural and technological solution to remove the gas from the atmosphere and to reach the objective of the

Paris agreement. It is necessary to estimate the evolution of CO2 emissions and evaluate different scenarios. The IPCC (Intergovernmental Panel on Climate Changes) is an organization dedicated to the study of different scenarios to evaluate the increase of average earth temperature, caused by the tonnes of CO2 emitted in the atmosphere. To have a positive effect on the actions, the CO2 present in the atmosphere needs to be nil or negative. The scenarios evaluated by IPCC are different, based on several energetic policies. An example is the S1 scenario, based on the sustainability concepts as active mobility and green energy. S5 is the scenario in which the fossil energy is the driving force for the global economy. S5 is more realistic, due to difficulties to obtain a complete transition to a renewable energy mix in the short-term. Low-Energy Demand (LED) is an interesting scenario in which the goals of the Paris agreement can be obtained without the implementation of new technology for CO2 removal. In figure 1.4 are shown the official publication of the scenarios by IPCC. It is visible that a "zero year", in which the CO2 is nil or negative, is reached in different years depending on the scenario. This is related to different energy and food demand for each scenario. However, each scenario shows a "zero year" near 2060 [5].

To accelerate the removal of carbon dioxide, new solutions for CO2 capture need to be implemented. At the current moment, research has the attention on two approaches:

- natural: forestation and reforestation, agro-forestation and carbon removal from the land.

- technological: carbon dioxide removal, utilization, and storage (CCS: Carbon Capture and Storage; CCU: Carbon Capture and Utilization), direct removal of CO2 from the atmosphere (Direct Air Capture), and production of bio-energy combined to carbon dioxide storage (BECCS).

The integration of new removal technologies shows important limits, as the maturity of the carbon market and the ability to obtain secure financing for the development of new technologies. Moreover, new policies and social impacts are fundamental for a CO2 removal technology-based zone.

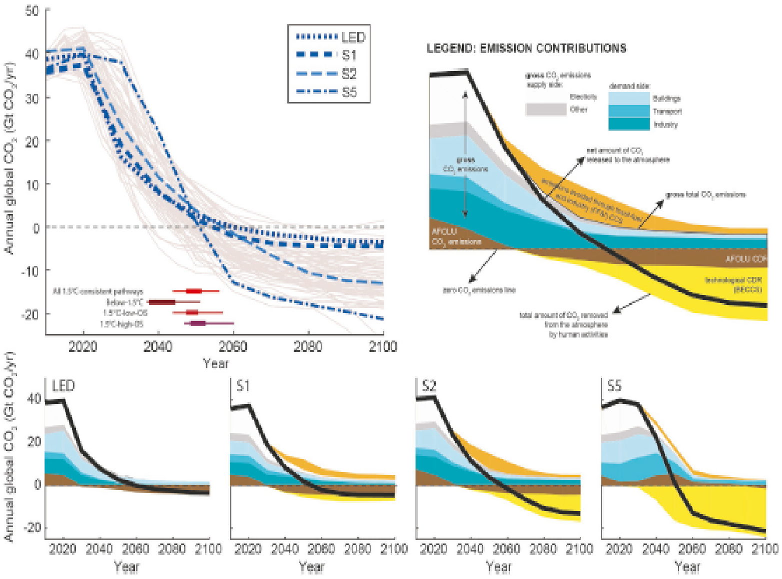

Figure 1.4: IPCC scenarios for carbon dioxide.S1 is a sustainability-oriented scenario, S2 is a middle-of the- road scenario and S5 is a fossil-fuel intensive and high energy demand scenario. LED is a scenario with particularly low energy demand. [3]

1.2 Technology for CO2 removal

In literature, are available a lot of papers for CO2 removal technologies. A lot of these, are based on the CCS integration in old energy plants. This integration shows a series of advantages because the space required for new technologies is minimum in the plants already in operation. Moreover, CCS application allows reducing carbon dioxide emissions in high consumption industrial sector. Examples are cement, steel, and iron industries. The additional cost of CCS systems is the main disadvantage for future marketing. CO2 capture methods are divided into three categories: post-combustion, pre-combustion, and oxyfuel combustion capture.

1.2.1 Post-Combustion

Post-combustion CO2 capture is useful to separate carbon dioxide from exhaust gases produced into the combustion chamber due to chemical reactions. It is a good solution because it is easy to apply for plants already in operation.Application examples are coal plants for energy production. CO2 removal unit is located following traditional treatment systems for sulfur oxide, nitrogen oxide, and particulate removal. In figure 1.5 is shown a flux diagram of an energy plant for energy production, with an added section for carbon dioxide separation. It is noticeable, how the addition of CO2 capture unit needs a compression of the gas for transport in a future storage site. The main limit is the low CO2 partial pressure in combustion products, which is responsible for the low driving force for gas separation. Post-combustion technologies for carbon dioxide removal include chemical absorption, adsorption, membrane separation, Ca-looping, and cryogenic separation. Chemical absorption is the most developed with several pilot plants and commissioned plants in the world. However, this process is highly energy-intensive and the trend of the research is to develop other alternatives[6].

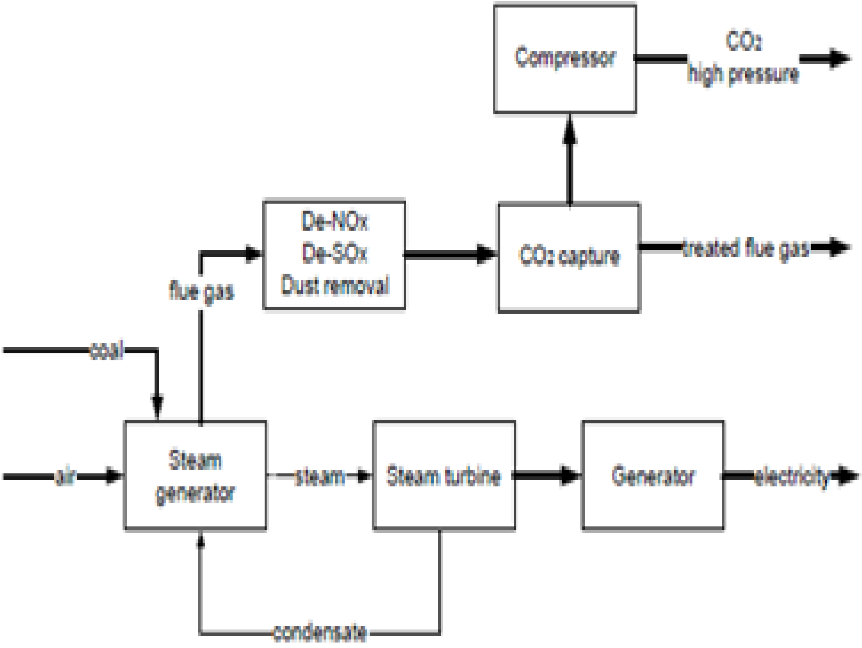

Figure 1.5: Flux diagram of a plant with CO2 capture section[6]

Chemical absorption is composed of two-steps. In the first step, exhaust gases enter into the absorption column, in counter-flow with solvent. In the component, CO2 is absorbed by the solvent and is formed a rich solution. Later, the rich solutions pass through a heat exchanger and goes to the second step of the process. The second step is composed of another column, named stripper. In the stripper, there is also a counter flow occurring with rich-loading solution flowing down the column and stripping steam generated in the reboiler upwards. In this way, using a final compressor, is obtained a flux with high CO2 purity (99 %). After, solvent returns to the first step. In figure 1.6 is shown the process scheme. The most common solvent is MEA (mono-ethanol-amine), in an aqueous solution at 20-30 % wt. The main issue of this technology is the thermal power required by the stripper, and the objective is to minimize this quantity. Other issues of MEA are the volatility, the large enthalpy of reaction with carbon as well as the formation of stable carbamate which limits its absorption capability. A way to improve the process is the use of alternative solvents. New solvents as amines mixture or multi-phase solvents highlight lower energy consumption, but two disadvantages are lower chemical stability and high cost. To increase efficiency, process modifications for example multi-step, or parameters optimization, are two solutions [7].

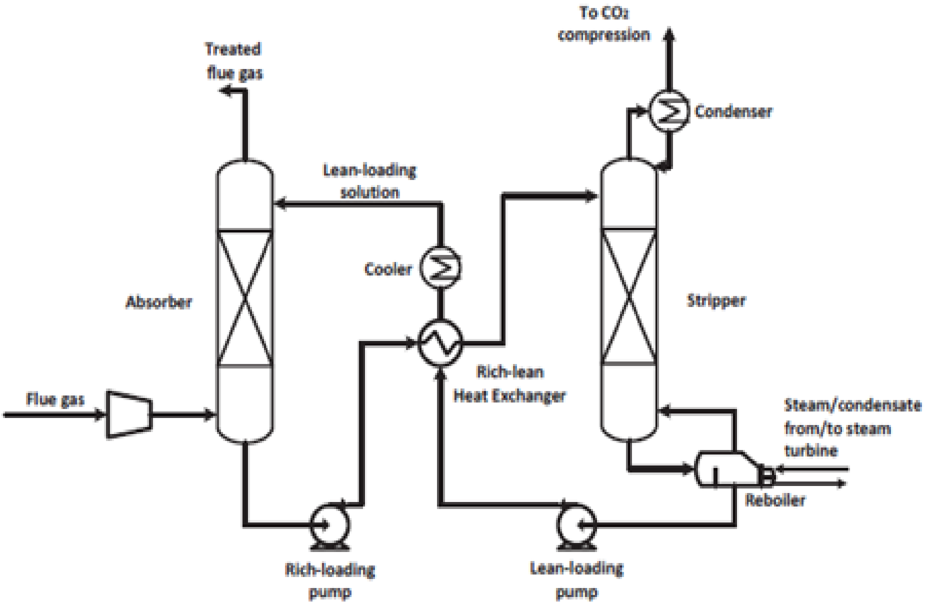

Figure 1.6: Schematic of Chemical Absorption Process [6]

Another process studied for post-combustion capture is the adsorption. Adsorption is based on gas-solid interactions, where gas molecules are attracted, due to electrical interactions, to the solid surface. Adsorption can be physical or chemical and depends on the operation parameters as pressure and temperature. In the field of CO2 capture, different technologies are based on cyclic works, with a variation of a single parameter. The most common are Temperature Swing Adsorption (TSA), in which absorbent is regenerated by a temperature increase, and Pressure Swing Absorption (PSA), in which the gas is captured at high pressure and regenerated at lower pressure. Other configurations are hybrid processes or Vacuum Swing Adsorption (VSA), very similar to PSA, but with lower pressure [8]. Positive aspects of the adsorption processes are: easily insertion in an operating plant, different operation choices, and minimum environmental impact. Adsorbent as zeolites, microporous, MOF (Metal-Organic Frameworks), and amino-based solvents, are used for this process. Adsorption has great perspectives, due to applications in which high reactivity of chemical absorption is not tolerable. Examples are food and drink industries [9]. Calcium-looping is a process based on Ca-O, derived from limestone, that reacts with CO2 to form CaCO3, reversibly. The loop is composed of two steps. In the first step, CO2 is captured in the carbonator, when is formed CaCO3, with an exothermic reaction, at a lower temperature (650-700 °C). The second step consists of a calcination reaction, in which CaCO3 produces solid calcium oxide (CaO) and gaseous CO2. The reaction is endothermic and is carried out at high temperatures (900-950 °C). Another process studied for post-combustion capture is the adsorption. In figure 1.7, is showed the flux diagram of the process proposed by Shimizu et al.. In the two steps, a fluidized bed mechanism is utilized [10]. The energy penalty is reduced with the application of Ca-looping. Moreover, the cost is lower in comparison with chemical absorption and the adsorbent is available from other industrial processes. The issues are the fast deactivation of the process and sorbent losses due to the mechanical impact into the fluidized bed. To improve performances, new solutions are: reactivation of the sorbents as hydration, doping with reagents, and pre-treatment. The perspectives are good, due to the feasibility to combine Ca-looping with other industrial processes.[7].

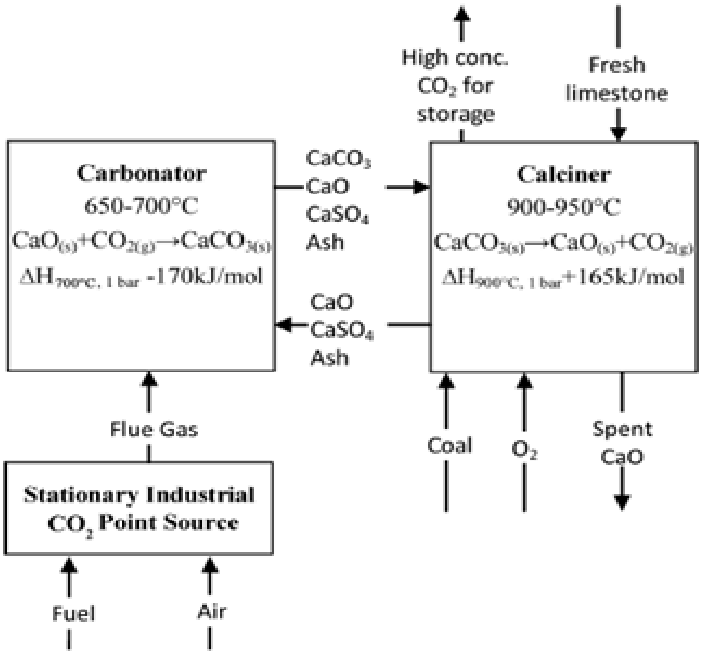

Figure 1.7: Schematic of Ca-looping Process [10]

The membrane separation technology is a promising alternative to chemical absorption. The main advantages are the absence of chemical reactions, low environmental impact, and energetic consumption. The membrane can be inserted easily in an operating plant. A typical scheme of the process is shown in figure 1.8. Many membrane are able to separate CO2 from a mixture of gases. There are two exits in a membrane: permeate, branch with higher CO2 concentration, and the retentate. Due to lower partial pressure, it is necessary to have a vacuum pump and/or a compressor to increase the driving force. Membranes can be classified into polymeric, organic, and mixed. The most common are polymeric membranes, which are already in the market. Polymeric membranes show stability limits at high temperatures. Moreover, membranes are classified by module, examples are spiral and hollow fibers. It is necessary a deep study in the material selection and module project to improve the separation and energy performances. Because the separation with membrane is the main topic of this study, technology is explained in the next chapters. The development of new technologies for post-combustion CO2 capture is one of the most diffuse topics in the scientific field. In the last years, hybrid solutions and alternative solutions are proposed. Examples are cryogenic separation, electro-chemical membranes, or liquid ions use . Research is focused to improve performances and reducing costs.

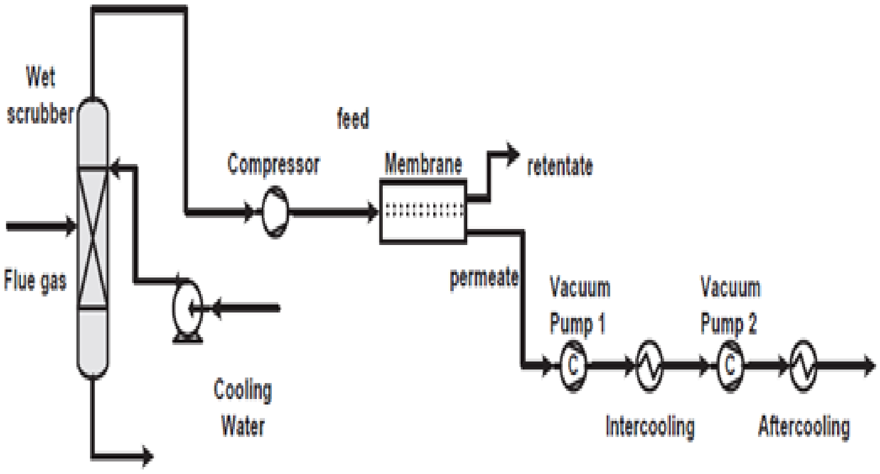

Figure 1.8: Schematic of Membrane Separation Process [6]

1.2.2 Pre-Combustion

Pre-combustion capture is based on fuel conversion into a synthesis gas named syngas, composed mainly of CO and H2. Successfully,the syngas is converted into a Water-Gas-Shifting (WSG) reactor in H2 and CO2, at high pressure. to obtain a high quantity of hydrogen. At the end, the CO2 is separated and a pure stream of hydrogen is produced. CO2 separation can be possible with the use of technologies described in the previous paragraph, as chemical absorption, membrane separations, or adsorption. The main application is the Integrated Gasification Combined Cycle (IGCC). The scheme, represented in figure 1.9, is composed of a gasification step, in which fuel is converted into syngas, with the help of air or oxygen, and water. The second step is the production of H2 in the shift reactor. The reaction may be carried out at a low temperature, to improve hydrogen production. Before sending a rich mixture, it is necessary a cooler and sulfur removal. Carbon dioxide separation happens before the turbine, to exploit high pressure [11]. Pre-combustion, typically, is more efficient than the post-combustion process, due to the high CO2 fraction into the mixture. An issue is the investment cost, very high due to the addition of components. At the moment, there are several commercial plant IGCC with chemical absorption or adsorption. New solutions as pre-combustion at low temperature is on the way.

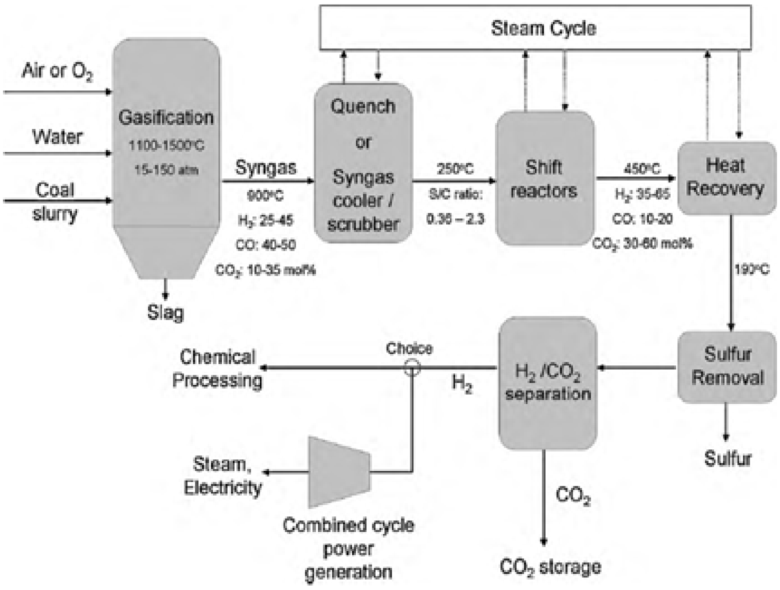

Figure 1.9: Schematic of IPCC Plant with Pre-Combustion Section [11]

1.2.3 Oxyfuel Combustion

The third option for CO2 capture is combustion in high oxygen concentrated ($\geq$95%) environment. Due to combustion, the flow is characterized by great concentrations of carbon dioxide and steam, with a lower presence of pollutants. Combustion products are easily adaptable to separation and CO2 capture, with high purity. In figure 1.10 is represented the scheme. The air separation unit (ASU) is necessary to produce a stream rich of oxygen. Moreover, several steps are needed to remove pollutants as particulate, sulfates, and nitrates. It is noticeable in the flow diagram, that after the particulate removal section, a fraction of exhaust gases are recirculated into the boiler. This step is very important, to control the flame temperature of the combustion process, and to avoid the increase of NOx formation. Oxyfuel combustion is a competitive technology, due to lower environmental impact and high purity carbon of dioxide. On the other side, there are high operational and investment costs, due to adding components to optimize the process. Moreover, energy consumption is higher than pre-and post-combustion technologies, and the efficiency decrease by a factor of 5-8%. Despite the limits, oxyfuel combustion can be competitive in the future [12] [13].

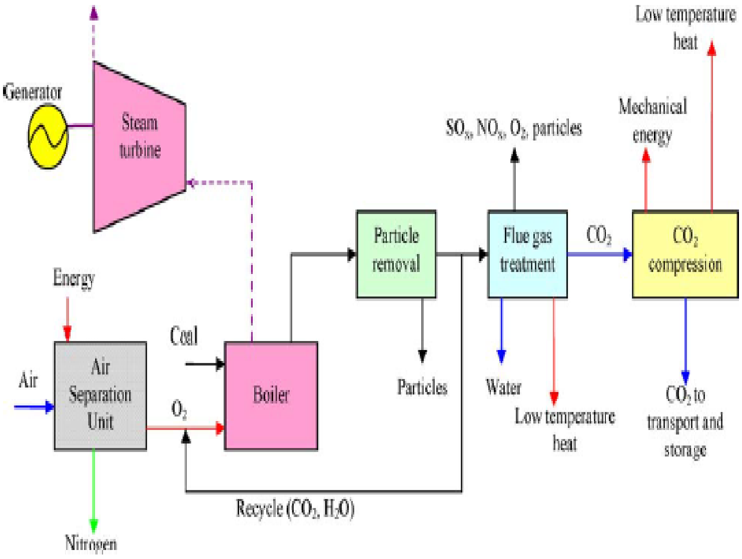

Figure 1.10: Schematic of Oxyfuel Combustion Process [12]

1.2.4 Chemical Looping Combustion

The main problem for the three technologies described previously, is the lower efficiency, due to energy consumption. In the last years, to avoid the problem, a new capture process has been developed, called Chemical Looping Combustion (CLC). In CLC, metal particles are utilized to transport O2 particles, through two reactors. In the combustion reactor, oxidase metal particles enter to oxidize fuel. In this way, particles are reduced in pure metal or less oxidase state. The first step is called reduction reaction and happens in the fuel reactor. Afterward, reduced particles go into the air reactor, in which they are oxidized to return to the original state, with an air flux. The result is a gas, composed of CO2 and steam. Steam is easily condensable and it is possible to obtain a pure stream of carbon dioxide. The main advantage of CLC, in comparison with other technologies, is the negligible energy consumption. The main issues are related to the choice of the particles for oxygen transport. In figure 1.11 the process scheme is showed [13][14].

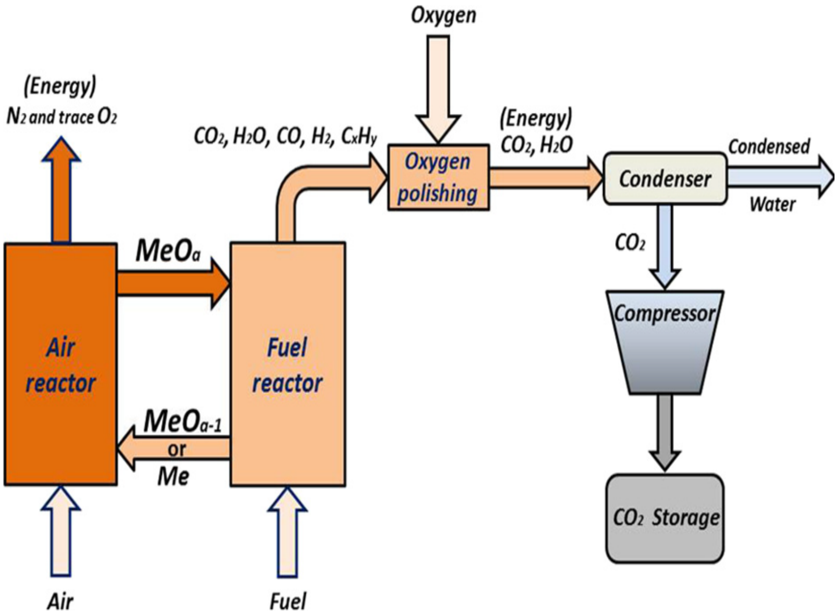

Figure 1.11: Schematic of Chemical looping process [13]

1.2.5 CO2 Transport and Storage

1.2.5.1 CO2 Transport

CO2 transportation process is performed via networks of pressurized pipelines and/or ships. CO2 can be transported in the solid, liquid, or gas phase, depending on physical properties. The best transport is with CO2 supercritical or dense-phase stream. The amount of impurities affect the thermophysical properties of the fluid. For example, water is important for the potential corrosion of the pipe steel. CO2 is typically compressed up to 80 bar to avoid two-phase flow regimes and density increase [15]. As the first stage in transportation, compression or liquefaction represents a significant use of energy. The pumping system is recommended to keep the CO2 under the super-critical phase all along the pipeline. Pipeline transportation is a mature technology. Over long distances, pipelines represent a significant capital cost, related to the installation of the pipeline, surge tank, control system, and booster pump. The selection of pipeline steel can impact the ability of the structure to withstand failures and corrosion. The cost of the material and installation is dependent on the diameter and length of the pipe. The key challenge is to understand the constraints for each transport technology to reduce the over-size and associated costs

[16].

1.2.5.2 CO2 Storage

Storage of carbon dioxide from a power station or industrial facilities can be feasibility done as a climate change mitigation option. There are many types of the underground storage site. The CO2 is injected at high pressures deep underground. Oil and gas wells are accessible and used for Enhanced Oil Recovery (EOR). In the EOR process, it is possible to achieve an oil with high viscosity in the extraction process. Coal beds usually contain methane. Methane can be replaced by carbon dioxide. Brine aquifer, which is created when a cap of impermeable rock is formed deep underground and prevents water and gas seeping upwards [15]. Most assessments of storage capacity consider that saline aquifers have the largest storage potential, while oil and gas fields offer economic incentive of additional hydrocarbon recovery when CO2 is injected. The main concern is to ensure that the fluid pressure does not increase sufficiently to induce fracturing. Over time, storage becomes more secure and the CO2 less likely to escape, but it is necessary to continuous monitoring. Moreover, sensitive CO2 leakage indicators include pressure monitoring and measuring CO2 flux at the surface over the storage site need to be developed. Ultimately, the capacity of permanent CO2 storage needs to be quantified on a global scale to ensure that all of the CO2 captured can be adequately stored [16].

1.2.6 Actual Situation

Before entering in the specific description about membrane separation, it is useful to have a global overview of technologies described in this chapter. It is helpful an index, called Technology Readiness Level (TRL). TRL is an index for the evaluation of technology pathways, through several R&D steps. The system is based on nine levels, each indicates different development grades. For example, TRL9 indicates a commercial technology, or TRL7 a technology in a demonstration state. The development state of CCS technologies is represented in figure 1.11, it is present in the 2018 IPCC report[7]. It is noticeable, that a lot of technologies are between TRL6 (pilot plants) and TRL7 (demonstration). In these levels are present polymeric membranes. There are few commercial technologies as amino-based chemical absorption for post-combustion and natural gas pre-combustion. IPCC shows that CO2 transport is in the last level of TRL. The storage situation is different because there are several solutions, but in the market, there is available only salt flats storage. Interesting solutions as oceans or mills storage are far from demonstration or market. TRL scheme is useful to understand the actual situation of CCS, and the need to invest in the R&D of these technologies, to respect environmental limits imposed by the Paris Congress, and limits the rise of average earth temperature [7].

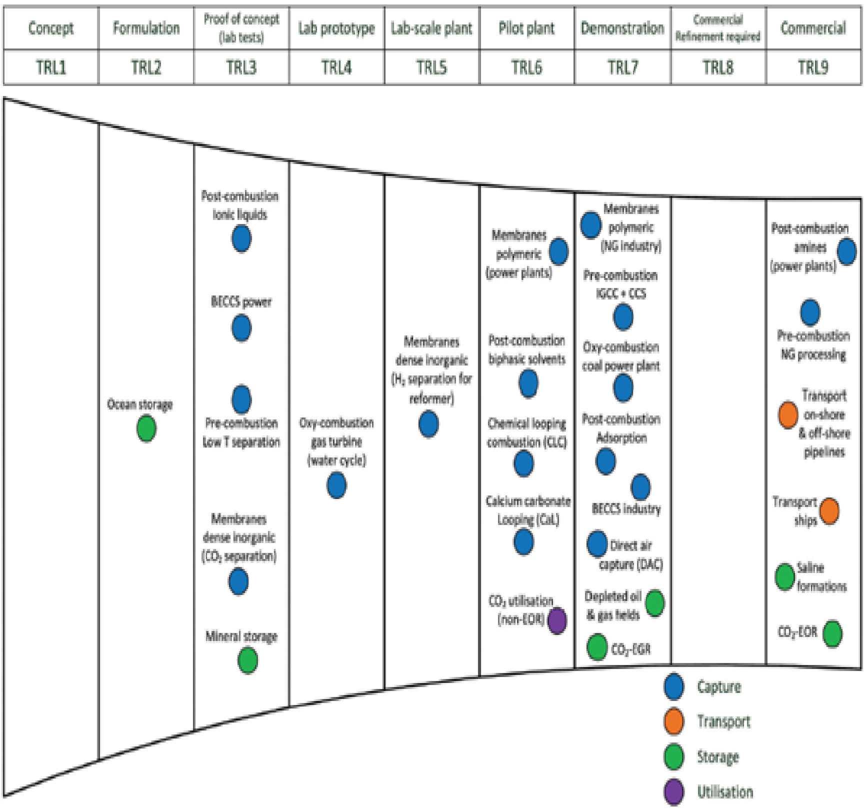

Figure 1.12: CCS technology TRL levels for carbone capture, transport, storage and utilisazion, IPCC, 2018 [7]

After describing, in an exhaustive way, an overview of CO2 capture technologies, the next chapter analyzes the state of the art of membranes. For the insights of capture technologies are suggested the bibliographical references.

1.3 Pulverized Coal Plants

1.3.1 Types of Coal

Coal is one of the most important source of electrical power in the world today. A lot of countries like China, Australia, South Africa, the United States, India, have coal as a lead source for energy production. The attractions of coal are security and cost-effectiveness. On the other hand, coal has a lower energy density than others and is more expensive to transport. Transport can be done by road over short distances, by rail, river or canal over long distances. Many types of coal contain significant amounts of sulfur which, when burnt, generates sulfur dioxide. Coal can also contain heavy metals which are released when the fuel is burnt. Coal combustion generates nitrogen oxides and more carbon dioxide, for each unit of energy produced, than any other fossil fuel.

There are several types of coal. The hardest is anthracite, which contains the highest percentage of carbon (up to 92%) and very little volatile matter or moisture. Anthracite is difficult to burn unless it is mixed with another fuel. For these reasons, anthracite is not widely used. The most abundant of coals are the bituminous coals. This coal contains high amounts of volatile matter and normally has between 76% and 86% of carbon (dry content). Moisture content is between 8% and 18%. They burn easily, especially when pulverized. Sub-bituminous coal is black or black-brown. This coal contains carbon in the range 70%-76% dry content and 18%-38% water. Sub-bituminous coal burns well and sulfur content is low. The last coal is lignite. It is brown and has a carbon content, in dry composition, of 65%-70%. Moisture content is 53%-63% [17].

1.3.2 Coal-Fired Power Generation

In coal-fired power generation, the electricity is produced from coal that burns, and the the exothermic reaction provides heat to a secondary cycle in which working fluid is steam. The hot and pressurised steam flows into steam turbine to generate electricity. A coal plant is composed of several components, as shown in figure 1.13. There is a fuel handling system in which the coal, deliveries from the mine, is converted into a form that can be readily burnt. In the modern plant, powders are produced to form a pulverized coal. The pulverized coal is sent to a combustion system where it is mixed with air, releasing chemical energy as heat. The heat energy converts the water in steam. In combustion chamber, ashes are produced.

In large part, they move to the bottom of the chamber and are removed as slag. The remains of ashes are carried away with the hot combustion gases. Steam goes into the steam turbine, usually composed of at least three elements, high-pressure turbine, intermediate-pressure turbine, and low-pressure turbine. Usually, there is a re-heater to improve efficiency. Exit steam from the low-pressure turbine goes to the condenser to return water.

The hot-flue gases, that exit from the combustion chamber, are rich in carbon dioxide and impurities. There are a series of cleaning systems to remove nitrogen oxides, fly ashes, and sulfur oxides. Methods for separation can be chemical or filtrating. Potentially, a coal plant with all these processes, including carbon dioxide capture, may be called a zero-emission plant [17].

In the world, different types of pulverized coal-fired power plants are available, depending on the steam conditions entering in the steam turbine. Subcritical refers to pressures below the critical point of water (221 bar), while supercritical refers to pressures above it. Ultra-supercritical refers to pressures above 221 bar and temperatures above 590°C [18]. The efficiency of subcritical plants ranges between 33% and 39%, it increases to 38-42% in supercritical plants and above 42% in ultra-supercritical plants. Subcritical and supercritical power plants account for more than 95% of the global capacity, with 80% of this contribution related to subcritical plants [18].

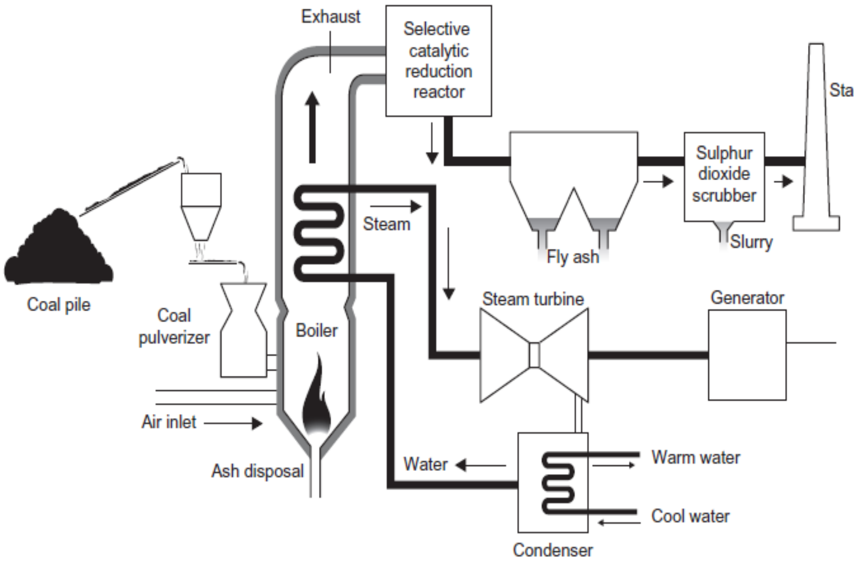

Figure 1.13: Schematic of a pulverized coal-fired plant [18]

1.4 Outline

This work aims to evaluate the technical and economic feasibility of a pulverized coal plant, with the introduction of a CO2 capture stage based on membrane separation. The main steps of the thesis are:

- description of state of the art for membranes, to understand: (i) positive and negative aspect of each membrane classes and (ii) modules.
- description of the inputs and assumptions required for the simulations, with all technical and economic factors.
- visualization and discussion of the results for relevant parameters, with the comparison of chosen membranes. Parameters are: Total energy requirement, plant efficiency, total membrane area, CO2 emitted and captured, capital cost, O&M cost, cost of CO2 avoided and captured, and cost of electricity.
- sensitivity analysis of main important factors, to understand the best combination to improve the system.

2 State of The Art of Membranes

Membrane technology is useful in several industrial processes such as purification of natural gas, air separation, and hydrogen separation. In the last decade, a lot of membranes are tested to understand the most suitable materials for post-combustion capture. In the following chapter, physical principles of gas separation with membrane and state of the art of membrane are showed, analyzing pros and cons.

2.1 Solution Gas Mechanisms

Gases diffuse into the membrane with different mechanisms. The most common is the solution-diffusion that characterizes a large part of polymeric based membranes. In the last decade, a mechanism based on the chemical reaction it has developed, introducing facilitated-transport of CO2. Finally, some inorganic membranes exploit different dimensions of CO2 with other gases for the separation.

2.1.1 Solution-Diffusion

Solution-diffusion describes gases and ions transport into dense membranes. Gas is absorbed on the membrane surface, diffuses into it, and, in the end, is desorbed. Figure 2.1 (a) shows the process. The parameters that describe the process are solubility (S), which depends on the membrane affinity and condensability, and diffusivity (D), related to gas kinetic. The mathematical theory of diffusion isentropic substances is based on the hypothesis that the rate of transfer of diffusing substance through unit area of a section is proportional to the concentration gradient measured normal to the section [19].

$$N_A = D_{AB}\frac{c_{A1} - c_{A2}}{z_2 - z_1} \tag{2.1}$$

where $N_A[mol_A/m^2s]$ is the molar flux of component A in the z-direction due to molecular diffusion.$D_{AB}[m^2/s]$ is the molecular diffusivity of the molecule A in B. z is the distance in m and c_A is the concentration of A in $[kg\ or\ mol_A/m^2]$.

The diffusion coefficient does not depend on the partial pressure of the gas. The solubility of the gas is directly proportional to the partial pressure, as stated in Henry's law:

$$S = \frac{c_A}{p_A}[mol/m^3Pa] \tag{2.2}$$

The mechanism of diffusion in porous solid changes as the different diameter of the pores and on the mean free path, which is the average distance traveled by a molecule of gas between two collisions. The mean free path is inversely proportional to the pressure and it is defined as:

$$\lambda = \frac{3.2\mu}{P}\sqrt{\frac{RT}{2\pi M}} \tag{2.3}$$

μ is the viscosity in $Pa * s$, P is the total pressure in N/m^2, T is the temperature in K, M is the molecular weight in kg/mol and $R = 8.3413 * 10^3$ is the gas constant in $N * m/mol * K$. To improve the model it is necessary to introduce a parameter that evaluates the unknown tortuous path of the molecule when it is greater than the thickness of the membrane. Moreover, in the equation of the molar flux, a new parameter needs to be inserted, called fractional free volume (FFV). FFV is the ratio between the total volume of the membrane minus the volume occupied by a polymeric chain, over the total volume of the membrane.

$$FFV = \frac{V_{membrane} - V_{occupied}}{V_{membrane}} \tag{2.4}$$

With FFV and tortuosity τ, the flux is evaluated as:

$$N_A = (FFV)D_{AB}\frac{c_{A1} - c_{A2}}{\tau(z_2 - z_1)} \tag{2.5}$$

The diffusion coefficient D is evaluated with the Knudsen gas molecule diffusion theory. D is independent of pressure while it depends on the average pore radius $\bar{r}$ and on the average molecular velocity for component A $\overline{v_A}$. The average molecular velocity can be evaluated by the kinetic theory of the gas [19].

$$D_{K,A} = \frac{2}{3}\overline{r v_A} \tag{2.6}$$

To describe membrane performances there are two parameters:

- permeability, defined as the flux of a specific gas through the membrane:

  $$P_i = \frac{J_i\, l}{\Delta p_i} \tag{2.7}$$

  where J_i is the flux of i-th gas through the membrane, l is the membrane thickness and Δp_i is the variation of partial pressure. In solution diffusion mechanism, permeability is function of diffusion coefficient (D) and solubility coefficient (S), therefore permeability for the i-th gas is described by the following formula:

  $$P_i = S_i\, D_i \tag{2.8}$$

  Permeability unit is barrer, where 1 $barrer = 1 * 10^{-10} cm^3 (STP) * cm * cm^{-2} * s{-}1 * (cm\ Hg)^{-1}$.

  Permeability is an intrinsic quantity. Sometimes, to evaluate membrane performances, is used permeance, a pratical quantity. Permeance expresses the flux penetrating for driving force unit. It is defined as:

  $$\frac{P_i}{l} = \frac{J_i}{\Delta p_i} \tag{2.9}$$

  Permeance unit is GPU (Gas Permeation Unit), where 1 $GPU = 1 * 10^{-6} cm^3 (STP) * cm * cm^{-2} * s{-}1 * (cm\ Hg)^{-1}$.

  From the operational point of view, it is easy to pass from permeance to permeability through membrane thickness.

- selectivity, is the preference of membrane to allow the passage for one species and not another. It is defined as:

  $$a_{ij} = \frac{P_i}{P_j} \tag{2.10}$$

Table 2.1: Condensability and Diffusivity of different gases

Gas	Kinetic Diameter (A°)	Critical Temperature (K)
CO_2	3.3	304.2
N_2	3.64	126.1
CH_4	3.8	190.7
H_2	2.89	33.3

where P_i e P_j indicate permeability of i-th and j-th gases.
Selectivity can be ideal if permeability of gases are evaluated in a pure phase, otherwise is real, in multi-component conditions. For low pressure and stiff polymers, ideal selectivity is a good approximation for the real conditions [20].

Carbon dioxide, as shown in table 2.1, has the highest critical temperature. In comparison with methane and nitrogen, CO2 has the smallest kinetic diameter. Therefore, separation of CO2 in post-combustion with the mixture at high content of nitrogen is an operation helped by the physics of the problem [21].

2.1.2 Facilitated Transport

Facilitated transport exploit interactions between CO2 and functional groups that enhanced gas transport through reversible reactions. Penetrating gas dissolves into the membrane when reacting with a carrier, fixed or mobile, forming a reaction product. In the last part of the membrane, at low partial pressure, the inverse reaction is carried out with the release of penetrating and carrier regeneration. Other inert gases are rejected. The process is shown in figure 2.1 (b). Today, the most common carrier are amine with the following reactions:

$$2\,RNH_2 + CO_2 \leftrightarrow RNHCOO^- + RNH_3^+ \tag{2.11}$$

$$RNH_2 + CO_2 + H_2O \leftrightarrow HCO_3^- + RNH_3^+ \tag{2.12}$$

$$2R_2NH + CO_2 \leftrightarrow R_2NH_2^+ + R_2NCOO^- \tag{2.13}$$

$$R_2NH + CO_2 + H_2O \leftrightarrow R_2NH_2^+ + HCO_3^- \tag{2.14}$$

$$R_3N + CO_2 + H_2O \leftrightarrow R_3NH^+ + HCO_3^- \tag{2.15}$$

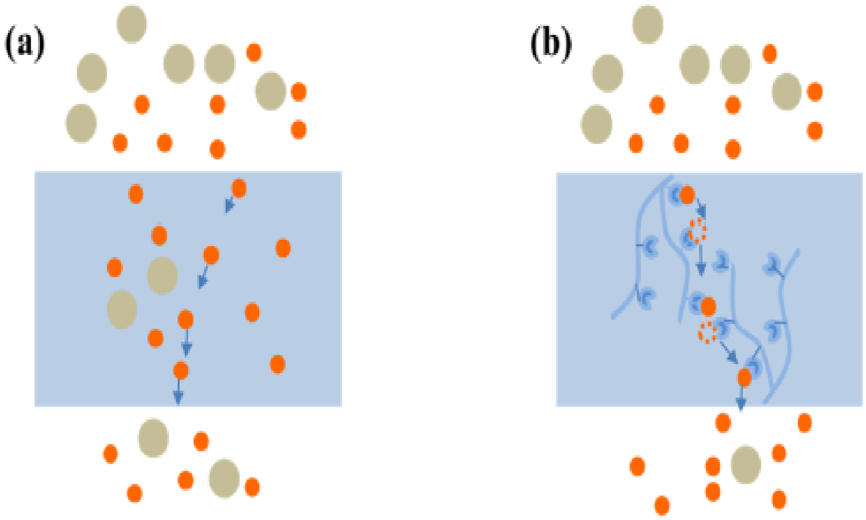

Figure 2.1: Transport Gas Mechanisms: (a) solution-diffusion, (b) facilitated transport. [21]

Primary and secondary amines can react without water, unlike tertiary amines. Other basic groups based on fluorine, potassium, can be utilized as a carrier [21].

2.1.3 Molecular Sieve

Molecular sieve exploits gas dimension differences. Gases with small kinetic diameters pass into the membrane while gases with big kinetic diameters are blocked. In this way, remembering that CO2 kinetic diameter is small than N2 and CH4, separation can be obtained. Microporous inorganic membranes use molecular sieve. This type of mechanism is not exploited in this work. For a complete explanation of the mechanism, it is recommended the references. [21].

2.2 Membranes

2.2.1 Dense Polymeric

Polymeric membranes are largely used in the industry. Over the years, the synthesis and production process of this membrane is tested and enhanced. Polymers can be divided into two classes: glasses and rubbers. Rubbers show high free volume into the major structure, regulated by chain dynamics. Glasses have less free volume but show high gas selection. Generally, rubbers have high permeability and low selectivity, glasses have low permeability and low selectivity. Polymeric membranes are based on solution-diffusion mechanism. One of the most studied polymeric class for membrane separation are polyimides (PI). PI has high thermal and chemical stability, and reproducibility is easy. The main problems of this type of membrane are physical aging and plasticization. In the last years, the tests carried out show high degradation for thin membranes in comparison with thick membranes. Because membrane technology is addressing thin and ultra-thin technology, with nano-orders thickness, a lot of methods are proposed to reduce aging and plasticization [21]. Cross-linking is the introduction of agents with specific functional groups into polymers. This method causes reduction of crystalline phase, rising the overall membrane performances [22]. Commercial membrane Matrimid®9725 is characterized by the permeability of 4 barrer and selectivity to N2 of 23. In the last years, a lot of experiments with membrane 6FDA are carried out. 6FDA is based on phenol-chains with fluorine atoms. Results are the low increase of permeability (15 barrer) and noticeable selectivity (50) [23]. Today, PI is not a possible candidate for carbon dioxide separation in combustion products, due to low partial pressure and low permeability. PEO/PEG membranes are polymers characterized by polar groups to increase CO2 affinity. Production cost is low and manufacturability is good. The main limit of this membrane is the crystallization that reduces the permeability. To avoid this problem, methods like cross-linking or co-polymerization are used. Co-polymerization is the creation of a material with a fraction of PEO/PEG plus other compounds with strong boundaries to obtain higher transport parameters [21]. Polaris® and Pebax® membranes are two examples of commercial types. Zhongde et al. have obtained a permeability of 1889 barrer and selectivity of 39, with cross-linking of PEG membrane with a liquid ionic material [24]. The use of benzoic acid in the membrane of Meshkat et al. causes a high rise of selectivity of Pebax®1657 membrane, reaching a value of 93 [25]. Another possible way to increase transport properties is blending.

Blending is a mixing process between two polymers to obtain a new material with better parameters. This process is highly used in industry and is characterized by lower cost [22]. Shirin et al. tested blended membrane composed by Pebax ® and VACc, an acetate organic compound, obtaining good performance and selectivity increase [26]. PEO/PEG membranes are most promising, they are the base for composite membrane research.

2.2.2 Facilitated Transport Membranes

Facilitated transport membranes show high permeability and selectivity at low pressure, due to reversible reaction between CO2 and fixed or mobile carrier. Overall, the performance obtained is higher than the membrane with the solution-diffusion mechanism. The most used carriers are amines (primary, secondary or tertiary) because they easily react with carbon dioxide forming carbonates. Subsequently, carbonates are reduced, due to reversible reaction, into H2O and CO2. These membranes are easily replicable and are easy to use. Amines are incorporated into the membrane with the blending process and they, provide an increase of membrane density. Examples are poly-ethylene/amines-based membranes (PEI), polyvinyl amine (PVA), and poly-acryl-amides (PAAm). Tests carried out recently show that PVAm has high transport performances at low pressure. High crystalline ratio and carrier saturation are the main problems for these membranes. Moreover, PVAm raises the water retention and contributes to the creation of defects-free membrane [21]. To avoid carried saturation, production of multi-layers membrane or increase carrier quantity into the structure are the solutions. Han et al. have obtained permeance of 1451 GPU and a CO2/N2 selectivity of 165 at 67°C, with a PVAm/PES membrane encapsulated into a nanotube structure [27]. PVA membrane, with poly-sulphone support and metakaolin disperse phase (MK), shows excellent performances for low pressure. Selectivity concerning nitrogen is 80 and permeability is 450 Barrer. Moreover, this membrane has good stability based on a 300-hours test [28]. Recently, new solutions and carriers are studied to optimize facilitated-transport membranes. Inter-facial polymerization is a solution to optimize structure membrane through the introduction of several perm-selectivity. Carboxylic groups, as a fixed carrier, show excellent anti-oxidation and perm-selectivity. Lately, natural enzymes or -OH groups are proposed as carriers nevertheless they present stability and activation limits [22].

2.2.3 Microporous Organic Membranes

Organic microporous membranes are characterized by high porosity and surface area. The main classes are intrinsic porosity polymers (PIM) and thermal re-arranged membranes (TR), which exploit high free volume and pores created by chains disorder. Recently, other classes as covalent organic membranes (COF) are investigated, based on molecular sieve mechanism. PIMs have twisted and rigid structures with interconnected pores, with a distribution of 0.4-0.8 nm. PIMs show high permeability due to high free volume. The representative membrane of this class is PIM-1, with good solubility and easy fabrication. The main limit is the low selectivity and, to avoid the problem, nitrates and nitrites are tested. A solution is to grow the chain's rigidity to enhance the diffusion mechanism through the introduction of rings aromatic compounds. Another negative aspect is physical aging; to reduce it, solutions as cross-linking and UV, chemical, and thermal are proposed with the consequence of permeability reduction [28]. Fuoco et al, test PIM membrane with fluorine groups, finding permeability of 1080 barrer and selectivity CO2/N2 of 10.6 [29]. Excellent permeability of 9709 barres is reached by Rose et al. adding TMN-trip functional groups to a PIM [30]. A good solution to increase PIM's performance is the introduction of filler. Also, TR membranes are rigid with interconnected pores. TR is not soluble and shows high thermal and chemical stability. An example is PI membranes thermally re-arranged to change cavity distribution into the structure and increase free volume. There are two types of structural changes: (a) casual re-order by chains due to chemical bonds; (b) chains are converted into a more rigid structure. TR has both large cavities to enhance gas transport and small cavities to enhance separation. Results are permeability and selectivity better than same material without thermal treatment [28]. Lee et al. tested diXTR membrane modified with a thermal densification process, obtaining a permeance of 2060 GPU and selectivity of 17.9 [31]. Lastly, there are a lot of new microporous organic membranes. COFs are membranes constituted by light elements (B, N, C, and O) connected with covalent bonds. COFs shows a low-density, organized structure with a channel for gas and high stability. COF's fabrication is limited due to the difficult production of free-defect material. COF's have high selectivity and low permeability and, due to their characteristic, applications are oriented to filler into mixed-matrix membranes. Other examples are PAR, based on poly-arylate, characterized by intra-molecular micro-vacuums and MMP, based on metal elements. In the work of Quiao et al., MMP shows high idrolityc stability, the preparation process is chemical. MMP-3 membrane synthesized starting from Amina-based polymers shows permeance of 3000 GPU and selectivity of 79 under dry and wet conditions [32]. MPF-1 are membranes based on metal frame-works [28].

2.2.4 Microporous Inorganic Membranes

Microporous Inorganic Membranes, based on molecular sieve mechanism, are a solution to obtain better performances. Zeolites are materials with uniform pores of 0.3-0.1 nm. It is possible to modify zeolites, substituting metallic ions or hydrogen with Si/Al cations. Zeolites are fabricated on the aluminum substrate to have high mechanical stability. The limit is large-scale free-defect production due to brittle nature [28]. Makertihartha et al. have obtained great results with SAPO-34 membrane based on silicon tube. With an optimized method of production, a free-defect membrane with 10000 barrer of permeability and selectivity CO2/N2 of 35 is obtained [33]. In the work of Twalbeh et al., silicon oxide-based membrane shows the enormous potential of zeolites into composite membranes, with a permeability of 10500 barrer [34]. Another class is graphene-based materials (GO). GO show good mechanical resistance, chemical stability and it is used a lot in industrial fields. Free-defects graphene is gas and liquid impermeable and, to have membrane useful for gas separation, chemical or physical modification are needed. A second issue is the large pore dimension; cationic control with small molecules to control space of different material layers is a solution to reduce pore dimension [28]. Today, GO membranes tested are few. An example is GOP tested by Zhou et al.; permeance of 120 GPU and selectivity of 12 for a mixture 15% CO2/85% N2 in volume is obtained, due to nano-channels for gas transport [35]. MOF membranes (Metal-Organic Frameworks) show great surface area and uniform ultra-porosity. The fabrication process is related to layer-by-layers steps and is solvent-free, with lower pressure. The main limit is low selectivity due to low CO2-structure interactions. To enhance selectivity, the introduction of material that increases carbon dioxide interaction is a solution. Thicknesses of MOF are small to reduce the presence of defects; the result is a reduction of permeability. The obstacles for commercialization are brittleness and incompatibility with several materials [28]. Rong et al show selectivity of 31,3 due to the introduction of particles with transition elements TMDCs into MOFs membrane [36]. Grafting chemical process with PDA into UiO-66 membranes, caused an increase of selectivity to 51,6 without modification of permeance of 1115 GPU[37].

2.2.5 Mixed-Matrix Membranes

Mixed-matrix membranes (MMM) are composed of a continuous polymeric phase, with good processability, and dispersed phase to increase performances. MMMs show the best separation properties. The most common problems are related to interface compatibility between two phases and agglomeration of nano-particles. Organic fillers are more compatibles than inorganics. MOFs, COFs, and ZIFs are some examples of organic fillers. Introducing polar groups, coatings, or make chemical processes as cross-linking, blending, or grafting are pathways to increase compatibility between two phases. It is noticeable, from literature, that -NH2 and -COOH groups increase compatibility. Filler's fraction that is possible to introduce into a polymeric matrix is very low. Today, it is difficult to find a MMM with more than 30% in weight of filler. Best fractions are obtained with cross-linking, where filler's fraction is 40% wt. MMM synthesis is complex and expensive [28].
Recently, Sun et. al have tested MMM with PIMs as polymeric phase and penta-fluorine as filler into carbon nanotubes. With 7,5% wt. of filler, the permeability of 29000 barrer and selectivity CO2/N2 of 24,2 is reached, with 1:1 flux of carbon dioxide and nitrogen [38]. MMM membrane PVA/ PEG with carbon nanotubes fillers in low percentage shows high selectivity of 174,33 in the work of Dilshad et al. [39]. Kheirtalab et al. use as an organic filler graphene oxide (GO) into a Pebax membrane. GO has created intramolecular extra-vacuums that increase permeability to 228,3 barrer, with good selectivity [40].
The introduction of MOFs fillers increases transport parameters, due to channel growth for selectivity and diffusivity. An example is the MMM-801/PIM membrane, which shows permeability of 9686 barrer and selectivity of 27. Moreover, physical aging is evaluated with continuous work on 90 days, and results show a negligible performance decrease. [41] Zeolites with functional groups as -NH2, in the work of Ding et al., cause an increase of 53% and 27% for permeability and selectivity of Pebax membrane [42].
Inorganic filler's use is more difficult due to its compatibility with the polymeric membrane. However, different solutions are tested in the last years. The introduction of titanium oxide (TiO2) into the Pebax membrane creates active sites for gas passage, increasing CO2 diffusion and overstep Robeson's limit [43].
Liquid ions (ILs) as fillers is another solution to increase compatibility with the polymeric phase. Kalantari et al. have tested a Pebax membrane with OMIM/PF6 as liquid ions solution, obtaining permeability of 300 barrer and selectivity of 248,6. Moreover, great mechanical stability is shown

[44]. MMM obtain great performance and overstep Robeson Limit and they are the main candidates to post-combustion CO2 capture with separation membranes process.

2.2.6 Robeson Plot

Robeson diagrams represent a visual guide to understand the state of the art of the membranes. These plots are characterized by permeability on the x-axis in barrer, and by selectivity CO2/X on the y-axis, where X is the gas from which carbon dioxide should be separated. Graphs are in log-scale. On the graph, all couple of data from the last years are inserted. Moreover, a straight line called Robeson Upper Bound is represented; this line shows a limit to reach the desirable performances. Then, if a membrane is represented over the Robeson Upper Bound, the membrane is a good candidate for future marketing [45]. As described previously, permeability and selectivity are the two important parameters for membranes. They constitute a trade-off because increasing one, the other decreases. Therefore, it is necessary to insert a membrane into the Robeson diagram, to compare it with other available in the literature and, to find methods to improve a specific parameter and places a membrane over the Robeson upper bound. In 2008, the last Robeson upper bound for CO2/N2 separation is published. Based on it, on the diagram in figure 2.2, membranes tested in the last years are inserted. The diagram shows different membranes classified by typologies. Dense polymeric membranes, due to lower permeability, do not reach the upper bound. Transport facilitated membranes are placed up to the upper bound, due to high performance. If the compatibility of the carrier is fixed, facilitated transport membranes could be candidates for future marketing. Microporous organic membranes have the advantage to increase permeability, but the lower selectivity reduces the number of the membrane that reach the upper bound; examples are COF and MMP. Microporous inorganic membranes are characterized by good performances. Today, GO, MOF, and zeolites-based membranes are placed over the Robeson upper bound. Finally, there are MMM membranes that are more than others. MMM, with the union of polymeric matrix and filler, reach the upper bound easily. They are a principal candidate for future marketing and, the possibility to change composition is a positive aspect to find the most suitable membrane for continuum operation in a post-combustion CO2-capture plant. It is noticeable, analyzing the last articles, a trend to mixed-matrix membranes. In 2020, more than twenty mixed-matrix membranes are tested, in comparison with other classes that date back to 2017-2018.

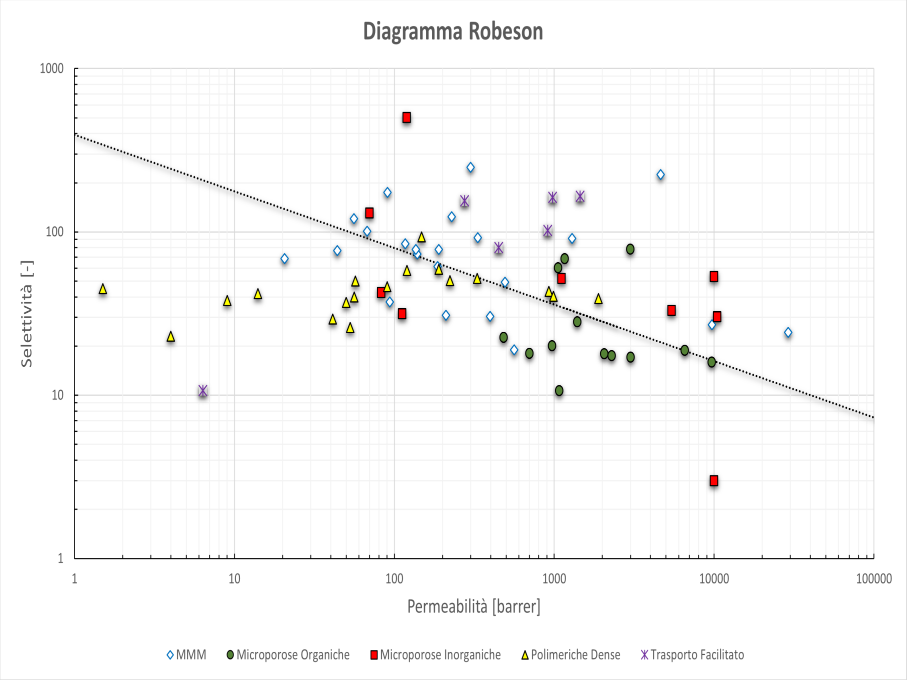

Figure 2.2: Robeson Diagram for CO2/N2 separation, on the x-axis the permeability in Barre, on y-axis the selectivity CO2/N2

2.3 Modules

Membrane modules consist of housing, sealing materials, and membrane. The industrial membranes can be packaged in a different configuration to respect some important requirements like high surface/volume ratio, low flow resistance, low construction cost, and membrane replacement. Typical module housing materials include stainless steel, titanium, and plastic. Stainless steel is most commonly used due to its good chemical and thermal stability as well as great robustness. Plastic is a cheaper option but limits the conditions with which the membranes can operate. There are four typologies of membrane modules: (i) tubular, (ii) plate-and-frame, (iii) spiral-wound, (iv) hollow fibers [46].

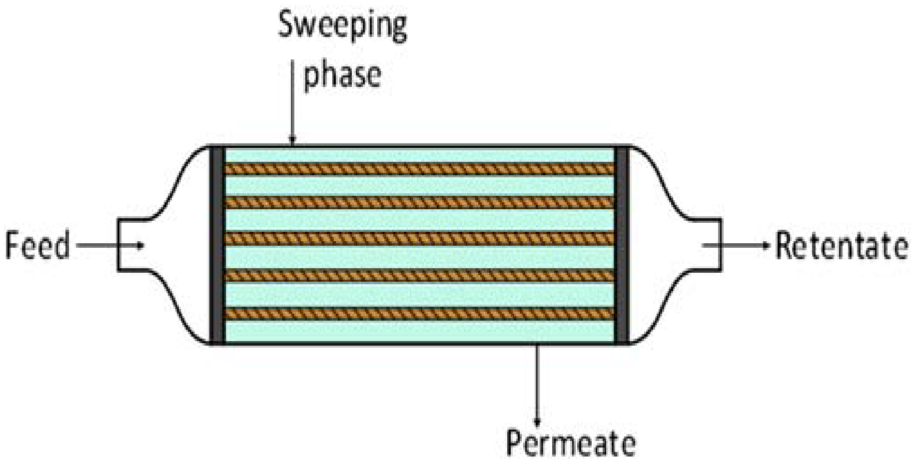

Figure 2.3: Schematic drawing of a tubular module [48]

2.3.1 Tubular

Tubular modules are composed of many membrane tubes assembled in a shell-and-tube arrangement. Tubes are usually made of porous fabric or plastic support with selective membranes on the inside. The Internal diameters range from 5 to 25 mm, and tube lengths are in the range of 0.6 to 6 m. Due to their large internal diameters, tubular modules are capable of dealing with the feed stream containing fairly large particles. They need a large pumping capacity because they are usually operated under turbulent flow conditions. Moreover, tubular modules have the lowest surface-area-to-volume ratio among all the four membrane configurations [47]. The high axial velocity limits are helpful to avoid the effect of polarization. Volumes of modules are also high, which need large floor space to operate. In a typical tubular membrane system, a large number of tubes are manifolded in series. The permeate is removed from each tube and sent to a permeate collection header. Figure 2.3 shows the scheme of the tubular membrane module [48].

2.3.2 Plate-and-Frame

In the plate-and-frame module, the selective layer is sandwiched between two support layers, which provide a flow channel to the fluid on both sides of the membrane. The sandwiched plates with the membrane can be built up vertically to increase the surface of the membrane.

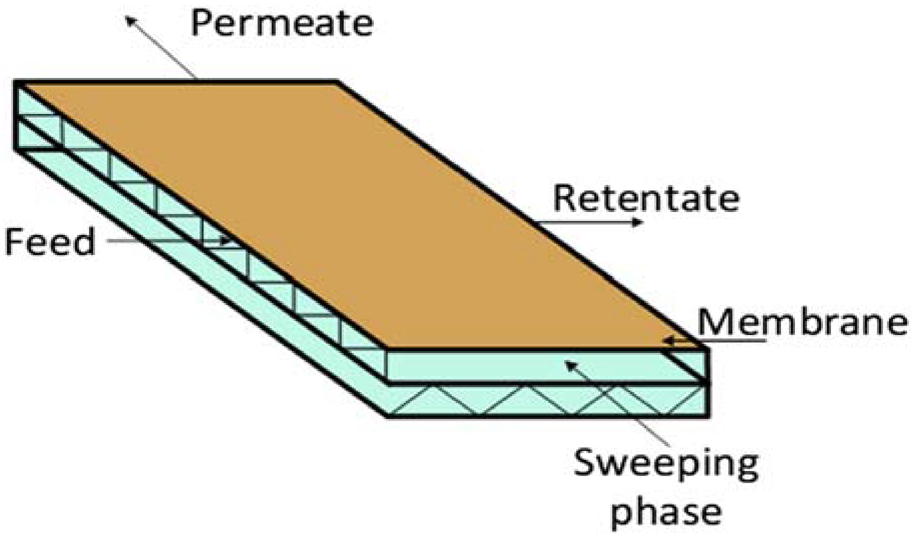

Figure 2.4: Schematic drawing of a plate module [48]

Flat sheet modules have channel gaps ranging from 0.5 to 10 mm and are of lengths ranging from 10 to 60 cm [47]. It is recommended a pretreatment. Fluid flow takes place parallel through the membrane module. Regarding packing density, energy consumption, and cost, flat sheet performances are lower concerning tubular modules. In figure 2.4 is illustrated the module.

2.3.3 Spiral-wound

The design of spiral-wound modules is similar to the flat sheet modules. In the spiral-wound modules, two membrane sheets are separated by a mesh-like spacer with the active membrane sides facing away. On the other two sides, another two mesh-like spacers with thicknesses in the range of 0.56-3 mm are placed as the feed channel spacers. The whole assembly is rolled around the perforated center tube in a spiral configuration. Spiral-wound modules are operated in the turbulent flow region due to the presence of feed spacers. The pressure drop is high due to the additional drag generated by feed spacers. Spiral-wound modules show a high surface area-volume ratio and the lowest capital cost. In the case of suspended particles, they can easily block the mesh-like spacers and feed channels. Therefore, spiral-wound modules require relatively clean feed that are with a minimum content of suspended particles [47].

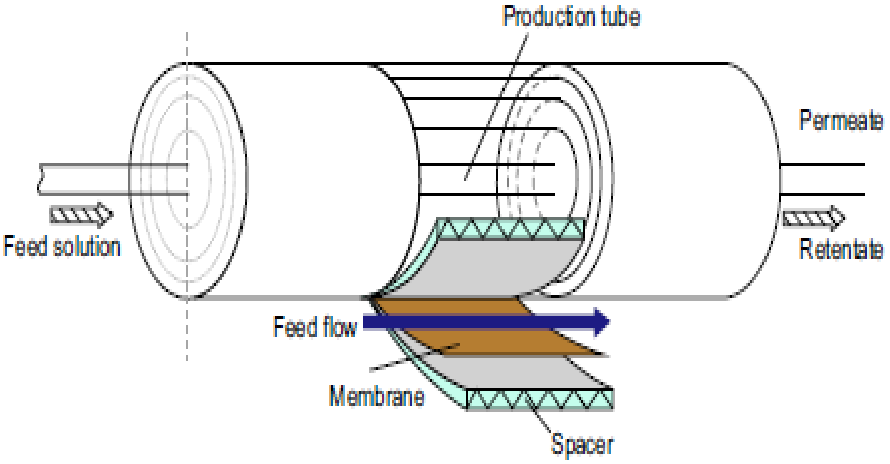

Figure 2.5: Schematic drawing of a spiral-wound module [48]

The membrane sheets are separated by polyester fabric or a thin plastic spacer. In figure 2.5 is illustrated the module.

2.3.4 Hollow Fibers

Hollow fiber modules are the thin tubular membranes in compact modules. Hollow fiber modules are composed of 50-3000 individual hollow fiber, bundled and sealed together on each end with epoxy. The fiber diameters typically range from 0.2 to 3 mm. The fiber lengths range from 18 to 120 cm. Hollow fiber modules have some very different characteristics from tubular modules. The pressure rating of hollow fiber modules is low, normally with a maximum of 2.5 bar. They are one of the more economical modules in terms of energy consumption, due to the combination of low crossflow rate and low-pressure drop. Hollow fiber modules have the highest surface-area-to-volume ratio among all the four membrane configurations, and their holdup volume is low. They are very high easy to clean. The main disadvantage is that their thin fibers are susceptible to get blocked by the feed with large particles when they are operated in the inside-out model. The pre-treatment to reduce the particle size to 100 μm is required [47]. Two arrangement types are illustrated in figure 2.6. The inside-out arrangement (the skin layer is on the lumen side) has better protection for the active layer.

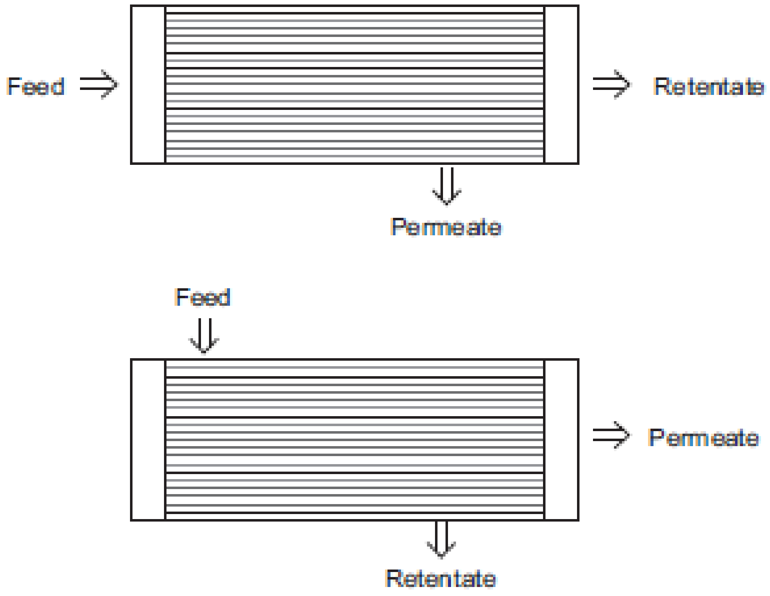

Figure 2.6: Schematic drawing of a hollow-fiber modules: (a) inside-out, (b) outside-in [48]

A disadvantage is that it needs a clean feed. The second arrangement is the outside-in (the skin layer is in the shell), that has the high membrane surface, while its disadvantage is channeling.

3 Techno-economic assessment

Tecno-economic assessment is explained in the following paragraphs. The analysis is carried out with the Integrated Environmental Control Model (IECM), an open-source software. To evaluate the performances of a pulverized coal plant with a CO2 capture section based on membrane separation, three membranes are chosen from the literature. Technical and economic performances are carried out to understand the feasibility of the technology.

3.1 Software

IECM is an open-source tool for calculating the performance, emissions, and cost of a fossil fuel plant. It is developed by Carnegie Mellon University and the Department of Engineering & Public Policy, in collaboration with the National Energy Technology Laboratory (NETL) and the United States Department of Energy. IECM shows the possibility to configure three types of plants: pulverized coal (PC), Natural Gas Combined Cycle (NGCC), and Integrated Gasification Combined Cycle (IGCC). Starting from these base plants, several configurations are possible, introducing all the post-combustion controls, including the carbon dioxide capture. Amine-based, ammonia-based, solid sorbent, and membrane are carbon capture technology available for the pulverized coal plant. The interface of the software is shown in figure 3.1 A complete simulation can be carried out, introducing data of the USA reference plants or from other plants with user definition. IECM carried out a technical evaluation of the plant performance, based on energy and mass balance equations. The economic analysis is based on the methodologies developed by the Electric Power Research Institute (EPRI). Methodologies are included in a Technical Assessment Guide, to provide a consistent basics for reporting cost and revenues. Moreover, there are two important tools. First, it is possible to carry out sensitivity analysis for all dependent variables available on the software. It is possible to set the range, number of points, and the minimum and maximum value. Second, it is possible to configure an uncertainty analysis, setting the sample size and sampling methods. The version used for the work is the IECM 11.4, released in 2020. The current version refers the prices to USD 2017 dollars. Analysis and graphs are modeled and visualized with the last version of Microsoft Excel.

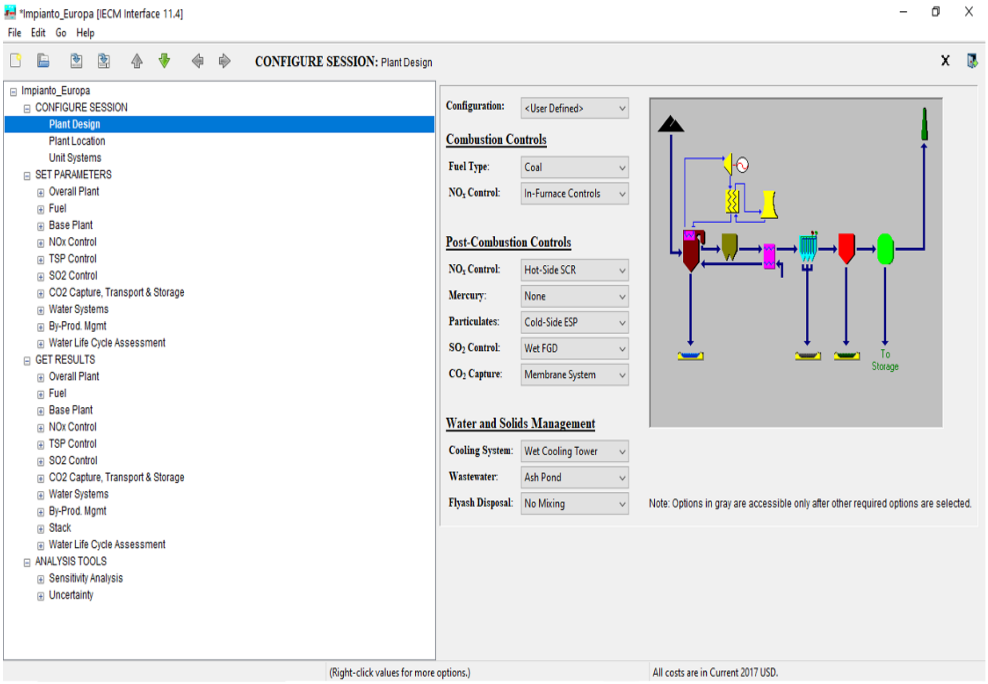

Configuration: <User Defined>

Combustion Controls

Fuel Type: Coal

NO_x Control: In-Furnace Controls

Post-Combustion Controls

NO_x Control: Hot-Side SCR

Mercury: None

Particulates: Cold-Side ESP

SO_2 Control: Wet FGD

CO_2 Capture: Membrane System

Water and Solids Management

Cooling System: Wet Cooling Tower

Wastewater: Ash Pond

Flyash Disposal: No Mixing

Note: Options in gray are accessible only after other required options are selected.

(Right-click values for more options.)

All costs are in Current 2017 USD.

Figure 3.1: The interface of IECM Software. In the left window (white), there are different voices of the plant. In the right window (grey), inputs of the specific section it showed, with the possibility of parameter modification [49]

3.2 Reference plant

The base plant needs to be defined in the first steps of the simulations. The pulverized coal plant chose for the current work is represented in figure 3.2. It is a typical new plant set by NETL, evaluated based on research and plants available in the USA. The plant has the conventional side for electricity production, with a furnace, turbine, and boiler. In the furnace, the first NOx control is added, in specific, a Low NOx burner is used. When flue gases exit from the furnace, they go to the hot side Selective Catalytic Reduction (SCR) to reduce nitrogen oxides. After, Electrostatic Filters (EP) to reduce particulate, and Wet Flue-Gas Desulphurization to reduce SOx are added. The last innovative control system is a section for the CO2 capture based on membrane separation. Moreover, it is noticeable a cooling tower for the cooling of flue gases before the release in the atmosphere.

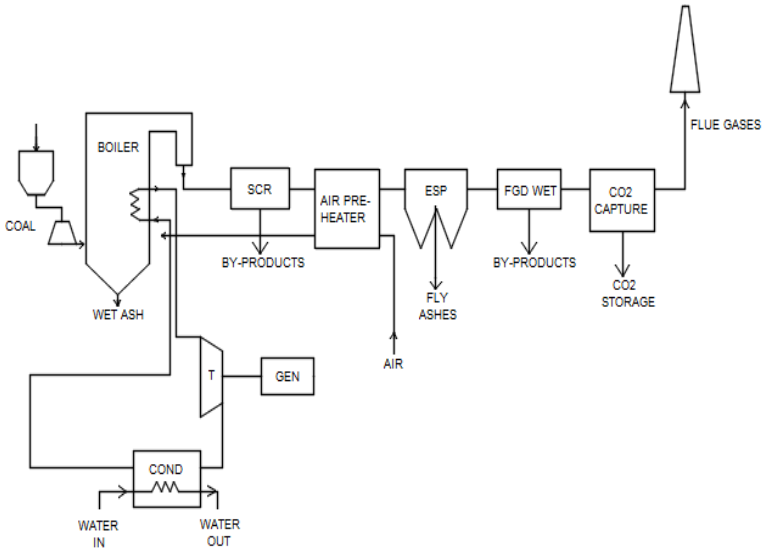

Figure 3.2: Scheme of reference plant used in the simulations

IECM gives the possibility to set the region of the plant, based on USA district or other. The state, when we select the plant in Texas, in US South Central State. The plant evaluated in the simulation is nearly similar to the real plant of Texas state. An example of a Texas plant, is the Fayette Power Plant, with three units for gross energy of 1760 MW. Units 1 and 2 are co-owned by the Lower Colorado River Authority (LCRA) and Austin Energy (AE). Focus on unit 1, it is a 600 MW sub-critical unit, with sub-bituminous coal from Wyoming as a fuel [50]. The Fayette Power Plant, using the data of the Energy Information Administration (EIA), released, last year, in the atmosphere near 9,800,000 tonnes of carbon dioxide [51]. For the simulation, based on data of the Fayette Power Plant, the gross electrical output of the 600 MW plant is simulated. The capacity factor

(CF) used is an average value, set by IECM and it is given by the analysis of NETL for the real power plants. CF is set to 75%. The Unit type is sub-critical. Other inputs required by the software are the temperature of the gas exiting economizer and the temperature of gas exit from air pre-heater. These parameters are set based on the average value of the NETL guide. The boiler firing type is tangential and the efficiency is evaluated automatically by the software. Boiler efficiency is based on the algorithm in "Steam: Its Generation and Use", by Babcock and Wilcox (8) and "Combustion, Fossil Power Systems", by Combustion Engineering, Inc. The boiler efficiency is the energy absorbed by the steam cycle divided by the energy in the fuel [52]. Table 3.1 shows the mainly important parameters of the base plant for the simulation.

Table 3.1: Parameters for the base plant

Gross Electrical Output (MWg)	600
Capacity Factor (%)	75
Unit Type	Sub-critical
Steam Cycle Heat Rate (kJ/kWh)	8219
Boiler Firing Type	Tangential
Boiler Efficiency(%)	89.41
Gas Temperature Exiting Economizer (°C)	371.1
Gas Temperature Exiting Air Preheater (°C)	148.9

3.2.1 Economic Parameters

Several economic and regulation parameters need to be fixed for the simulation. The emission constraints are set automatically by the software. The sulfur dioxide emission constraint is defined by the 1979 revised New Source Performance Standards (NSPS) and it is evaluated as the potential emission of the coal, minus the amount of sulfur retained in the ash streams. Nitrogen oxide emission constraints combined the emissions of NO2 and NO3, with NSPS values. The limit depends on the fuel type. Particulate emission constraint is defined by the NSPS standards of 1978 [49]. The values for the current simulations are reported in Table 3.2

The economic analysis is referred to the 2017 year dollar cost. Other economic parameters to be set are the discount rate (before taxes), which is equal to the sum of return of debt plus return on equity and fixed charge factor (FCF), the revenue required to finance the power based on the capital expenditures. The percent of equity and debt is automatically set by the

IECM. The inflation rate, taxes, process contingency cost, pre-production cost, and O&M parameters for the base plant are reported by NETL guide. For a description of the numbers and models used, it is recommended the references for the User Manual of IECM and Pulverized Coal Model Costs for IECM software [52].The plant life time is selected to 30 years, with five years for the construction. The last important value is the internal cost of electricity for component allocations [49]. In the software, three options are available: base plant (assumed to be a coal plant combustion boiler, air preheater, and disposal site), user-specified, or total plant Cost Of Electricity (COE). Table 3.3 shows the economic assumptions for the base plant.

Table 3.2: Emission Constraints

Sulfur Dioxide Emission Constraint (mg/kJ)	0.258
Nitrogen Oxide (Equiv. NO2) Emission Constraint (%)	0.06449
Particulate Emission Constraint (mg/kJ)	0.0129

3.3 Fuel

IECM gives the possibility to choose the coal from a database by NETL, with several coal types extracted in the USA. As described previously, the base plant analyzed uses sub-bituminous coal extracted in Wyoming. From the database, Wyoming Powder River Basin coal composition is imported. The coal shows a good amount of carbon and low content of sulfur. The main problem is the high percentage of moisture, up to 30%. in weight. Also, the IECM gives the composition of the ashes. For the Wyoming coal, the main components of the ashes are the SiO2 and Al2O3 that have together the 93% wt. The auxiliary gas composition is composed mainly of methane and ethane, with a heating value of 52.29 MJ/kg. Table 3.4 shows the composition of Wyoming Powder River Basin coal.

Table 3.3: Economic Assumption for base plant

Discount Rate (Before Taxes) (fraction)	0.103
Fixed Charge Factor (FCF) (fraction)	0.1473
Inflation Rate (%/yr)	3
Plant or Project Book Life (years)	30
Percent Debt (%)	45
Percent Equity (Preferred Stock) (%)	10
Percent Equity (Common Stock) (%)	45
Internal Electricity Price ($/MWh)	56.23
Construction Time (years)	5
Land Use Cost ($/acre)	3000
Fixed Operating Cost (months)	1
Variable Operating Cost (months)	1
Miscellaneous Capital Cost (% TPI)	2
Inventory Capital (% TPC)	0.06
Operating Labor Rate ($/hr)	34.65
Number of Operating Jobs	20
Number of Operating Shifts (shifts/day)	4.75
Total Maintenance Cost (% TPC)	1.866
Maintenance Cost Allocated to Labor (% TMC)	35
Administrative & Support Cost (% total labor)	7

Table 3.4: Sub-bituminous Wyoming Powder River Basin Coal (wt %)

Carbon (wt %)	48.18
Hydrogen (wt %)	3.31
Oxygen (wt %)	11.87
Chlorine (wt %)	0.01
Sulfur (wt %)	0.37
Nitrogen (wt %)	0.7
Ash (wt %)	5.32
Moisture (wt %)	30.24
Higher Heating Value (MJ/kg)	19.40

3.3.1 Economic Parameters

There are few economic inputs to be introduced in the software. Concerning coal, the total delivered cost (as-fired) is the total cost delivered, assumed to contain any cost of cleaning and transportation. It is a default value extracted from the database, based on the coal type used. Moreover, the auxiliary gas cost is related to the cost of the natural gas and it is edited by NETL [49]. In Table 3.5 are reported the costs.

Table 3.5: Fuel costs

Total Delivered Cost (as-fired) ($/tonne)	9.645
Auxiliary Gas Cost ($/mscm)	260.2

3.4 Post-Combustion Controls

3.4.1 NOx Control

There are two steps for the control of NOx. The first reduction of NOx is in the furnace, with the use of a Low NOx Burner (LNB) with Overfire Air Technology (OFA). Their special design leads to the production of air during the process and reduces the formation of NOx in the fuel or reduces the temperature, to decrease the formation of thermal NOx. OFA systems divert a portion of the combustion air away from the primary combustion zone. The only input required for the LNB & OFA is the removal efficiency of NOx, the value is based on the last data available in the literature [53]. The second reduction of NOx is related to post-combustion, with the use of a Hot-Side Selective Catalytic Reduction (SCR). SCR has been developed to reduce the NOx gases to pure nitrogen. In the process, ammonia (NH3) vapors reduce the NOx gases into environmentally friendly N2 and H2O on a catalyst site. In the software, inputs as actual NOx removal efficiency, steam to Ammonia Ratio, and catalyst activity are required. The data used are referred to the literature [54]. The data chosen for the simulations are represented in table 3.6.

3.4.2 Particulate Control

In the plant, it is also included, a Cold-Side Electrostatic Precipitator (ESP). ESP has great particulate removal and covers a temperature range from ambient to 850 °C. The pressure losses are typically less than 1 bar and the electrical power consumption is acceptable. Today, ESP is widely used in industrial applications and power plants. Efficiency and collector plate spacing is required by the software, value can be visualized in table 3.6 and are taken from literature [55].

3.4.3 SOx Control

The last common system for pollutants control is referred to as SOx. One common system is the Wet Flue-Gas desulfurization (FGD). Wet FGD is based on the contact of flue gas containing sulfur compounds and a reagent slurry, with a high-efficiency removal near 90%. The reagent chosen in this simulation is limestone, and removal efficiency of SO2, particulate and chlorine, are required by the software [56]. Parameters are shown in table 3.6.

Table 3.6: Pollutants Treatment Control Systems Inputs

NOx control - LNB & OFA	
Actual NOx Removal Efficiency (%)	32
NOx control - Hot-Side SCR	
Actual NOx Removal Efficiency (%)	61
Steam to Ammonia Ratio (mol H2O/mol NH3)	20
Particulate control - ESP	
Particulate Removal Efficiency (%)	99
Actual SO2 Removal Efficiency (%)	25
Collector Plate Spacing (centimeters)	30,5
SOx control - Wet FGD	
Maximum SO2 Removal Efficiency (%)	98
Scrubber SO2 Removal Efficiency (%)	69
Scrubber SO3 Removal Efficiency (%)	50
Particulate Removal Efficiency (%)	50
Chlorine Removal Efficiency (%)	90

3.4.4 Economic Parameters

For the control systems, economic parameters are directly evaluated by the software. For the LNB & OFA NOx reduction, base capital costs, including retrofit are automatically evaluated by the software. It is the base capital cost with the retrofit cost factor. The fixed O&M cost is related as a percentage of the total capital cost and it is equal to 1.5. For the hot-side SCR, more inputs need to be required. Process contingency cost is referred to global plant. IECM, with the data of NETL, provides also the cost for the catalyst and ammonia. ESP costs are mainly related to the water and waste disposal cost, evaluated directly by the IECM. Limestone and Lime Cost are also introduced as input for the SOx removal. All the economic parameters for the pollutants controls are showed in table 3.7 For a deeper analysis of models and cost used by IECM and NETL, is suggested the reading of Pulverized Coal-Fired Power Plants and Air Pollution Controls, published by IECM during the 2019 [52].

Table 3.7: Economics input for Air Pollution Controls

NOx control - LNB & OFA	
Combustion Modifications ($/kw-gross)	14.25
Combustion Modifications O&M (%TPC)	1.5
NOx control - Hot-Side SCR	
General Facilities Capital (%PFC)	10
Engineering & Home Office Fees (E) (%PFC)	10
Catalyst Cost ($/cu m)	6003
Ammonia Cost ($/tonne)	149.9
Particulate control - ESP	
General Facilities Capital (%PFC)	1
Engineering & Home Office Fees (E) (%PFC)	5
Water Cost ($/kliter)	0.2983
Waste Disposal Cost ($/tonne)	18.79
SOx control - Wet FGD	
General Facilities Capital (%PFC)	10
Engineering & Home Office Fees (E) (%PFC)	10
Limestone Cost ($/tonne)	25.39
Lime Cost ($/tonne)	110.3
Waste Disposal Cost ($/tonne)	14.47

3.5 CO2 Capture, Transport and Storage

The main purpose of the thesis is the assessment of a coal plant with the introduction of a CO2 capture section. The CO2 section is needed to achieve the goal of the Paris Agreement, for the reduction of carbon dioxide emission. The principal argument of the current work is the explanation and analysis of a membrane for CO2 capture. IECM has a different configuration for the CO2 section. In this work, the performance of membranes is studied for two configurations: 2-Step with Air Sweep and 2-Stage Cascade.

3.5.1 2-Step with Air Sweep

In this configuration, two membrane modules are used in the system, in which boiler combustion air is used as a sweep gas for one membrane module. The first is a cross-flow membrane module, the permeate stream from this membrane is sent to a cryogenic purification unit for further purification and compression, ready for transport and storage. The second membrane module is a counter-flow membrane with a boiler combustion air as a membrane sweep gas to recover the permeated CO2. The permeate stream from the counter-flow membrane module is recycled back to the boiler, which in turn increases the CO2 concentration in the flue gas stream entering the capture system[57]. A vacuum pump is used before the rich CO2 stream enters the section for purification and compression. In figure 3.3 the scheme of the 2-step with air sweep configuration is shown. Inputs required are the CO2 Purification configuration, set to 95%, due to environmental global goals and the CO2 removed in the cross-flow membrane, set as default to 50%. For the current configuration, it is required to introduce the membrane characteristic parameters (e.g., permeance, and CO2/N2 selectivity). The membrane operation temperature is fixed to 50°C. In the next paragraphs are described the membranes chosen for the simulation. Moreover input for vacuum pumps, as efficiency and pressure value, is taken from the NETL reference value [57]. Moving for the simulation, in the section of purification, the rate of CO2 recovery needs to be set. This value, according to global rules, is set to 95%. The CO2 product pressure is set to 13 MPa, and the compressor efficiency is 80 %, by default value [49].

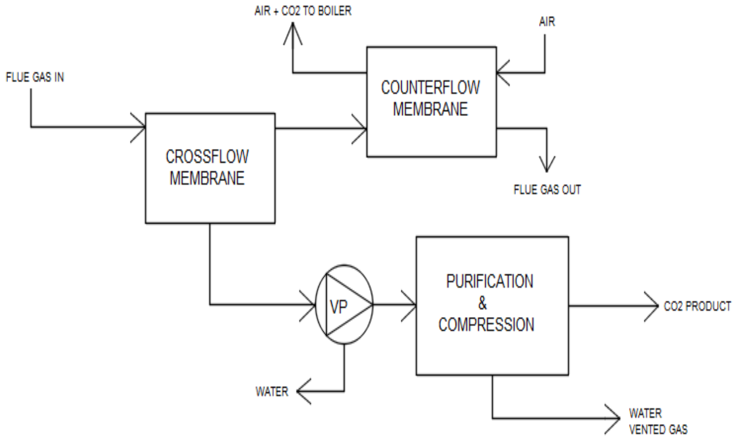

Figure 3.3: 2-Step with Air Sweep Configuration. In the crossflow membrane the permeate exit and, after the purification and compression, is ready for transportation. The counterflow membrane is used for the recovery of CO2, using combustion air as sweep gas [49].

3.5.2 2-Stage Cascade

The second configuration used a simpler two-stage system for carbon dioxide capture. Flue gases enter the first stage when there are two outputs. The permeate goes to the vacuum pump and compressor before it moves to the second stage. The retentate goes to an expander before releasing it into the atmosphere. In the second stage, the exit retentate is recirculated to the first stage. Stream with rich-CO2 is sent to a compressor, ready for transport and storage as shown in figure 3.4. Similar to the previous case, parameters need to be set. In the current configuration, the maximum efficiency possible for the absorber on an annual average basis is the input. This value is used as a limit in calculating the actual CO2 removal efficiency for compliance. The value is set to 90%. Same as air sweep gas configuration, compressor, vacuum pump, and expander efficiency are set. Also, it is requested the permeate-side pressure. This value is set to 0.2 bar as an IECM default. In the end, as the previous case, CO2 product pressure, and purity are set. Table 3.8 shows different inputs for the two configurations.

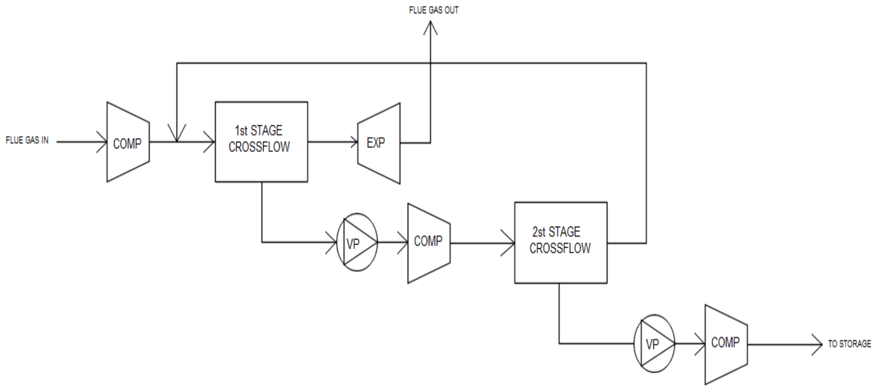

Figure 3.4: 2-Stage Cascade Configuration with crossflow membranes. In the first stage, retentate exit and going to the atmosphere with an expansion, permeate is sent to the second stage, in which the retentate is recycled back to the first stage and permeate is ready for transport and storage [49].

Table 3.8: CO2 Capture section input

	2-Step/Sweep	**2-Stage/Cas**
CO2 Removed in Membrane (%)	90.91	N/A
Membrane Temperature (°C)	50	50
Pressure Drop @ Crossflow (bar)	0.1	N/A
Vacuum Pressure Cross-Flow(bar)	0.2	N/A
Efficiency of turbomachines (%)	85	85
CO2 Recovery Rate (%)	95	N/A
CO2 Product Purity (%)	95	95
CO2 Product Pressure (MPa)	13	13
CO2 Removal Efficiency (%)	N/A	90
Permeate-side Pressure (bar)	N/A	0.2

3.5.3 Membranes

For the analysis of the system, different membranes taken from the literature are compared, to find the optimum membrane from the technical and economic point of view. For a more realistic comparison, it is useful to start with a commercial membrane. Membrane Pebax-1657 is a series available in the market. The membrane is a resin, based on poly(ether block amide), it offers excellent properties for CO2 separating membranes. It is a thermoplastic elastomer combining linear chains of the hard polyamide (PA) segment for mechanical strength, and flexible polyether (PE) that offers good permeability, due to chain mobility. In the market, there are several Pebax, characterized by different grades of composition. Pebax-MH 1657 is composed of 40% aliphatic polyamide and 60% of poly(ethylene glycol). Figure 3.5 shows the chemical structure of the membrane[58]. The most recent data highlight a permeability of 56 barrer and a selectivity CO2/N2 of 40 at 35 °C [59].

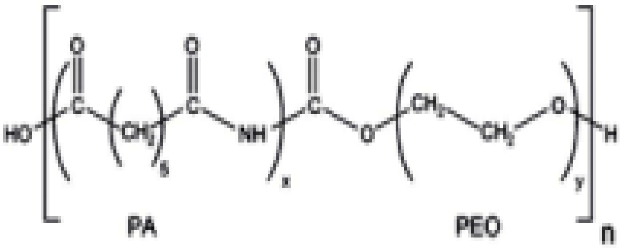

Figure 3.5: Pebax-MH 1657 chemical monomer structure, composed by two chains of PA and PEO [58]

Ke Duan et al. synthesize the COF-5 nanosheet and dispersed the filler in Pebax-MH 1657 matrix. COF-5 is a rigid structural material with a fixed pore size and high porosity and it is obtained with a sonochemical method. As the MMMs described previously, Pebax-MH 1657/COF-5 is prepared with a solution-casting method. The difference between the pristine Pebax membrane and the new membrane is shown in figure 3.6. Also for this MMM, several configurations are proposed. The best is obtained with the 0,4% in wt. of COF-5 disperse. Permeability of 493 barrer and selectivity CO2/N2 of 49,3 are measured at 30°C [60].

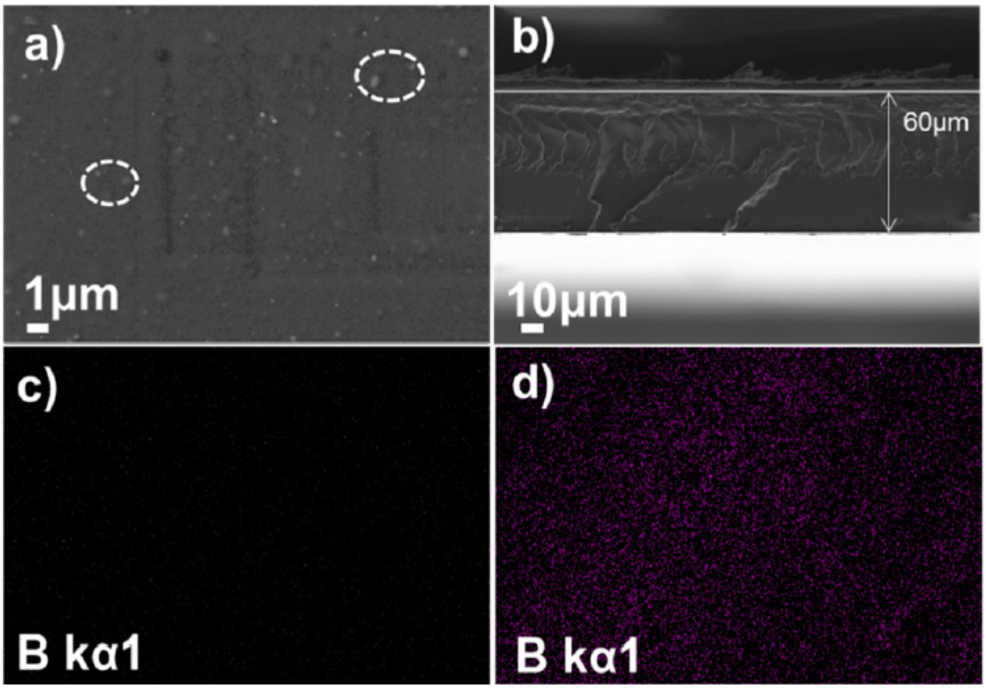

Figure 3.6: Pebax-MH 1657/COF-5 Microscopic visualizer.(a) surface; (b) cross-section; (c) pristine Pebax membrane; (d) COF-5 Pebax membrane (0.4 wt%). [60]

To increase the selectivity of a commercial Pebax membrane, Shin et al. tested a new MMM composed of a blend of Pebax and PEG. Oligomers PEG-MEA was added to improve the permeability of the membrane. The effect of PEG-MEA additives is the rise of fractional free volume. The membrane is easily obtained with a blending process, with the 50% wt. of PEG-MEA [61]. To simulated IECM, the characterization of membranes is required. Comparing the performance of the three membranes described is one of the aims of this paper. One of the inputs of the software is the permeance, measured in GPU. Permeance is easily obtained by dividing the permeability by the thickness of the membrane. To respect the bounds of the software, permeance needs to stay in the range of 1000-4000 GPU. For the pristine Pebax, the thickness is smaller than the other two membranes, due to lower performance and due to the need to obtain a more sophisticated module. Other inputs required by the software are the CO2/N2 selectivity and operation temperature, which is fixed to 50 °C. Table 3.9 shows the characterization of the membrane used for this work.

Table 3.9: Membranes Characterization at 50 °C

	Pebax	**Pebax/COF-5**	**Pebax/PEGMEA**
Thickness (μm)	0.08	0.15	0.15
Permeance (GPU)	1037.5	3287	3820
Sel. CO2/N2	43.3	49.3	43.3

Table 3.10: CO2 Storage Characteristic

State	Texas
Reservoir Depth (meters)	1372
Reservoir Thickness (meters)	152.4
Reservoir Horizontal Permeability (mD)	100
Reservoir Porosity (%)	27.5
Storage Coefficient (%)	5.58
Reservoir Surface Temperature (°C)	49.28

3.5.4 Transport and Storage

IECM provide the estimation of a carbon dioxide transport and storage. The transport method is through pipelines. Region and total pipeline length needs to be set, at the same way of the minimum outlet pressure, that is the pressure of the storage site. Due to location of base plant, the pipeline region is the central region, with a length of 100 km and an outlet pressure of 10.3 MPa.

For the storage setup, the options are geological or Enhanced Oil Recovery (EOR). IECM, thanks to NETL, has a database of a series of storage, characterized by typical parameters as depth, thickness, porosity and others. The reservoir used for the simulation is displaced in Texas. In table 3.10 is showed the characteristic of it. The performance of the storage is based on Law & Bachu model, see the references for a background on the model [49].

3.5.5 Economic Parameters

The Economics analysis of carbon capture systems is one of the most critical points today. It is difficult to find the costs of technology at the lab-stage. IECM economic is based on EPRI standards, which are the most accurate for the CO2 capture section.

Capital cost estimation starts with the estimation of a membrane module and frame. Actually, the cost of a commercial module is the big problem of technology. The cost of a commercial membrane is between 500-700 \$/m2, due to fabrication and materials. In literature, estimations give the ideal cost for commercial penetration on the technology to 50 \$/m2 [62]. Other works, consider a cost in the range of 80-200 \$/m2[63] [64]. For the current simulation, a default value of 80 \$/m2 is used for the membrane module [65]. The frame cost is dependent on the area and the referred frame cost, equal to 0.238 M\$. The installation cost of the compressor, vacuum pump, and other components is based on literature. In the following tables, the details about the capital cost and O%M cost are described [66].

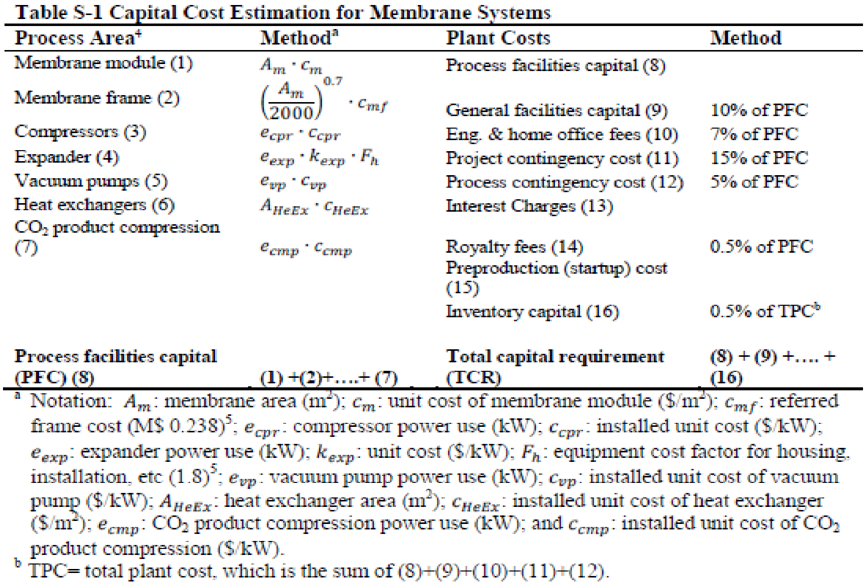

Table S-1 Capital Cost Estimation for Membrane Systems

Process Area[+]	**Method**[a]	**Plant Costs**	**Method**
Membrane module (1)	$A_m \cdot c_m$	Process facilities capital (8)	
Membrane frame (2)	$\left(\frac{A_m}{2000}\right)^{0.7} \cdot c_{mf}$	General facilities capital (9)	10% of PFC
Compressors (3)	$e_{cpr} \cdot c_{cpr}$	Eng. & home office fees (10)	7% of PFC
Expander (4)	$e_{exp} \cdot k_{exp} \cdot F_h$	Project contingency cost (11)	15% of PFC
Vacuum pumps (5)	$e_{vp} \cdot c_{vp}$	Process contingency cost (12)	5% of PFC
Heat exchangers (6)	$A_{HeEx} \cdot c_{HeEx}$	Interest Charges (13)	
CO_2 product compression (7)	$e_{cmp} \cdot c_{cmp}$	Royalty fees (14)	0.5% of PFC
		Preproduction (startup) cost (15)	
		Inventory capital (16)	0.5% of TPC[b]
Process facilities capital (PFC) (8)	**(1) +(2)+….+ (7)**	**Total capital requirement (TCR)**	**(8) + (9) +…. + (16)**

[a] Notation: A_m: membrane area (m^2); c_m: unit cost of membrane module (\$/m^2); c_{mf}: referred frame cost (M\$ 0.238)^5; e_{cpr}: compressor power use (kW); c_{cpr}: installed unit cost (\$/kW); e_{exp}: expander power use (kW); k_{exp}: unit cost (\$/kW); F_h: equipment cost factor for housing, installation, etc (1.8)^5; e_{vp}: vacuum pump power use (kW); c_{vp}: installed unit cost of vacuum pump (\$/kW); A_{HeEx}: heat exchanger area (m^2); c_{HeEx}: installed unit cost of heat exchanger (\$/m^2); e_{cmp}: CO_2 product compression power use (kW); and c_{cmp}: installed unit cost of CO_2 product compression (\$/kW).

[b] TPC= total plant cost, which is the sum of (8)+(9)+(10)+(11)+(12).

Figure 3.7: Capital Cost of Membrane System [66][57]

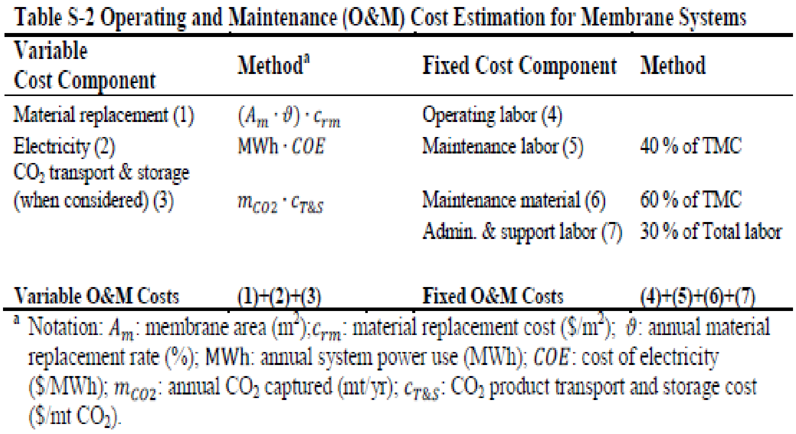

Table S-2 Operating and Maintenance (O&M) Cost Estimation for Membrane Systems

Variable Cost Component	Method[a]	Fixed Cost Component	Method
Material replacement (1)	$(A_m \cdot \vartheta) \cdot c_{rm}$	Operating labor (4)	
Electricity (2)	MWh · COE	Maintenance labor (5)	40 % of TMC
CO_2 transport & storage (when considered) (3)	$m_{CO2} \cdot c_{T\&S}$	Maintenance material (6)	60 % of TMC
		Admin. & support labor (7)	30 % of Total labor
Variable O&M Costs	**(1)+(2)+(3)**	**Fixed O&M Costs**	**(4)+(5)+(6)+(7)**

[a] Notation: A_m: membrane area (m^2); c_{rm}: material replacement cost (\$/m^2); ϑ: annual material replacement rate (%); MWh: annual system power use (MWh); COE: cost of electricity (\$/MWh); m_{CO2}: annual CO_2 captured (mt/yr); $c_{T\&S}$: CO_2 product transport and storage cost (\$/mt CO_2).

Figure 3.8: O & M Cost of Membrane System [66][57]

Table 3.11: Characteristic Cost of CO2 section components [66]

Membrane Module Cost ($/sq m)	80
Membrane Frame Cost (M$)	0.238
Gas compressor installed cost ($/hp)	500
Gas vacuum pump installed cost ($/hp)	1000
Gas expander unit cost ($/kW)	500
Heat exchanger capital cost ($/m2)	300
CO2 product compression installed cost ($/kW)	900
Membrane Material Replacement Cost ($/sq m)	15
Membrane Material Life Time (years)	5

For transport, the capital cost display does not require inputs. For the operational cost, the booster pump operating cost as a percentage of the process facilities capital needs to be defined. Also, the cost for maintenance materials and labor costs are required. Storage requires the operation duration and the management values for the maintenance. All these parameters are showed in the next table [57].

Table 3.12: Transport and Storage Economics

Transport	
Booster Pump Operating Cost (%PFC)	1.5
Fixed O&M Cost ($/km-yr)	3100
Storage	
Operation Duration (years)	30
Contingency Factor (%)	20
PISC and Site Closure Duration (years)	50

3.6 Water systems and by-products management

IECM has the option to include the type of water systems and the management of by-products. In the current plant, a wet cooling tower is installed. The ambient conditions are set by default due to USA meteorological real conditions. Cooling water inlet temperature needs to be specified with the cycles of concentration. This is a measure of the degree to which dissolved solids are being concentrated in the circulating water and it is estimated in terms of the concentration ratio of dissolved solids in the circulating versus makeup water. Moreover, the percent of the quantity of cooling water as drift loss is an input. The cooling water inlet temperature is set to 32 °C and the cycles of concentration are equal to 4.

The by-product management is referred to as the bottom ash, fly ash, flue gases, and wastewater. For all treatments, the simulation does not need inputs.

3.6.1 Economic Parameters

IECM does not need the economic input for the by-products management. The capital cost of the water system is evaluated directly by the software with the input of the base plant. For the operational and management cost, other inputs are required. The cost of the water is set in the previous system for pollutants treatment, the aluminum cost is set to 407.7 $/tonne and the total maintenance cost is equal to 2 percent of the total plant cost (TPC).

4 Results

4.1 Energy Analysis

Simulations with IECM are carried out to understand the effect of different membranes and configurations in the plant. Simulations show that the first issue of the performance, with the inclusion of a CO2 capture section, is the plant efficiency. The introduction of a specific section for carbon dioxide capture naturally increase the energy requirements. The global efficiency for the referent plant is 34.15 %, with a net electrical output of 548.4 MW. The introduction of CO2 section based on 2-Stage Cascade configuration reduces dramatically the efficiency, with a reduction of the 40%. Three membranes are simulated in the plant, and results show that the Pebax/COF-5 has the better efficiency, with 22.48 % in 2-stage cascade configuration. Commercial Pebax and Pebax/PEG-MEA show efficiencies of 21.59 %. It is noticeable that the efficiency is better if the membrane has a good selectivity respect to permeability. The air sweep configuration shows better efficiencies, in comparison with 2-Stage Cascade, due to less components required for the process that means lower energy consumption. Also in this case, the best efficiency is related to Pebax/COF-5, with a value of 28.12 %, greater than six percentage points respect to same membrane in 2-Stage Cascade. In the air sweep configuration, the variation of efficiency is lower. Other membranes show 27.93 % of efficiency, very close to value of Pebax/COF-5. In the figure 4.1 the plant efficiencies are visualized.

The energy requirement for the reference plant is half related to the power plant section. The other half is related mainly to SOx systems and cooling towers, with a lower contribution of ESP and NOx systems. It is noticeable in figure 4.2 the contribution of different sections in the energy requirements.

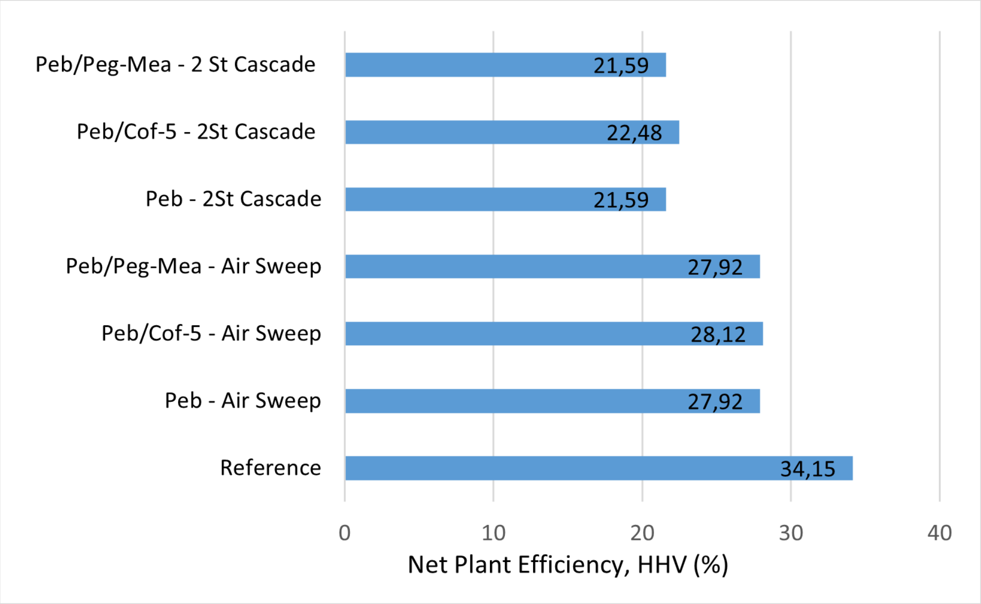

Figure 4.1: Net plant efficiency, HHV (%), for reference plant, commercial Pebax (Peb), Pebax/COF-5 (Peb/Cof-5), Pebax/PEG-MEA (Peb/Peg-Mea) in air sweep and 2-stage cascade configurations.

The net power produced for the reference plant is 548.4 MW, with 51.6 MW of 600 MW used internally. As described previously, the main contribution is the power section, with 26.1 MW. The CO2 capture section is the most energy-intensive system. Plant with air sweep configuration shows a contribution of CO2 capture to total energy requirements equal to 55%, for each membrane. Commercial Pebax and Pebax/PEG-MEA require 84.31 MW for the CO2 section, Pebax/COF-5, due to better selectivity, needs 81.57 MW. Even worse is the other configuration. Energy required for a 2-stage membrane contributes to 75% of the global energy consumption. Also, in this case, the best membrane is the Pebax/COF-5 with a consumption of 177 MW, in comparison with the other two membranes that require 191.3 MW. In conclusion, with the introduction of a section for CO2 capture, the net output decreases by 20% for air sweep and 40% for 2-stage cascade. Graphs in figures 4.3 and 4.4 show the different contributions on the global energy requirement, using Pebax/COF-5 membrane. Details about energy consumption are available in Appendix B. The results show the need to optimize the process to avoid an important cut for net efficiency.

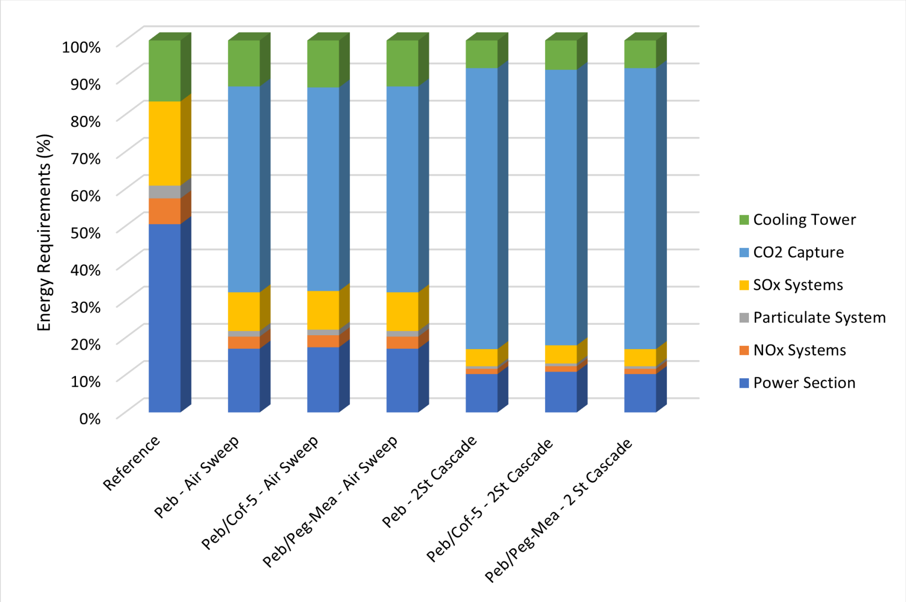

Figure 4.2: Contribution of different plant sections on the global energy requirement of the plant, for the reference plant and new plant with carbon capture, in air sweep and 2-stage cascade configurations with Pebax, Pebax/COF-5, and Pebax/PEG-MEA.

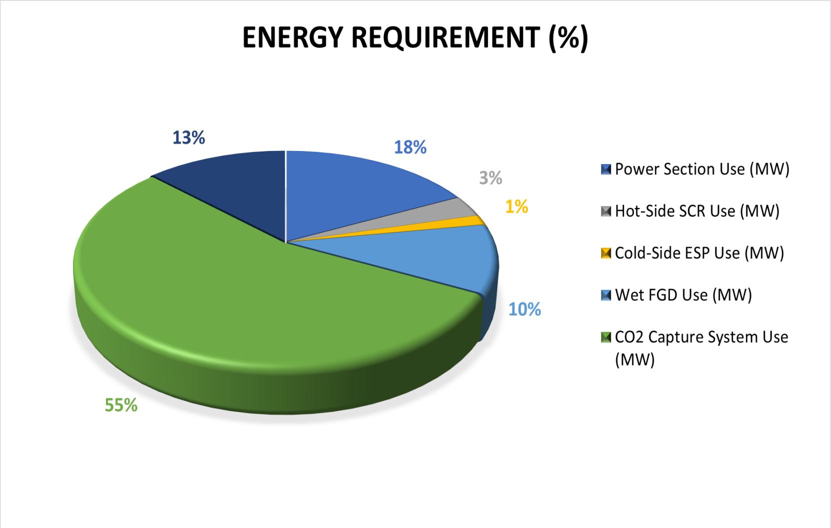

Figure 4.3: Contribution to global consumption in air sweep configuration with Pebax/COF-5 membrane.

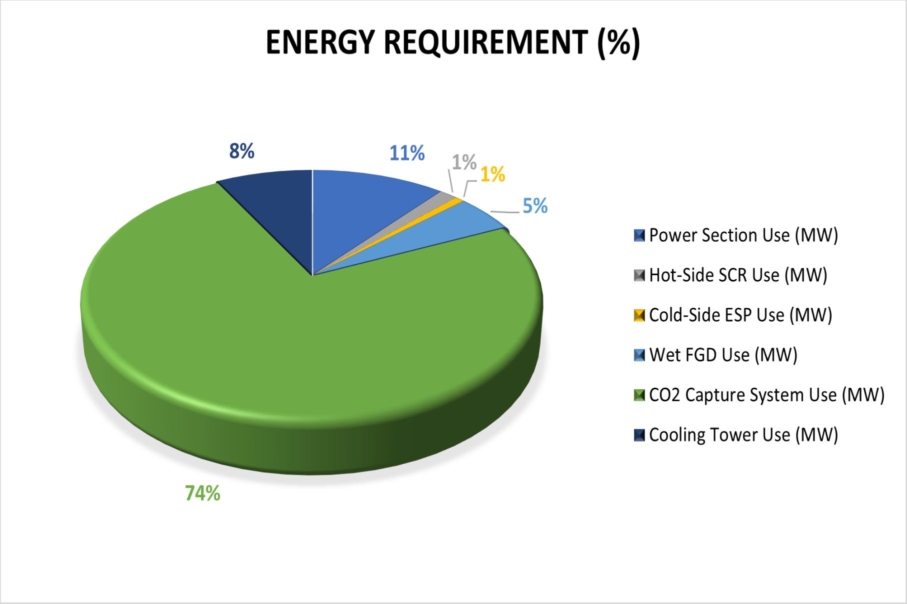

Figure 4.4: Contribution to global consumption in 2-stage cascade configuration with Pebax/COF-5 membrane.

To understand which are the critical points of the carbon capture system, it could be interesting to analyze several parameters . The membrane area is the most important parameter for a based-membrane system. IECM provides an estimation of the membrane area, available in appendix A, based on an empirical model with a polynomial equation, function of permeability and selectivity [57]. As discussed previously, the result areas are high. Despite this issue, it is interesting to evaluate how to change of the area depends on configuration and membranes. Moreover, the result can be extracted and used for comparison with different membrane modules. Table 4.1 shows the area values. The air sweep configuration shows high areas. Commercial Pebax membrane has an area of $4.92 * 10^6 m^2$, due principally to lower permeability. If permeability rise, the flux on the membrane increases and it is easier to reach capture goals with a lower area. For this reason, areas of Pebax/COF-5 and Pebax/PEG-MEA decrease to $1.433 * 10^6 m^2$ and $1.413 * 10^6 m^2$ respectively. The difference between these two membranes is the highest permeability of Pebax/PEG-MEA. In the 2-stage cascade, the area is reduced drastically, due to different system configurations. Commercial Pebax shows an area of $1.501 * 10^6 m^2$, so much lower than air sweep. Another difference is the area of Pebax/PEG-MEA, equal to $4.079 * 10^5 m^2$, so much lower respect to Pebax/COF-5, equal to

$7.086 * 10^5 m^2$. This result is due to different systems.

Table 4.1: Membranes Area of Pebax-1657 membranes ($10^5 m^2$)

Membrane	**Air Sweep**	**2-St Cascade**
Commercial	49.20	15.01
with COF-5	14.33	7.09
with PEG-MEA	14.13	4.08

As described previously, the CO2 capture section has a big impact on the energy requirements for a pulverized coal power plant. The energy required depends on the configuration of the section. Air sweep needs the introduction of a vacuum pump for the correct treatment of the permeate and a compressor for the purification and compression of carbon dioxide before transport and storage. For analyzed membranes, a high fraction of energy is required by the purification and compression stage. Commercial Pebax and Pebax/PEG-MEA, required 55 MW with a CO2/N2 selectivity of 43.3. If the selectivity increases, the energy required is lower due to the high purity of CO2. It is the case of Pebax/COF-5, with consume of 53.18 MW. The vacuum pump requires 35% of energy, with an average value of 29 MW. 2-stage cascade has a more sophisticated configuration. It requires a lot of components to obtain good performance. The big impact is related to the feed compressor and vacuum pumps. Feed compressor is necessary to increase the pressure to improve the capture parameters. The feed pressure is very sensitive to selectivity. The simulations are set to obtain the standard pressure drop of 20 bar between feed and permeate. For Pebax and Pebax/PEG-MEA, it has an incidence of 39% (109.2 MW) on the global CO2 section requirements. Pebax/COF-5 shows a lower requirement that has an incidence of 34% (83.6 MW). The second important contribution is related to the vacuum pump, due to vacuum conditions requirements. The higher consumption is for COF-5 filler membranes, with 87.94 MW in comparison to other membranes with 85.29 MW. Vacuum pumps energy requirements and feeds compressor energy requirement are one of the critical trade-offs for 2.-stage cascade configuration. In terms of energy, an advantage of the 2-stage cascade is the lower energy required by the section of purification and compression. The reason is that with this configuration, the carbon dioxide exit from the second stage has high purity and does not require an intensive process for purification. The only power required is related to the compression for future transport and storage. From air-sweep to 2-stage cascade the consumption of the purification and compression section decrease from 55 MW to 41 MW.

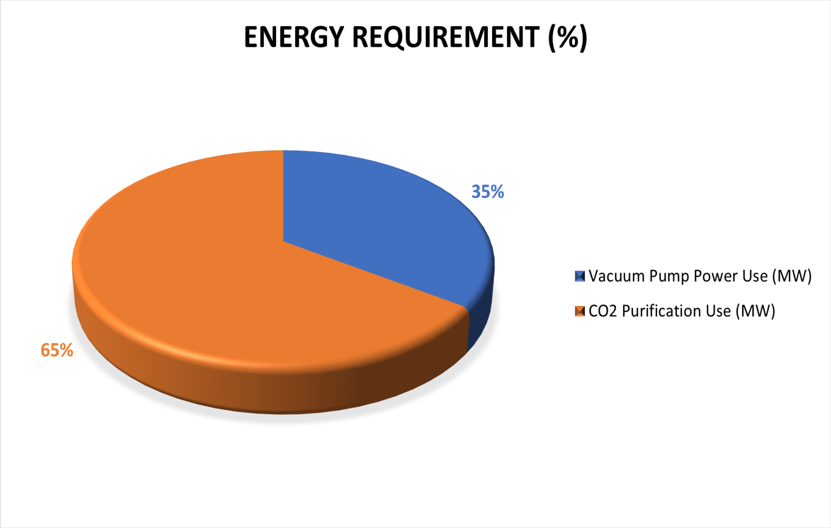

Figure 4.5: Contribution to CO2 section consumption in air sweep configuration with Pebax/COF-5 membrane.

Figure 4.5 and 4.6, table 4.2 show this results for Pebax-COF-5. All data about energy consumption are available in appendix B: (i) commercial Pebax (tables B.1 and B.7), (ii) Pebax/COF-5 (tables B.3 and B.9), (iii) Pebax/PEG-MEA (tables B.5 and B.11).

Table 4.2: Energy requirement for Pebax/COF-5, 2-step Air Sweep and 2-stage Cascade

Energy Requirement (MW)	Air-Sweep	2-St Cascade
CO2 Capture System Use (MW)	81.57	177.00
Vacuum Pump Power Use (MW)	28.38	87.94
CO2 Purification Use (MW)	53.18	41.02
Feed Compressor Use (MW)	//	83.60
Expander Use (MW)	//	35.34

CO2 captured and emitted are important parameters to compare membranes and configurations. IECM software gives as output the CO2 product tonnes in a year, the emission in kg/kWh, and the carbon dioxide captured.

The CO2 product is the quantity of CO2 that is produced by the section of purification and compression and is ready to go for transport and storage.

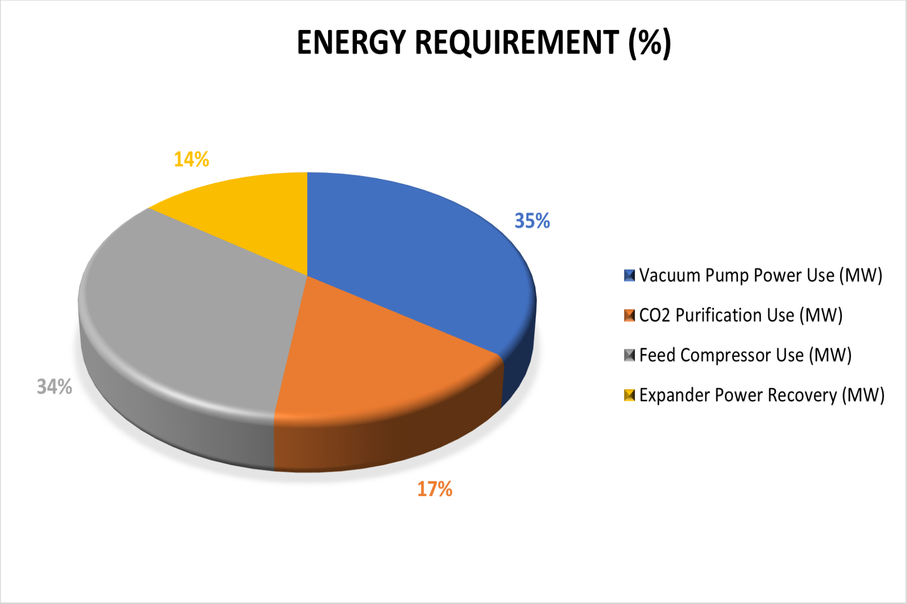

Figure 4.6: Contribution to CO2 section consumption in 2-stage cascade configuration with Pebax/COF-5 membrane.

Air sweep produces fewer tonnes of CO2 in comparison with a 2-stage cascade, with a value of 2.9 Mtonnes/year for each membrane. The 2-stage cascade, with a more complex configuration and high energy penalty, produce plus than 3.1 Mtonnes/year. Reference plant has a big value of emission, equal to 0.960 kg/kWh. The introduction of a carbon capture section decreases this quantity by 80%. The CO2 emitted depends on the configuration and membranes, specifically on the selectivity more than permeability. Commercial and composite PEG/MEA Pebax produce a CO2 emission of 0.191 kg/kWh for the air-sweep and a less value of 0.152 for a 2-stage cascade. Better are the performances of Pebax/COF-5, with a reduction to 0.146 kg/kWh in air-sweep and 0.162 in 2-stage cascade. The complementary parameter is the quantity of CO2 captured. It is related to CO2 emitted. If the carbon dioxide emitted is lower the CO2 captured is higher. Results show that with a 2-stage cascade, more than 1 kg/kWh of carbon dioxide is captured. Interesting is the fact that the quantity of captured CO2 is higher for Pebax/PEG-MEA and commercial Pebax, equal to 1.368 kg/kWh. For air-sweep configuration, the value is good but lower than the 2-stage cascade 0.986 kg/kWh of carbon dioxide is captured for Pebax and Pebax/PEG-MEA, 0.973 kg/kWh for Pebax-COF-5. Figure 4.7 visualize the parameters described.

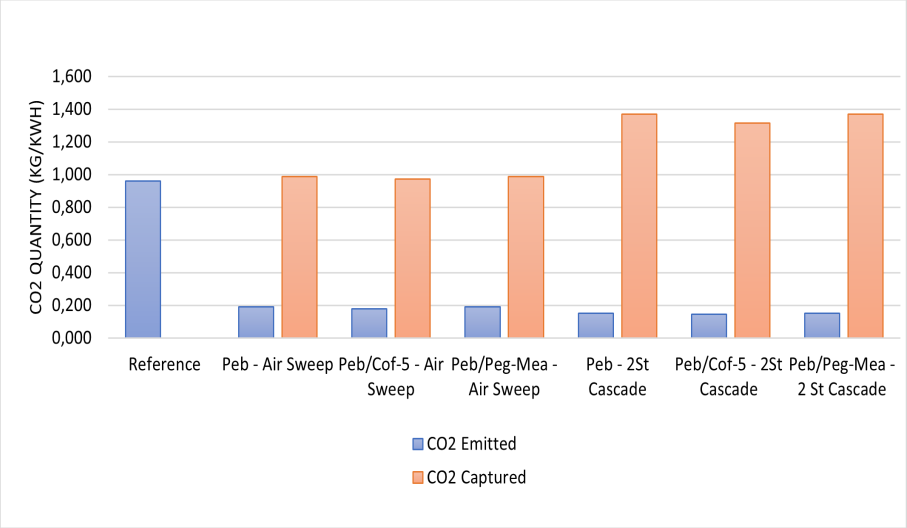

Figure 4.7: CO2 captured and emitted in kg/kWh for the reference plant and new plant with CO2 capture section, for air sweep and 2-stage cascade, and all three membranes analyzed.

4.2 Economic Analysis

The most important economic factors are evaluated with the simulations in IECM. The introduction of a CO2 capture section in a plant should be easy from the construction point of view, due to post-combustion configuration. On the other side, the capital cost is the main obstacle for the market penetration of technology. IECM calculates the total capital cost of the plant. For each section, the capital value in M$ is visualized. Capital cost related to the reference plant are strictly related to the base configuration (power cycle, furnace) and control systems. The overall value is 707 M$ with a Total Capital Requirement (TCR) of 973.8 M$. The introduction of air-sweep configuration causes a surge in capital cost. The cost is related to the performance parameters of the membrane. Commercial Pebax membrane increases the capital cost of 84%, with a total value of 1302 M$ and a contribution of the CO2 section of 560,7 M$.
TCR move from 973.8 M$ to 2344 M$, with an increase of 140%. Novel membranes Pebax/COF-5 and Pebax/PEG-MEA show the lower impact of the CO2 section in total capital cost. Cost is halved to 255 M$ and the total capital cost is equal to 994 M$. 2-stage cascade is different. Firstly, there is no drastic modification changing the membrane.

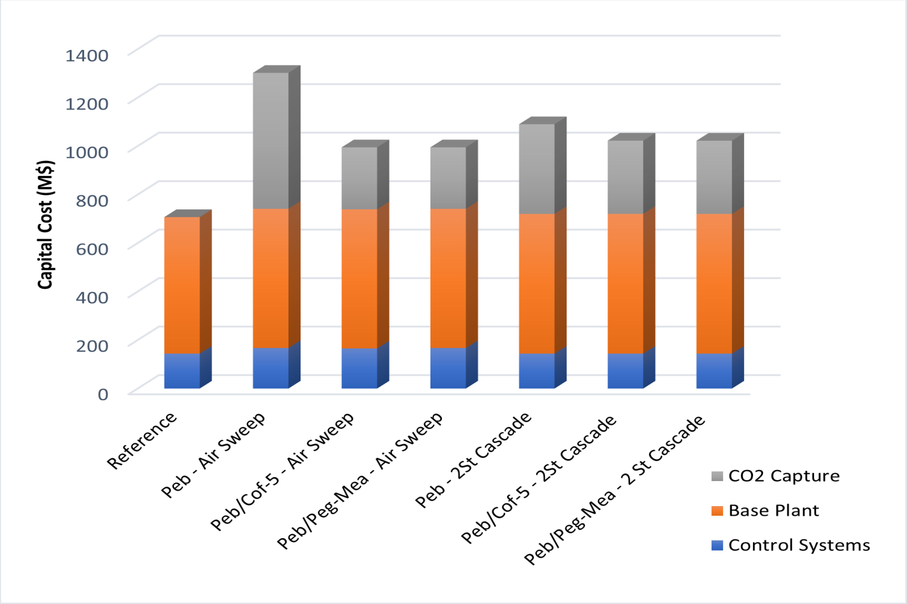

Figure 4.8: Capital Cost for the reference plant and new plant with CO2 capture section, for the two configurations and three membranes

Secondly, the overall capital cost of the membrane has low impact. The Pebax commercial membrane has major benefits with the current configuration. The capital cost of the CO2 section is reduced to 370 M$. Composite membranes that show best results for air-sweep, increase their capital cost with a 2-stage cascade. With Pebax/COF-5, the capital cost of the section is 302.10 M$, with a total cost of 1022 M$, higher than the air-sweep configuration. Same results for the Pebax/PEG-MEA. TCR is near to air sweep, with a not-negligible reduction only for commercial Pebax. Graphical visualization is available in figure 4.8, all voices of capital cost are available in appendix B, under the economics tables.

Operative and maintenance costs are related to the operative point of view of a plant. O&M cost is very important for economic analysis. For the reference plant, the big part of the O&M is related to the base plant. The pollutants control systems have a total O&M cost of 23.65 M$/yr, with a great percentage related to the SO2 control system, with 16.27 M$/yr. The introduction of the carbon capture section increases the maintenance and operating cost, due to the inclusion of new components, membrane replacements, and additional labor costs. In the air sweep configuration, the use of a commercial Pebax membrane causes an additional cost of 115.50 M$/yr, near to four times the global cost of all control systems.

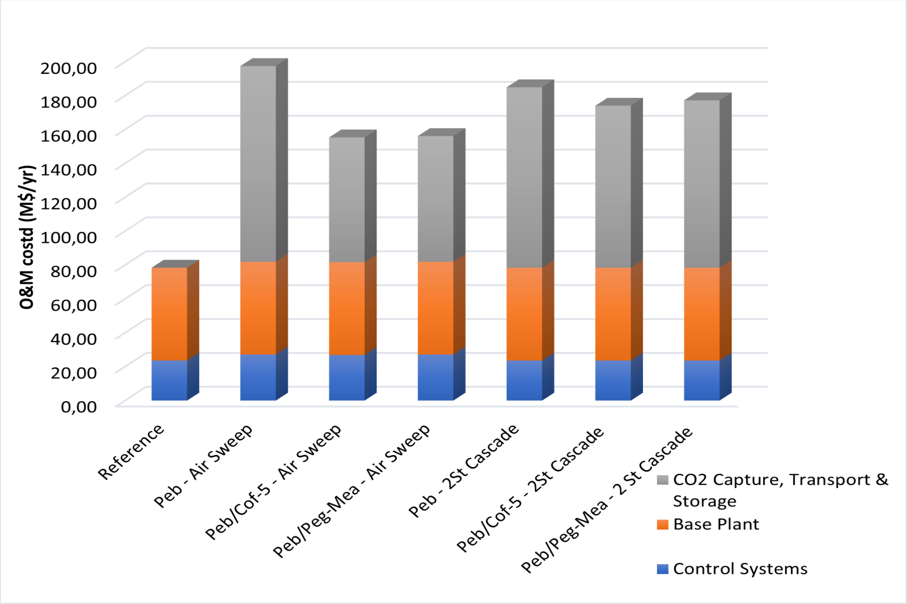

Figure 4.9: Operation and Maintenance for the reference plant and new plant with CO2 capture section, for the two configurations and three membranes

If the permeance of the membrane increases, the O&M costs related to CO2 capture decrease. Pebax/COF-5 shows a value cost of 73.65 M$/yr, Pebax/PEG-MEA causes a O&M costs of 74.18 M$/yr. Configuration modifications do not change a lot the maintenance and operation costs. Commercial Pebax shows the lower cost in comparison with air sweep, equal to 106.50 M$/yr. On the other hand, the other two membranes increase the cost to 95.64 M$/yr (Pebax/COF-5) and 98.80 M$/yr (Pebax/PEG-MEA). In conclusion, the introduction of the CO2 section increases the OPEX costs. Total O&M costs are more or less equal for all configurations and membranes, except for commercial Pebax in air sweep configuration, due to lower permeance. Figure 4.8 shows the visualization and the incidence of O&M costs. All voices of capital cost are available in appendix B, under the economics tables.

Capital cost for carbon dioxide system based on membrane separation is the main cost of a pulverized coal plant. The main issue is the membrane module, due to the high cost of materials, fabrication, and processes for the module construction. The cost of the module is the biggest trade-off for the configuration. The current simulations are carried out with a default cost of 80 $/m2, which is optimistic. Starting with the air sweep configuration, a big membrane area means a high cost of the membrane module. Due to lower performance, the commercial Pebax matrix has the biggest area that means a membrane module capital cost of 385.80 M$. Improving the performance, with a focus on permeance, the area is reduced and the module cost is highly reduced to 113.20 M$ with Pebax/COF-5, and 110.90 M$ with Pebax/PEG-MEA. The membrane frame is another important voice of capital cost. The frame is strictly related to the area, with high capital cost in the case of commercial Pebax, with 10% of incidence. The frame structure cost is half reduced with the Pebax/COF-5 and Pebax/PEG-MEA. The high requirements in terms of CO2 purity, increases the cost of the purification unit. This cost does not depend on the different membrane and has a value of 81 M$. The cost of the vacuum pump is the lowest in this configuration and does not depend on membrane typologies. More complex is the capital cost in a 2-stage cascade configuration, due to many components in the system. As described previously, with a 2-stage cascade, the membrane area is drastically reduced. The result is that the module capital cost decrease of 80% for commercial Pebax (73.60 M$) and Pebax/PEG-MEA (20 M$), and 70% for Pebax/COF-5 (34.74 M$). In the same way, the membrane frame structure cost is very low, with the best value for highly-permeable membrane Pebax/PEG-MEA, with a cost of 9.65 M$). Another positive aspect is the net decrease of the purification and compression section. This is related to lower difficulty to produce high purity CO2 and to the high partial pressure of the gas. The cryogenic separation is not required in the 2-stage cascade. In contrast with a cost of 81 M$ in air sweep, the CO2 separation, and purification unit has a constant capital cost of 36.28 M$. On the other hand, a 2-stage cascade requires the introduction of the two vacuum pumps. Pressure drop required of 20 means that vacuum pumps work at a pressure of 0.1 bar. All these requirements increase the cost drastically, reaching a capital requirement of 112.10 M$ for Pebax and Pebax/PEG-MEA, and 115.60 M$ for the Pebax/COF-5. An important contribution to the capital cost of the 2-stage cascade is related to the feed compressor to increase the pressure before entering the membrane module. This parameter is strictly related to the pressure drop in the membrane and it is related to selectivity. Feed compressor capital requirement is 71.78 M$ for Pebax and Pebax/PEG-MEA. For Pebax/COF-5, due to high selectivity, feed compressor capital cost is 54.93 M$. Moreover, the capital cost increases due to the presence of an expander, with an incidence of 10% and a heat exchanger, with an incidence of 4%. Figures 4.10 and 4.11 show the contribution of components to the capital cost of the CO2 section for Pebax/COF-5. Values for Pebax/COF-5 are reported in table 4.3, for other membranes are available in appendix B.

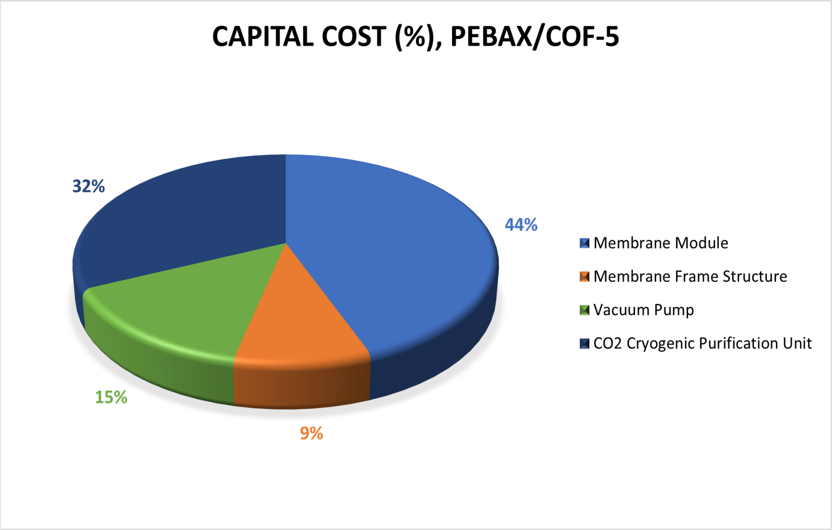

Figure 4.10: Contribution to CO2 section capital cost in air sweep configuration with Pebax/COF-5 membrane.

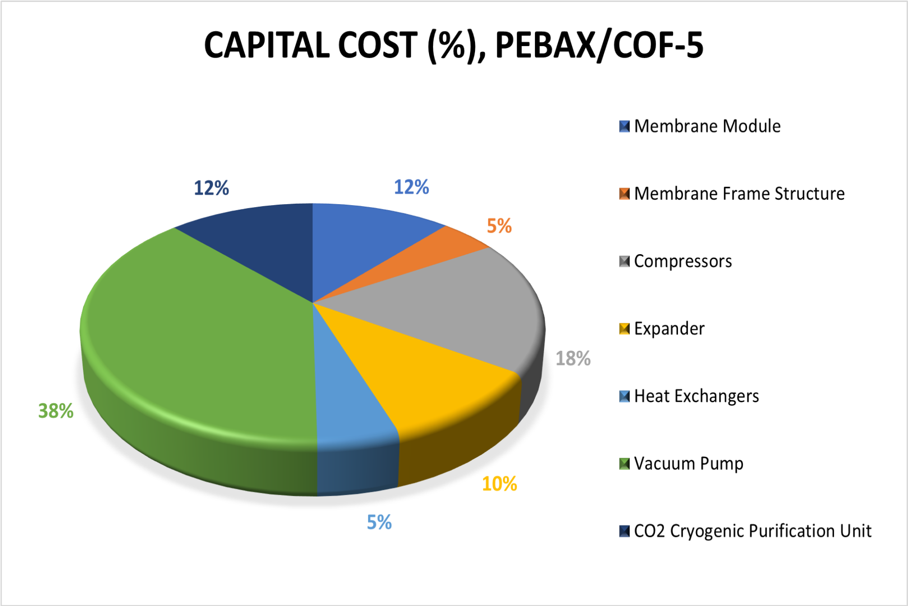

Figure 4.11: Contribution to CO2 section capital cost in 2-stage cascade configuration with Pebax/COF-5 membrane.

Table 4.3: CO2 section capital cost for Pebax/COF-5, in the two configurations

Capital Cost (M$)	Air Sweep	2-St Cascade
Total Capital Cost	255.50	302.10
Membrane Module	113.20	34.74
Membrane Frame Structure	23.38	14.21
Feed Compressor	//	54.93
Expander	//	31.36
Heat Exchanger	//	14.99
Vacuum Pump	38.52	115.60
CO2 Cryogenic Purification Unit	81.15	36.28

Carbon dioxide capture section adds several operation and maintenance costs. During the operation, membrane is object of degradation. The membrane replacement is mandatory for a pulverized coal plant that operates for many years. Membrane is replaced every five years and total cost depends on the area. Pebax has the high cost membrane replacement in air sweep, equal to 19.74 M$/yr. Pebax/COF-5 and Pebax/PEG-MEA shows a lower cost of 5.79 M$/yr. In the 2-stage cascade, due to less area required, membrane replacement cost decreases of 80% for pristine Pebax (4.02 M$/yr), 70% for Pebax/COF-5 (1.90 M$/yr). Pebax/PEG-MEA shows the better cost, with 1.09 M$/yr. Electricity is important for the system and is counted in the O&M cost. 2-stage cascade required high electricity due to many components. The electricity O&M cost depends on the selectivity of the membrane. Pebax/COF-5 required 49.12 M$/yr of electricity, compared with 53.09 M$/yr for other two membranes. Air Sweep electricity requirement is lower influenced by the membrane performance. The value is around 24 M$/yr for each membrane, with best value of Pebax/COF-5 of 23.73 M$/yr. O&M costs include also a percentage related to transport and storage. These cost are independent from the system configuration. CO2 transport includes maintenance and labour operation, with a value of 5.50 M$/yr. CO2 storage has an higher value of 14.50 M$/yr, due to high controls routine requirement. In conclusion, driving force of operation and maintenance cost is the electricity requirements. In general, 2-stage cascade has higher O&M cost, with a best value of Pebax/COF-5 (95.64 M$/yr). Air sweep has overall lower cost requirement, with a 74 M$/yr for Pebax/COF-5 and Pebax/PEG-MEA. The only difference is that commercial Pebax requires high fixed cost, due to lower performance.

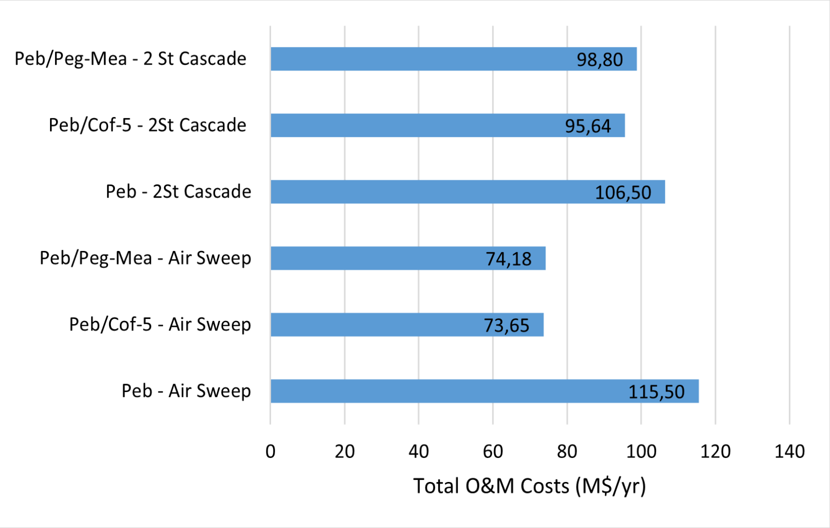

Figure 4.12: Operation and maintenance costs of CO2 capture section, for air-sweep and 2-stage cascade and all membranes

The cost is higher for air sweep (115.50 M$/yr) respect to 2-stage cascade (106.50 M$/yr). Total O&M costs are noticeable in the figure 4.12.

To complete the comparison and the effect of the carbon capture system in a pulverized coal plant, other costs need to be analysed. Reference plant produces a cost of electricity of 58.4 $/MWh. It is evaluated with the simulation of the same plant without the CO2 capture section. As seen previously, the introduction of the carbon capture section inevitably increases consumption and cost. The cost of electricity depends on the configuration and type of membrane. Commercial Pebax adds a cost of 117.60 $/MWh in the air sweep, with a global cost of 176 $/MWh, more than four times the reference cost, including transport and storage. The choice of a better membrane helps to reduce the cost of electricity. Pebax/COF-5 and Pebax/PEG-MEA produce a cost of electricity of 127 $/MWh in air sweep, with an addition of 84.81 $/MWh, including transport and storage. 2-stage cascade is characterized by feed compressor, expander, and heat exchanger. The addition of the components increases the cost of electricity in comparison to air sweep configuration. The better result is obtained with the Pebax/COF-5, with a cost of electricity equal to 154.30 $/MWh, including transport and storage. Pebax/PEG-MEA shows a cost of 160.20 $/MWh, including transport and storage. The cost of electricity without transport and storage is a little bit lower. Pebax/COF-5, for example, shows a value of 120.20 $/MWh in air sweep and 145.70 $/MWh in a 2-stage cascade. In figure 4.13 results are visualized. The cost of CO2 avoided is an important output to compare the different carbon capture technologies. The cost of CO2 avoided depends on the value of the cost of electricity (COE) and emission ratio (ER) for the current case and reference case. Equations and methods used for the calculation are available in appendix A. The introduction of a carbon capture system based on membrane separation in the Fayette power plant is more expensive. The best cost is obtained in air sweep with Pebax/COF-5, with a cost of CO2 avoided of 87.90 $/tonne. The result is near the value of the cost of CO2 avoided for Pebax/PEG-MEA (90.28 $/tonne). Critical is the cost for commercial Pebax due to the worst performance and a big area. In the air sweep, the cost of CO2 avoided is 152.90 $/tonne, with a small decrease in the case of a 2-stage cascade (140 $/tonne). 2-stage cascade shows an increase in the cost of CO2 avoided for the other two membranes. The cost of CO2 captured is the last important economic factor for a complete analysis. The calculation method is reported in appendix A. Great results are obtained with composite Pebax in the case of air sweep, with a cost of around 63 $/tonne. Commercial Pebax is not-convenient, with the highest cost of 112.30 $/tonne. On the other hand, pristine Pebax shows great improvements in the 2-stage cascade, with a reduction of 30% of the cost of CO2 captured, with a value of 76.03 $/tonne. For Pebax/COF-5 and Pebax/PEG-MEA, the cost increases a little bit, with a value of 65.28 $/tonne and 66.87 $/tonne respectively. These results are shown in figure 4.14.

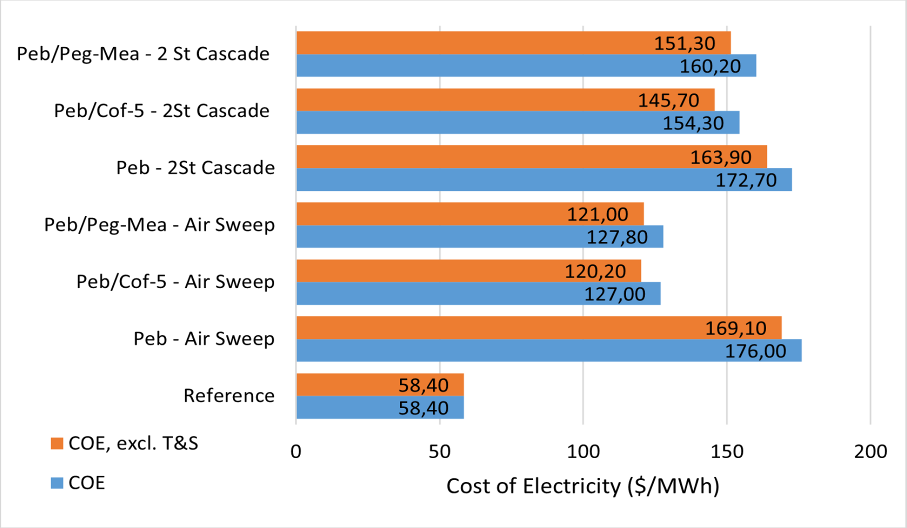

Figure 4.13: Cost of Electricity for the reference plant and plant with CO2 capture section, including or not transport and storage, for all configurations and membranes

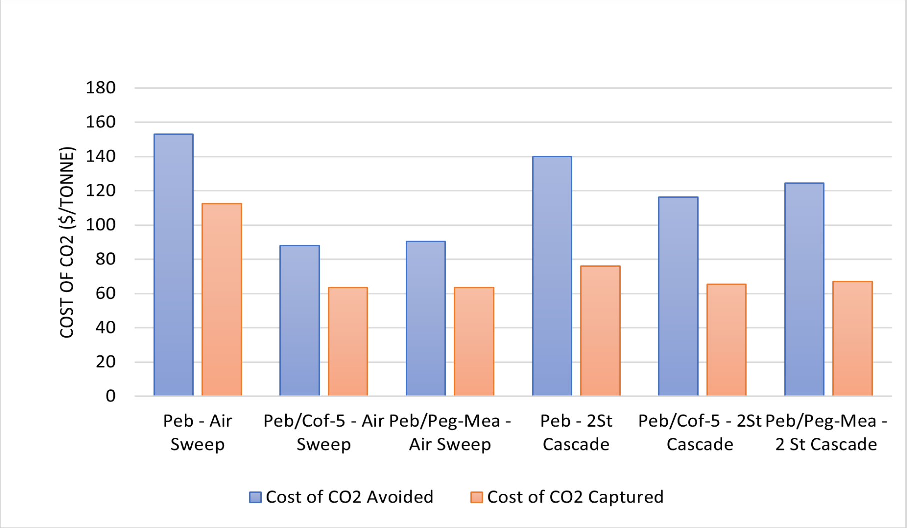

Figure 4.14: Cost of CO2 captured and avoided for air sweep and 2-stage cascade and all membranes

5 Sensitivity Analysis

To understand the effect of the different driving force on the critical parameters of the system, it is necessary to carry out sensitivity analysis. In this chapter, different sensitivity analyses are carried out. It is noticeable, exploring the results of the simulation, that total membrane area is the first critical point of the plant, due to the high area required and high cost of the module. Secondly, the high energy requirements are dependent on the characteristic parameter of the membrane and pressure drop. Specifically, in a 2-stage cascade configuration, feed compressor use variations are helpful to understand the limits of the configuration. Moreover, for each configuration, the effect of several parameters on the cost of CO2 captured is visualized.

5.1 2-step Air Sweep

The total area of the membrane in a 2-step air sweep is one of the critical points. As described in table 4.1, the total area required is higher than 10.0e5 m^2. Moreover, it is noticeable that the introduction of a better membrane reduces the area. Mathematical models used in air sweep configuration are described in appendix A. Total membrane area is a function of permeance and selectivity CO2/N2, with a polynomial function that depends on the square permeance and the selectivity. For details, it is recommended the equations in Appendix A. Due to models, the influence of the permeance is more determinant in comparison to selectivity to reduce total membrane area. In figure 5.1 it is showed the variation of the membrane area with the selectivity (CO2/N2), for three different values of permeance. It is noticeable that the membrane area does not change increasing the selectivity, this is related to the lower effect on the global formula. On the other hand, the effect of permeance is very remarkable. Moving from 1000 GPU to 2500 GPU, there is an important reduction in the area of 60% (from $50 * 10^5$ to $20 * 10^5$).

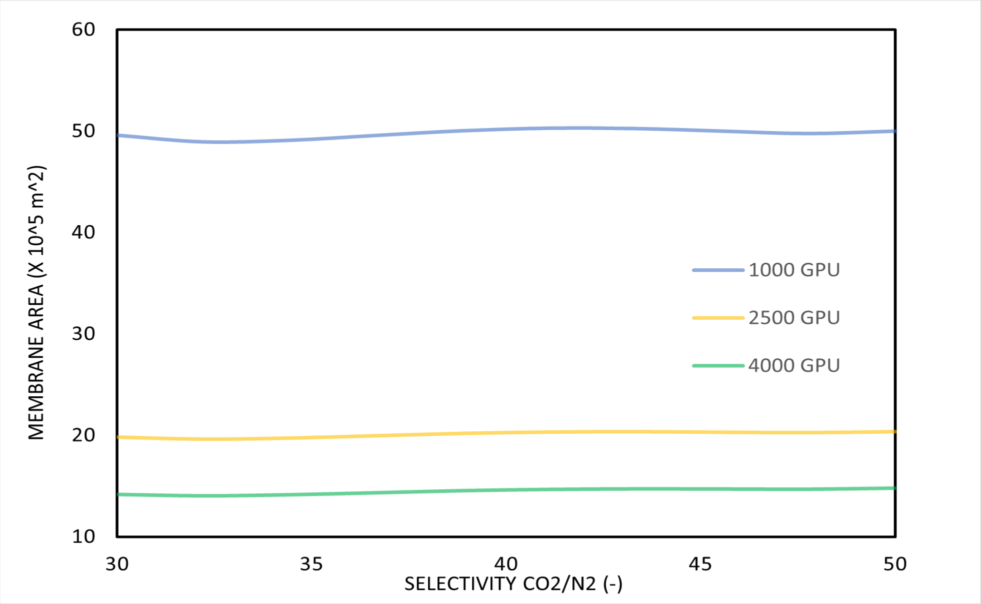

Figure 5.1: Total Membrane Area (m^2) Vs Selectivity (CO2/N2) and Permeance (GPU), for 2-step Air Sweep

This is related to the major effect of permeance and global contribution to the formula, especially the last terms with the permeance square. Moreover, the reduction in the area continue if the permeance increase, and it is easy to see visualizing the trend of 4000 GPU line on the plot 4.1. In conclusion, to improve the membrane area it is required to increase the permeance, and this concept explains the minimum area required with the Pebax/PEG-MEA and Pebax/COF-5.

The introduction of the carbon capture section increases the energy requirement. In a 2-step air sweep, the configuration is simpler and the only required energy is related to the vacuum pump and purification compressor. The vacuum pump energy is related to the efficiency of the component. If the efficiency increases, the consume of the CO2 section decreases. The plot in figure 5.2 shows the effect of the vacuum pump efficiency on the uses of the CO2 capture system, changing the purity of the product. IECM software gives the possibility to choose three types of purity for air sweeps: low purity, 95%, and 99.99%. Higher is the purity, lower is the energy requirement because it is easier to process carbon dioxide. It is visualized in the plot the variation from low purity to 99.99%. Also, the contribution of the efficiency is not negligible, because increasing from 50% to 100%, the capture system requirement goes down of 30%.

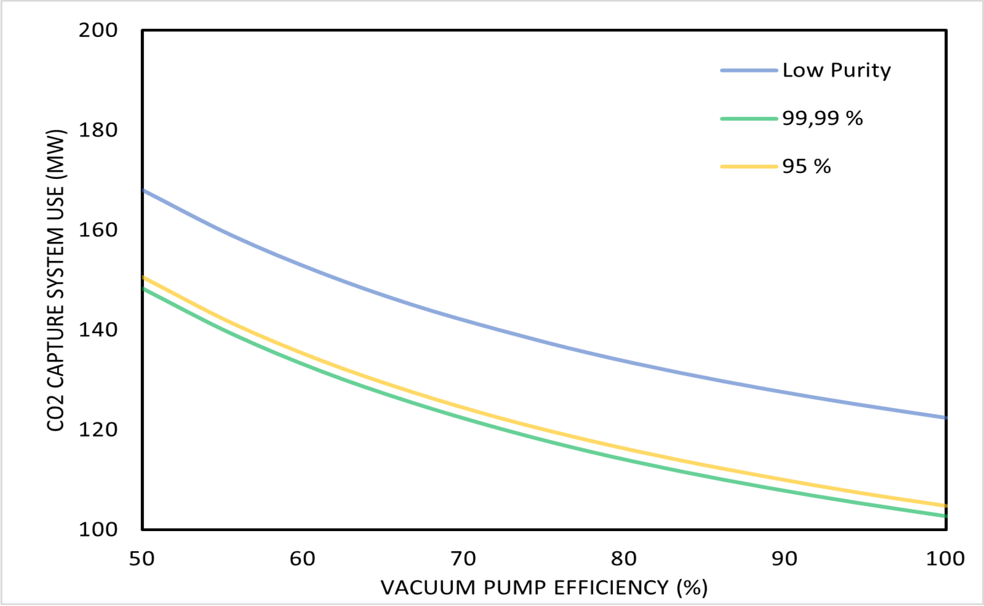

Figure 5.2: CO2 Capture System Use (MW) Vs Vacuum Pump Efficiency (%) and Product Purity (%), for 2-step Air Sweep, 3500 GPU, 35 CO2/N2

Compressor for purification is the second important contribution to global consumption of the CO2 capture section. Driving forces for the optimization of the component are the efficiency and the product pressure, that influence the energy requirement. In figure 5.3 it is represented the trend of CO2 capture system use versus compressor efficiency and pressure of the product sent to the storage. As expected, the increase in the pressure required much energy. In some cases, higher pressure is required for transport and storage. The effect of the pressure is constant, with a slight reduction if the pressure decreases. Much important is the effect of efficiency. The actual efficiency is around (80-85)%, but the performance improvement reduces the energy requirement. In comparison with the previous graph, the reduction is very lower and means that to optimize the energy request of the carbon capture section, improvements in vacuum pumps are the best choice. Moreover, if the efficiency increases it is reflected directly in the capital cost of the component.

Another parameter to be optimized is the cost of CO2 captured because it is the value that compares different carbon capture technologies. It depends on the emission and cost of electricity for reference and new plant. The first step is to analyze the variation of the cost of CO2 captured with the membrane characteristic parameters.

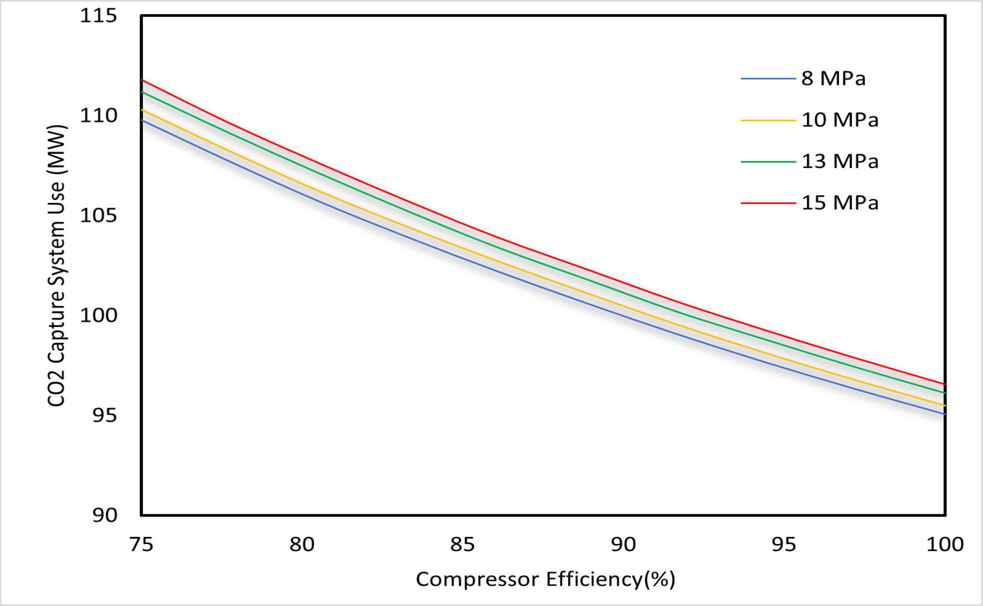

Figure 5.3: CO2 Capture System Use (MW) Vs Compressor Efficiency (%) and Product Pressure (MPA), for 2-step Air Sweep

It is visualized in chapter 4 that, with the introduction of membrane separation, the CO2 emitted decreases a lot, the result is slightly different for three membranes. On the other hand, COE changes a lot depending on the membranes, and in particular, permeance, because, as described in figure 5.1, membrane area and consequently the cost decreases with a growth of the permeance. Figure 5.4 shows the effect of selectivity and permeance on the cost of CO2 captured. Similarly to the membrane area, the cost is very sensible to the permeance. Changing the permeance from 1000 GPU to 4000 GPU, a reduction of 40% is obtained. Selectivity does not change a lot the cost of CO2 captured, but an improvement from 30 to 50 permits to decrease the cost of 4 $/tonn, with 4000 GPU. In conclusion, a better membrane has a cost of CO2 captured lower and it is reflected in the previous simulations, with the best cost available with Pebax/PEG-MEA and Pebax/COF-5.

One of the main limits of the technology today is the membrane module cost. It influences a lot the effectiveness of the carbon capture and it is reflected directly in the cost of carbon dioxide captured. It is noticeable in figure 5.5, the effect of membrane module cost and permeance on the cost of CO2 captured. Membrane module cost is correlated to the COE.

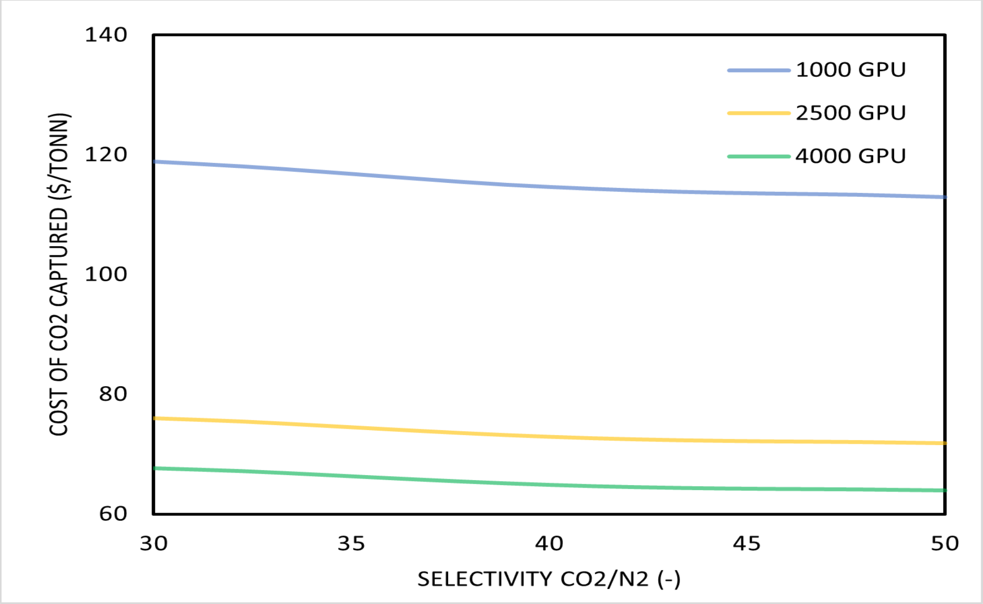

Figure 5.4: Cost of CO2 Captured ($/tonn) Vs Selectivity CO2/N2 and Permeance (GPU), for 2-step Air Sweep

It is noticeable that a reduction of the module cost provides a great decrease in the cost of CO2, especially at lower permeance. For a 4000 GPU, the commercial actual cost of 500 $\$/m^2$ reflects a not feasible cost of 153.2 $/tonn. If the cost is reduced to the value of 150 $\$/m^2$, which reflects a mid-term scenario, the cost is reduced by 50%. The estimated cost for the market penetration is 50 $\$/m^2$, which is equivalent to 60 $/tonn, which is a good value to compare with other technologies. The cost of CO2 captured increases if the permeance is reduced, and with lower permeance, a similar case of commercial Pebax, the cost is very sensible to membrane module and commercially infeasible.

5.2 2-stage Cascade

2-stage cascade shows globally less area, due to configuration and the no presence of air sweep technology. The total area is influenced by permeance and selective in a different way. Concerning air-sweep, selectivity has an important role and, if it increases total area required is higher. It is related to the model applied for this configuration. The model is based on a series of equations described in appendix A.

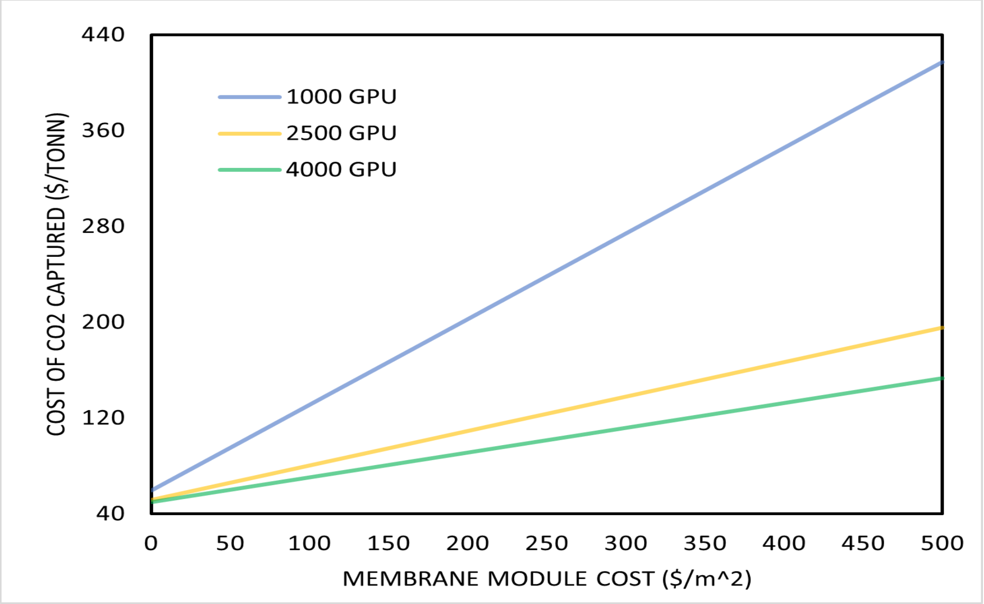

Figure 5.5: Cost of CO2 Captured ($/tonn) Vs Membrane Module Cost ($/$m^2$) and Permeance (GPU), for 2-step Air Sweep

In figure 5.6, it is shown the effect of permeance and selectivity on the membrane area. The reduction of the area with the permeance is much effective at lower permeance, but if the permeance increases for a value higher than 2000 GPU, the reduction is very negligible. For selectivity, a 60 CO2/N2 selectivity provides the highest area, with 45e5 m^2 for 1000 GPU. The reduction of the selectivity decreases the area. With a selectivity of 40, the membrane area is reduced by 75%. In conclusion, the effect of selectivity is more important than permeance. The trend is the opposite in comparison with air-sweep. 2-stage cascade has more degree of freedom as input for the simulation. This configuration requires a feed compressor to increase the partial pressure before entering the membrane. The feed pressure is a key parameter to understand how the area is modified.

Moreover, the CO2 efficiency, which evaluates the percentage of removing carbon dioxide in the membrane, influences the required area. Figure 5.7 shows the modification of membrane area, changing the max CO2 efficiency, for a range of feed pressure between 2 and 6 bar. Today, standards for CO2 efficiency are of 90% to reach the goal required by the Paris agreement. The membrane area increases with the removal efficiency, due to the high quantity of CO2 to be removed.

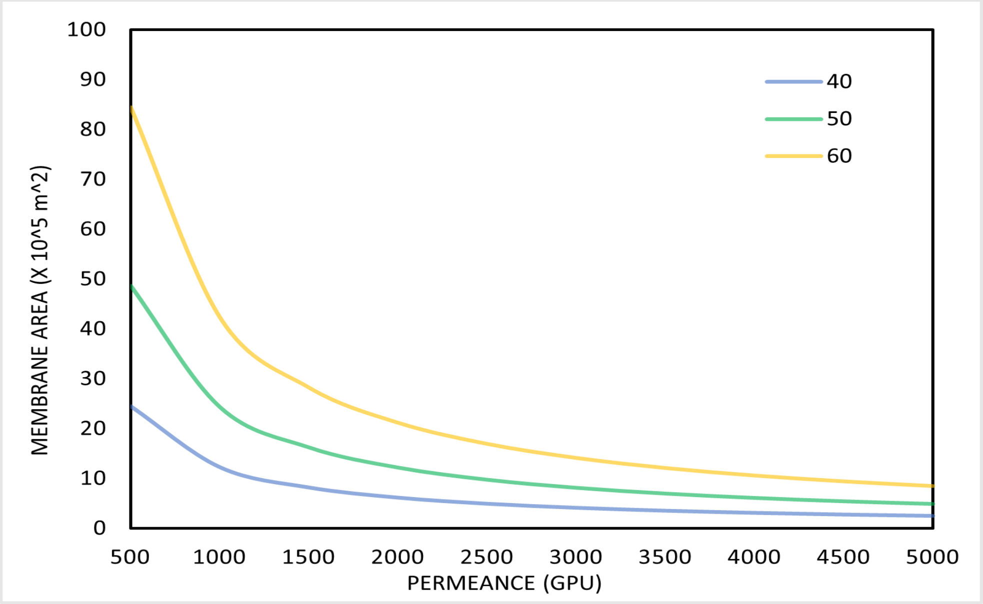

Figure 5.6: Total Membrane Area (m^2) Vs Permeance (GPU) and Selectivity CO2/N2 (GPU), for 2-stage cascade

It is noticeable that the effect of feed pressure is important because an increase in the feed pressure from 2 to 6 bar, causes a significant decrease in the area of 60% for an 80% removal efficiency. The trend has a maximum area in the range (70-80)%. If the feed pressure increase the curve tends to be flat. In comparison with the air-sweep technology, 2-stage cascade area optimization is more difficult and involves a large number of parameters.

CO2 capture use includes the addition of feed compressor, expander, and heat exchanger compared to air-sweep. Results of the simulation show the high contribution of the feed compressor on the global energy requirement. In figure 5.8, the effect of max CO2 efficiency and feed pressure on the CO2 capture system use are visualized. Higher pressure means that the energy required by the compressor increase, due to the pressure ratio. To minimize the compressor work, the feed pressure needs to be much lower as possible. This result shows an important trade-off because at lower pressure the feed compressor cost is lower but the membrane area is maximum. CO2 efficiency affects the CO2 capture system use. Curves show a minimum value of the request for a lower and physical infeasible value of max CO2 efficiency. The negative aspect is that the efficiency required is at a minimum 90%, and the required work, for a standard value of permeance (1000 GPU) and selectivity CO2/N2 (50), is very high.

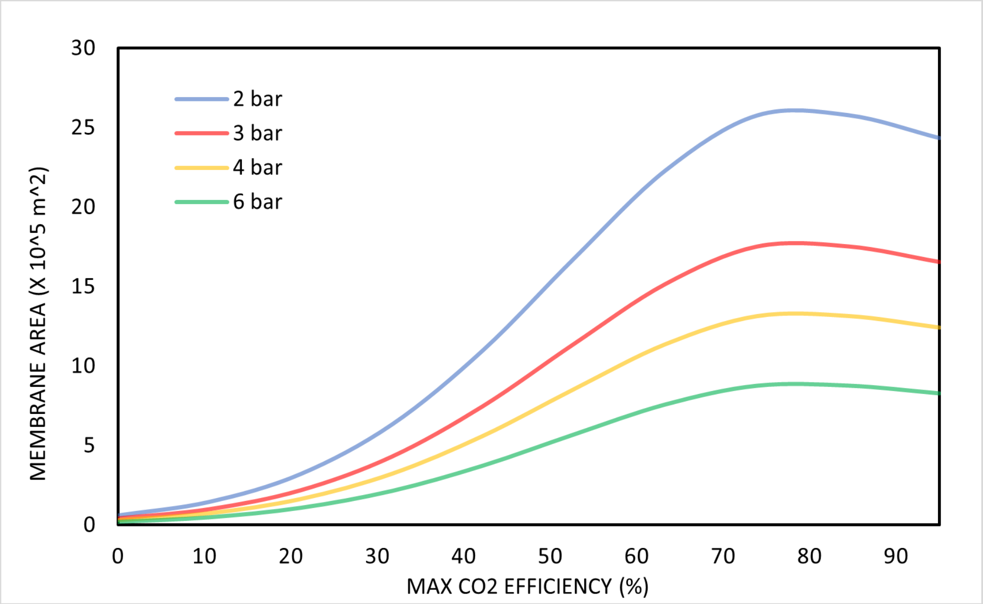

Figure 5.7: Total Membrane Area (m^2) Vs Max CO2 Efficiency (%) and Feed Pressure (bar), 2-stage cascade, 1000 GPU, 50 CO2/N2

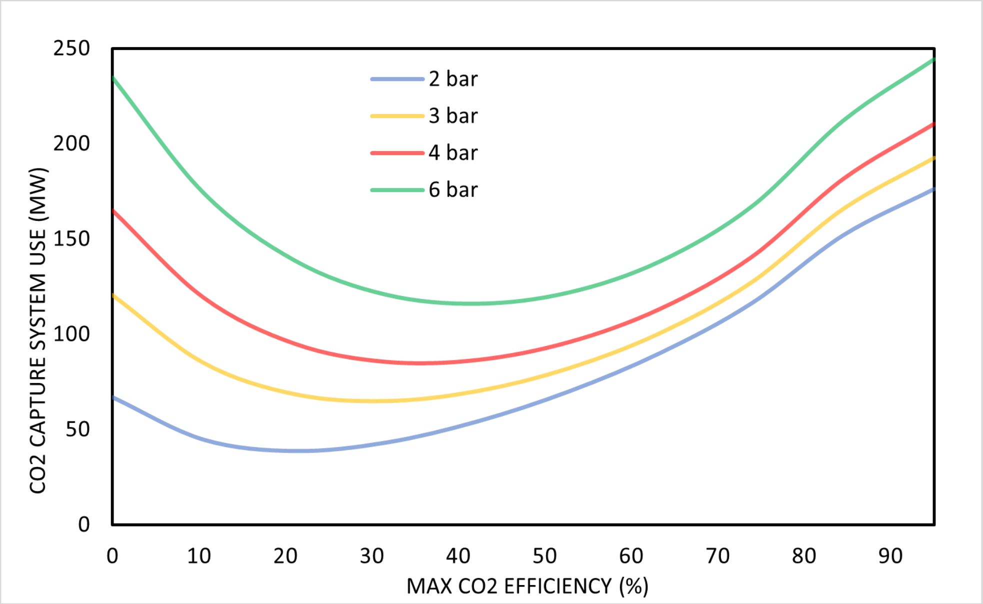

Figure 5.8: CO2 Capture System Use (MW) Vs Max CO2 Efficiency (%) and Feed Pressure (bar), 2-stage cascade, 1000 GPU, 50 CO2/N2

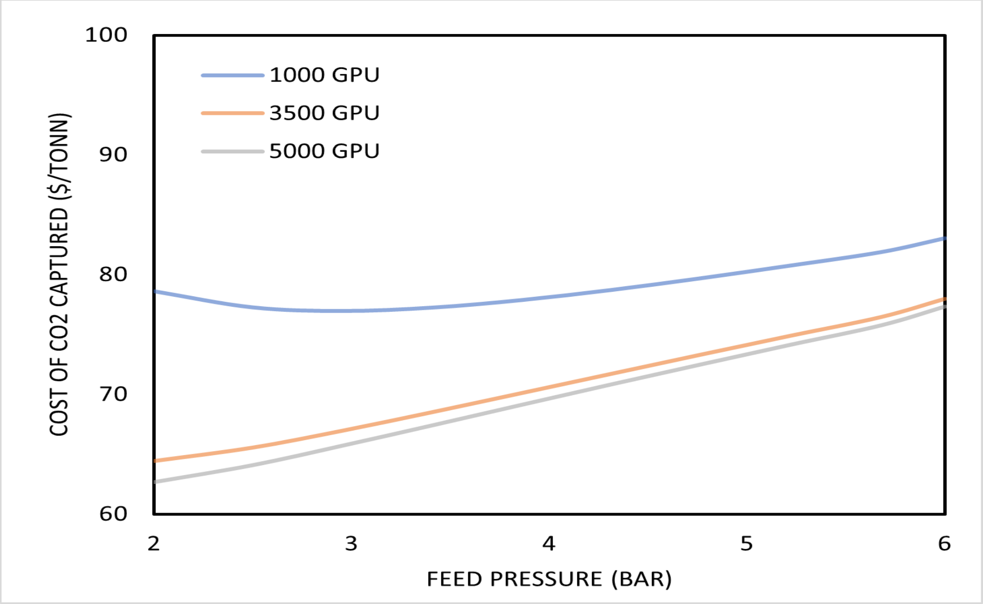

.

Figure 5.9: Cost of CO2 Captured ($/tonn) Vs Feed Pressure bar and Permeance, 2-stage cascade

The critical point of the system is to optimize the cost of CO2 captured. It is dependent on the pressure ratio and, the pressure is slightly dependent on the characteristic of the membrane. The improvement of the membrane performance can reduce the cost of CO2 captured. Figure 5.9 shows the effect of permeance and feed pressure on the cost of CO2 captured. Results show that an increase in the feed pressure corresponds to an increase in the cost of CO2 captured. The effect of permeance is negligible at a high value, but the difference is crucial between 1000 GPU and 3500 GPU.

Also in this configuration, the cost of CO2 captured depends on the permeance and selectivity. In the air-sweep, the effect of selectivity is negligible. In a 2-stage cascade, the selectivity has more impact, especially at lower permeance. Figure 5.10 shows the relationship between the cost of CO2 captured, permeance, and selectivity. There is a noticeable great distance between very lower permeance of 500 GPU and others, higher than 2000 GPU. If the permeance increases, the effect in the reduction of the cost is less impacting. The best value is related to the maximum permeance of 5000 GPU, at the moment it is really difficult to obtain. According to all critical parameters for the 2-stage cascade, the curve shows a minimum value, with a selectivity around 65. The effect of selectivity is more complicated.

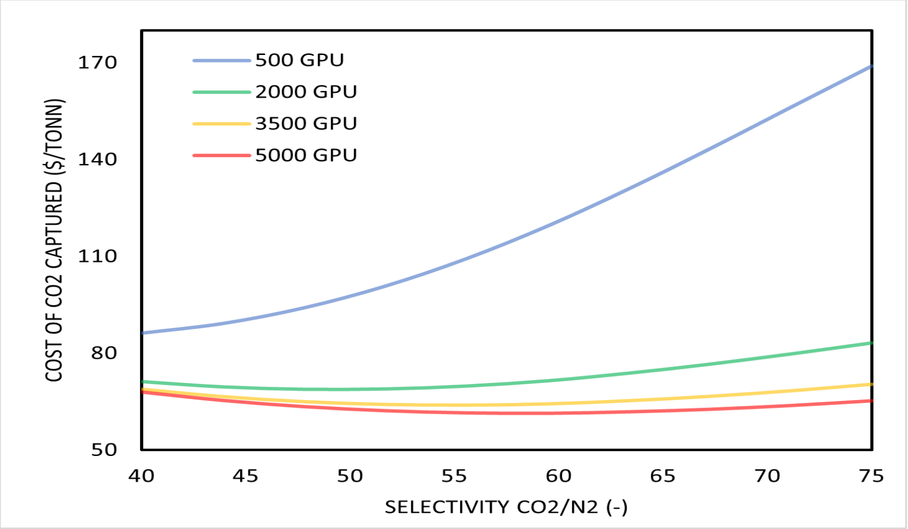

Figure 5.10: Cost of CO2 Captured ($/tonn) Vs Selectivity CO2/N2 and Permeance (GPU), for 2-stage Cascade

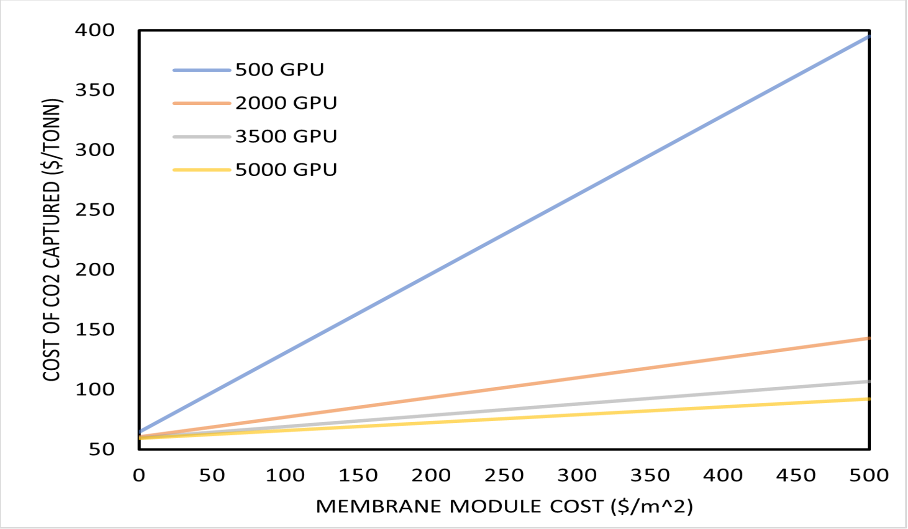

Figure 5.11: Cost of CO2 Captured ($/tonn) Vs Membrane Module Cost ($/$m^2$) and Permeance (GPU), for 2-stage cascade, 50 CO2/N2

For a 2000 GPU membrane, the cost of CO2 captured is equal with a selectivity of 40 and 75. Different is the case with 500 GPU when the increase in selectivity causes a great increase in the cost. Very close to the air-sweep case, the cost of CO2 captured is dependent on membrane module cost and permeance. The plot is shown in figure 5.11. In an equal way, module cost causes an increase in the cost of CO2 captured, with a fast growth for lower permeance.

To conclude, the optimization of the critical parameters is the key to improve the market penetration of technology. Air-sweep is relatively easier to optimize and shows less degree of freedom due to configuration and less presence of components. 2-stage cascade, due to the high number of components, is more complicated to optimize and several trade-offs are required to make the system technically and economically feasible.

6 Conclusion

This work highlights the pros. and cons. of the introduction of a CO2 section based on membrane separation in a PC plant. The simulations show that are required further investigations in the performance of the membranes and for the optimization of energy consumption and overall costs. The work shows that the introduction of the filler in the commercial Pebax-MH/1657 membrane influences a lot of the parameters and improves the feasibility of the system. The two different configurations (2-step air sweep and 2-stage cascade) show positive and negative technological aspects: (i) membrane area is lower for 2-stage cascade, with the best performance obtained by Pebax/PEG-MEA with $4.08 * 10^5 m^2$. The same membrane shows a value of $14.13 * 10^5 m^2$ in a 2-step air sweep. The membrane area is highly reduced with the introduction of composite membranes, due to high permeability and selectivity. (ii) The efficiency is even better for the 2-step air sweep because has lower energy consumption compared with other configuration. Also, in this case, the best value is obtained with Pebax/PEG-MEA, with a value of 27.92 %; in a 2-stage cascade, the plant efficiency is 21.59 % with the same membrane. It is related to the compressor, expander and additional vacuum pumps required in a 2-stage cascade. (iii) The CO2 capture section decreases carbon dioxide emissions. The best value is obtained in the case of the 2-stage cascade, with PEG/MEA filler in the Pebax-1657 membrane. In the sensitivity analyses emerges that the membrane area depends on the permeance and selectivity of the membrane. In the 2-step air sweep, the permeance required further optimization to reduce the total area. The total membrane area in the 2-stage cascade is influenced by selectivity and feed pressure. In the 2-stage cascade, the feed pressure generates a trade-off in the optimization of total membrane area and feed compressor use.

From the economic point of view, the following considerations can be done: (i) the overall capital cost increases with the introduction of the CO2 capture section. The use of the composite matrix shows great improvements, especially in the 2-step air sweep when the cost of membrane modules is the principal parameter to influence the capital cost. In a 2-stage cascade, the capital cost is less influenced by the type of membrane and it is highly dependent on the cost of the components like vacuum pumps and compressors. The lowest cost is related to Pebax/COF-5 membrane; (ii) operation and maintenance costs are one of the critical issues of the CO2 capture section. CO2 section required additional cost in the membrane replacement, electricity, transport, and storage. The lowest cost is related to Pebax/COF-5 membrane; (iii) the cost of CO2 captured is the most important parameter to understand the real effectiveness of the carbon capture technology. With the commercial Pebax, the membrane technology is not comparable with other technology. Pebax/COF-5 and Pebax/PEG-MEA, in both two configurations, show the very interesting cost of CO2 captured, around 63 $/tonne for 2-step air sweep and 65 $/tonne for 2-stage cascade; (iv) cost of electricity is increased due to compressors and vacuum pumps introduced in the plant. Better values are obtained with the air-sweep configuration because it is not required for the feed compressor and there is only one vacuum pump. Pebax/COF-5 shows the best cost of electricity, with a value of 120.20 $/MWh for Pebax/COF-5. Transport and storage influence this value, with an additional cost, as 127$/MWh for 2-step air sweep with Pebax/COF-5. In the 2-step air sweep, the cost of CO2 captured is very dependent on the performance of membrane and membrane module cost, that is the real parameter to be optimized for the penetration in the market of the technology. In the 2-stage cascade, the cost of CO2 captured depends on the feed pressure, because the compressor requires more electricity, on the module cost and performance at the same way of the 2-step air sweep.

Further analyses are required, due to immature investigation of the technologies and difficulty to understand the real effect of the membrane separation technology in an operating plant. This work can be used as a preliminary analysis, before testing the membranes to evaluate the effect of permeability and selectivity on the overall plant. Membrane research is an infinite field and it will have in future a lot of possibilities. It is suggested two types of use of this work: (i) the procedure for the simulations can be used before the evaluation of characteristic parameters of the membrane in the laboratory, to understand if the membrane is suitable for the reference plant; (ii) results can be used for a comparison and a preliminary analysis to understand the aspects to improves. Moreover, it is recommended to focus the attention on the materials and processes for the fabrication of the membrane, to reduce the membrane module cost. It is not possible the commercial use of membrane separation technology in the field of carbon capture with the actual module cost of 500 $\$/m^2$. The choice of mixed-matrix membranes is the best solution because the several degrees of freedom in the choice of the filler increases the possibility to obtain great performances. In conclusion, to speed up the feasibility of this technology, a lot of simulations, laboratory tests, and publications need to be carried out. Actually, there are few works available in the literature, and the validation of the membrane separation technology is still far.

A Mathematical Models

In this section, mathematical models used for the simulation in IECM ambient are described. The models are developed by the Carnage University and NETL.

A.1 2-step Air Sweep

2-stage air sweep is based on the scheme described in figure 4.3. The configuration is composed of a cross-flow membrane and a counter-flow membrane.

A.1.1 Counter-Current Flow Separation Model

This model is based on a multi-component gas separation model described by Coker et al. Several assumptions are required for the model: membrane module operate in steady-state, hollow fiber is divided into a series of N space with perfect mixing, no axial mixing, shell side pressure change is negligible and bore side pressure change can be described by the Hagen-Poiseuille equation. Figure A.1 shows the schematic view of counter-current model.[57]

The governing equations are:

- membrane area at segment k, that is divided into N equal area increments.

  $$\Delta A_k = \frac{2\pi R_o L N_f}{N} \tag{A.1}$$

  where L is the permeating length of the hollow fiber in the module (m), N_f is the number of fibers in the module, R_o is the outlet radius.

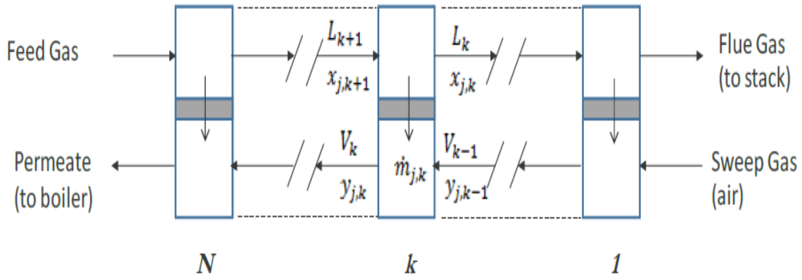

Figure A.1: Counter-Current flow scheme for membrane module.[57]

- flue gas component j and total stream flow rates at segment k.

$$l_{j,k} = x_{j,k} L_k \tag{A.2}$$

$$v_{j,k} = y_{j,k} V_k \tag{A.3}$$

where L_k and V_k are the total feed and permeate flow rates leaving stage k (kmol/s). $x_{j,k}$ and $y_{j,k}$ are the molar fraction of the components respectively. $l_{j,k}$ and $v_{j,k}$ are the flow rates of components j leaving stage k on the high and low pressure side of the membrane. The total feed and permeate flow rates on stage k are the sum of the components described previous and, with R the number of stages, the flow rates are evaluated with the following equations:

$$L_k = \sum_{j=1}^{R} l_{j,k} \tag{A.4}$$

$$V_k = \sum_{j=1}^{R} v_{j,k} \tag{A.5}$$

- mass balance of component j at segment k

$$l_{j,k+1} - l_{j,k} + v_{j,k-1} - v_j = 0 \tag{A.6}$$

- mass balance of total stream flow rates at segment k

$$L_{k+1} - L_k + V_{k-1} - V_k = 0 \tag{A.7}$$

- permeation of component j at segment

$$\dot{m}_{j,k} = l_{j,k+1} - l_{j,k} = Q_j \Delta A_k (x_{j,k} P_{L_k} - y_{j,k} P_{V_k}) \tag{A.8}$$

where $\dot{m}_{j,k}$ is the mass-flow rate of component j that leaves stage k (kmol/s) due to permeation throught the membrane. Q_j is the permeance, P_{L_k} and P_{V_k} are the feed and permeate pressures on stage k (Pa).

All the governing equations are combined and reformulate in the following equation:

$$B_{j,k} l_{j,k-1} + C_{j,k} l_{j,k} + D_{j,k} l_{j,k+1} = 0 \tag{A.9}$$

The result is a tri-diagonal matrix, showed in figure A.2.

$$\begin{bmatrix} C_{j,1} & D_{j,1} & & & & \\ B_{j,2} & C_{j,2} & D_{j,2} & & & \\ \cdots & \cdots & \cdots & \cdots & \cdots & \\ & B_{j,k} & C_{j,k} & D_{j,k} & & \\ \cdots & \cdots & \cdots & \cdots & \cdots & \\ & & B_{j,N-1} & C_{j,N-1} & D_{j,N-1} & \\ & & & B_{j,N} & C_{j,N} & \end{bmatrix} \begin{bmatrix} l_{j,1} \\ l_{j,2} \\ \cdots \\ l_{j,k} \\ \cdots \\ l_{j,N-1} \\ l_{j,N} \end{bmatrix} = \begin{bmatrix} -v_{j,0} \\ 0 \\ \cdots \\ 0 \\ \cdots \\ 0 \\ -D_{j,k} l_{k+1} \end{bmatrix}$$

Figure A.2: Tri-diagonal matrix for the counter current model.[57]

The coefficients are:

$$B_{j,k} = \frac{-V_{k-1}}{P_{V_{k-1}} \Delta A_{k-1} Q_j} (1 - \frac{\Delta A_{k-1} Q_j P_{L_{k-1}}}{L_{k-1}} \tag{A.10}$$

$$C_{j,k} = 1 + \frac{V_{k-1}}{P_{V_{k-1}} \Delta A_{k-1} Q_j} + \frac{V_k}{P_{V_k} \Delta A_{k-1} Q_j} (1 + \frac{\Delta A_{k-1} Q_j P_{L_k}}{L_k} \tag{A.11}$$

$$D_{j,k} = \frac{-V_k}{P_{V_k} \Delta A_{k-1} Q_j} - 1 \tag{A.12}$$

To solve the matrix Thomas algorithm is used, an initial guess has to be provided for the component flow rates at each segment. For further insights it is recommended the article published by Coker et al. [67]

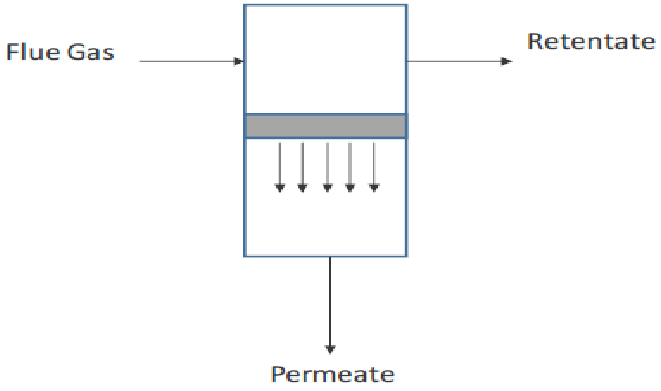

Figure A.3: Schematic of Cross-Flow Membrane Module[57]

A.1.2 Cross-Flow Separation Model

This model is based on calculations by Shindo et al, for membrane with the permeate stream is vertical to the feed stream. Several hypotheses are required: permeation rates obey Fick's law, the gas permeability is the same as that of the pure gas, the effective thickness is constant, concentration gradients in the permeation direction are negligible and pressure drops on both the feed and permeate sides are negligible. Figure A.3 shows the schematic model. [57]

The first step for the model resolution is to define a list of dimensionless variables to be used in the governing equations:

$$s = A\frac{Q_m P_h}{/}F_f\delta \tag{A.13}$$

$$s_t = A_t\frac{Q_m P_h}{/}F_f\delta \tag{A.14}$$

$$f = \frac{F}{/}F_f \tag{A.15}$$

$$f_o = \frac{F_o}{/}F_f \tag{A.16}$$

$$\theta = 1 - f_o \tag{A.17}$$

$$g = G/F_f \tag{A.18}$$

$$\gamma = P_l/P_h \tag{A.19}$$

$$q_l = Q_l / Q_m \tag{A.20}$$

where A and A_t are the membrane area and total membrane area respectively. F, F_f and F_o are the feed-side flow rate, feed flow rate and reject flow rate. f and f_o are the dimensionless flow rate on the feed stream and on the feed stream at the outlet. G and g are the flow rate on the permeate stream parallel to the feed stream and the dimensionless flow rate on the permeate stream, respectively. P_h, P_i are the pressure of the feed and permeate stream. Q and q are the permeability and his ratio. s and s_t are the dimensionless areas. γ the pressure ratio, δ the membrane thickness, θ the stage cut.

The governing equations are described by the following equations:

$$\frac{dx_i}{df} = \frac{q_i(x_i - \gamma y_i) - x_i \sum_{k=1}^{n} q_k(x_k - \gamma y_k)}{f \sum_{k=1}^{n} q_k(x_k - \gamma y_k)} \tag{A.21}$$

where x is the mole fraction of the feed-side gas component, y is the mole fraction of the permeate-side gas component. The range of the index i is from 1 to n-1.

$$\frac{ds}{df} = \frac{-1}{\sum_{k=1}^{n} q_k(x_k - \gamma y_k)} \tag{A.22}$$

$$x_n = 1 - \sum_{k=1}^{n} x_k \tag{A.23}$$

$$\sum_{k=1}^{n} x_k = \frac{x_j q_k / q_i}{\gamma((q_k - q_i) - 1) + (x_i / y_i}) = 1 \tag{A.24}$$

$$y_i = \frac{x_j q_k / q_i}{\gamma((q_k - q_i) - 1) + (x_i / y_i}) \tag{A.25}$$

$$y_n = 1 - \sum_{k=1}^{n} y_k \tag{A.26}$$

The Runge-Kutta-Gill algorithm is used to solve differential equations, while the Newton's iterative algorithm is used to solve y_i at the permeate stream. The overall mass balance for a single component at outlet of the permeate stream is:

$$x_{fi} = x_{oi}(1-\theta) + y_{pi}\theta \tag{A.27}$$

At the end, with the reduced-order performance model provided by NETL, parametric equations for total membrane area is produced, function of permeance and selectivity:

$$Tot_{M}emb_{A}rea(m^2/tCO2) = 1.71e4 + 7.680x + 8.087y + 1.123e - 3y^2 \tag{A.28}$$

The previous equations is referred to a carbon dioxide removal efficiency of 50% in cross-flow and 90% in counter-current. x is the CO2/N2 selectivity and y is the permeance in GPU.

A.1.3 Vacuum Pump

A three-stage vacuum pump with inter-cooling is simulated by NETL and Carnage University in Aspen Plus. The inlet flue gas temperature is fixed at 50°C. The inter-cooling temperature is 38°C for the two stages and 43°C for the outlet. The following equation for water removal efficiency, cooling duty, and vacuum power use are produced with the reduced-order and regression method:

$$Eff, H_2O, condensed(fraction) = 0.16401 + 2.9630 * x_{H_2O,in} - 2,7409 * (x_{H_2Oin})^2 \tag{A.29}$$

$$Qcool(MJ/kmolinletgas) = 8.811 - 30.22 * p_{in}(bar) + 41.306 * x2.9630 * x_{H_2O,in} \tag{A.30}$$

$$W_vacuum(kWh/kmolinletgas) = 2.93735 - 6.6168 * p_{in}(bar) - 1.3136 * x_{H_2O,in} \tag{A.31}$$

A.2 2-stage Cascade

2-stage Cascade is based on the scheme described in figure 4.4. It includes a two-step cross-flow membrane, vacuum pumps, compressors, and expanders.

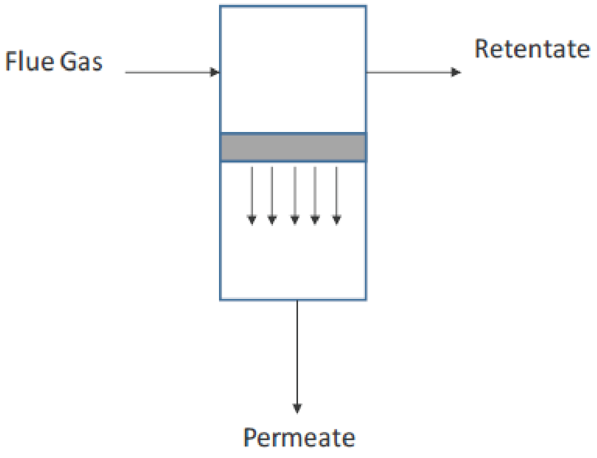

Figure A.4: Schematic of Cross-Flow Membrane Module[68]

A.2.1 Binary Gas Separation

The membrane module for the two-stage cascade is based on a binary gas separation. Transport flux is through polymeric membranes is expressed as:

$$J = \frac{P^*}{\delta}(xP_f - yP_p) \tag{A.32}$$

where J is the volumetric flux $cm^3/(cm^2.s))$, P^* is the gas permeability $cm^3.cm/(cm^2.s.cmHg))$, δ is the membrane thickness (cm), P_f and P_p are the pressures in the feed and permeate sides (cmHg), and x and y are the concentrations of CO2 in the feed and permeate streams (vol %). In figure A.4 the scheme for the cross-flow membrane is showed.

The following hypothesis are required: isothermal conditions, negligible pressure drop and constant gas permeability independent of pressure. Equations are described by Geankoplis. [68]

$$-ydq = J_{CO2}dA = \frac{P^*_{CO2}}{\delta}[xP_f - yP_p]dA \tag{A.33}$$

$$-(1-y)dq = J_{N2}dA = \frac{P^*_{N2}}{\delta}[(1-x)P_f - (1-y)P_p]dA \tag{A.34}$$

Dividing the first equation by second, the next equivalence is obtained:

$$\frac{y}{1-y} = \frac{\alpha(1-y/\Phi}{(1-x)-(1-y)/\Phi} \tag{A.35}$$

where A is the membrane area, q is the gas flow rate $(cm^3)/s$, α is the membrane selectivity CO2/N2 and Φ is the pressure ratio for feed versus permeate sides. For the governing equations, membrane selectivity, pressure ratio and stage cut are the key parameters for a membrane gas separation process. The equation are solved applied mathematical transformation, and the area is evaluated by the following formula:

$$A_m = \frac{tq_f}{P_f P_{N2}^*} \int_{i_o}^{i_f} \frac{(1-\theta^*)(1-x)}{(f_i-1)[1/1+i-1/\Phi(1/(1+f_i)]} di \tag{A.36}$$

where:

$$\theta^* = 1 - q/q_f \tag{A.37}$$

$$i = x/(1-x) \tag{A.38}$$

$$u = -Di + (D^2 i^2 - 2Ei + F^2)^{0.5} \tag{A.39}$$

$$D = 0.5[\frac{1-\alpha}{\Phi} + \alpha] \tag{A.40}$$

$$E = \frac{\alpha}{2} - DF \tag{A.41}$$

$$F = -0.5[\frac{1-\alpha}{\Phi} - 1] \tag{A.42}$$

$$R = \frac{1}{2D-1} \tag{A.43}$$

$$S = \frac{\alpha(D-1)+F}{(2D-1)(\alpha/2-F)} \tag{A.44}$$

$$T = \frac{1}{(1-D-E/F)} \tag{A.45}$$

$$f_i = (Di - F) + (D^2 i^2 - 2Ei + F^2)^{0.5} \tag{A.46}$$

Membrane area can be solved using the analytical approach above via an iterative process.

A.2.2 Power Use of Major Equipment

In the configuration, compressor and vacuum pumps are required due to increasing the partial pressure of CO2 at the inlet and outlet. The energy use is estimated as:

$$E = \frac{1}{\eta} Q \frac{\gamma R T}{\gamma - 1} [\dot{\phi}^{y-1/y} - 1] \tag{A.47}$$

where E is the equipment power use (W), Q is the gas flow rate through the equipment (mole/s); T is the operating temperature (K), η is the equipment efficiency (%); γ is the adiabatic expansion factor, $\dot{\phi}$ is the pressure ratio across the compressor or vacuum pump.

A.2.3 Heat Exchanger

Heat exchangers are needed to maintain a stable operation. The main parameter to evaluate the operation of a heat exchanger is the area, evaluated as:

$$A_{HEX} = \frac{q}{U \frac{\Delta T_2 - \Delta T_1}{ln \frac{\Delta T_2}{\Delta T_1}}} \tag{A.48}$$

where A_{HEX} is the heat exchange area (m^2), ΔT are the temperature differences across the component, U is the heat transfer coefficient (W/m^2). The heat transfer coefficient is 110 (W/m^2) for pressurized gases and 50 (W/m^2) for atmospheric gases.

A.3 Cost of CO2 Avoided and Captured

Many analysts like to express the cost of an environmental control system in terms of the cost per ton of pollutant removed or avoided. For energy-intensive CO2 controls there is a big difference between the cost per ton CO2 removed and the cost per ton "avoided" based on net plant capacity.

Cost of CO2 avoided is the difference between the cost of electricity in the capture plant and the reference plant, divided by the difference between the CO2 emissions in the reference plant and the capture plant:

$$Cost\ of\ CO_2\ Avoided = \frac{COE_{cap} - COE_{ref}}{CO_2\ emission_{ref} - CO_2\ emission_{cap}} \tag{A.49}$$

in which COE is the cost of electricity for the capture plant (cap) and reference plant (ref).

Cost of CO2 Captured is evaluated by the following formula:

$$Cost\ of\ CO_2\ Captured = \frac{COE\ Excl\ T\&S_{cap} - COE_{ref}}{CO_2\ emission_{cap}} \tag{A.50}$$

where $COE\ Excl\ T\&S_{cap}$ is the cost of electricity without transport and storage.

AppendixB

B Tables

Table B.1: Techno-Analysis with commercial Pebax, 2-step Air Sweep

Technical Parameters	Reference	w/Pebax
Gross Electrical Output (MW)	600	600
Net Electrical Output (MW)	548.4	447.7
Annual Operating Hours (hours)	6574	6574
Net Plant Efficiency. HHV (%)	34.15	27.92
Base Plant Use (MW)	26.10	26.10
Hot-Side SCR Use (MW)	3.57	4.93
Cold-Side ESP Use (MW)	1.77	2.29
WET FGD Use (MW)	11.67	15.85
CO2 Capture System Use (MW)	//	84.31
Cooling Tower Use (MW)	8.46	18.84
CO2 Product (tonn/year)	//	2.9e6
Vacuum Pump Power Use (MW)	//	29.31
CO2 Purification Use (MW)	//	55.00
CO2 Emitted (kg/kWh)	0.960	0.191
CO2 Captured (kg/kWh)	//	0.986

Table B.2: Economic-Analysis with commercial Pebax, 2-step Air Sweep

Economic Parameters	Reference	w/Pebax
Capital Cost (M$)		
In-Furnace NOx Control	13.71	13.71
Post Combustion NOx Control	20.36	24.61
TSP Control	27.12	35.00
SO2 Control	82.92	93.92
Total Control System	144.11	167.24
Cooling Tower	33.55	44.66
Base Plant	529.4	529.4
CO2 Capture	//	560.70
Total	707	1302
Total Capital Requirement	973.8	2344.0
O&M Cost (M$/yr)		
In-Furnace NOx Control	0.28	0.28
Post Combustion NOx Control	3.58	3.58
TSP Control	3.53	3.53
SO2 Control	16.27	16.27
Total Control System	23.65	23.65
Cooling Tower	7.57	7.57
Base Plant	47.21	47.21
CO2 Capture	//	115.50
Total	78.43	172.60
CO2 Section Capital Cost (M$)		
Membrane Module	//	385.80
Membrane Frame Structure	//	55.16
Vacuum Pump	//	38.52
CO2 Cryogenic Purification Unit	//	81.15
CO2 Section Capital O&M Cost (M$/yr)		
Membrane Replacement	//	19.74
Electricity	//	24.53
CO2 Transport	//	5.86
CO2 Storage	//	14.29
Total Variable Cost	//	64.41
Total Fixed Cost	//	51.11
Total O&M Cost	//	115.50
Total Levelized Annual Cost (M$/yr)	222.00	518.10
Cost of Electricity ($/MWh)	58.4	176.00
Cost of Electricity, excl, T&S ($/MWh)	58.4	169.10
Cost of CO2 Avoided ($/tonne)	//	152.90
Cost of CO2 Captured ($/tonne)	//	112.30

Table B.3: Techno-Analysis with Pebax/COF-5, 2-step Air Sweep

Technical Parameters	Reference	w/COF-5
Gross Electrical Output (MW)	600	600
Net Electrical Output (MW)	548.4	450.92
Annual Operating Hours (hours)	6574	6574
Net Plant Efficiency. HHV (%)	34.15	28.12
Base Plant Use (MW)	26.10	26.10
Hot-Side SCR Use (MW)	3.57	4.82
Cold-Side ESP Use (MW)	1.77	2.25
WET FGD Use (MW)	11.67	15.50
CO2 Capture System Use (MW)	//	81.57
Cooling Tower Use (MW)	8.46	18.84
CO2 Product (tonn/year)	//	2.86e6
Vacuum Pump Power Use (MW)	//	28.380
CO2 Purification Use (MW)	//	53.18
CO2 Emitted (kg/kWh)	0.960	0.179
CO2 Captured (kg/kWh)	//	0.973

Table B.4: Economic-Analysis with Pebax/COF-5, 2-step Air Sweep

Economic Parameters	Reference	w/COF-5
Capital Cost (M$)		
In-Furnace NOx Control	13.71	13.71
Post Combustion NOx Control	20.36	24.28
TSP Control	27.12	34.31
SO2 Control	82.92	93.06
Total Control System	144.11	165.36
Cooling Tower	33.55	44.54
Base Plant	529.4	529.4
CO2 Capture	//	255.50
Total	707	995
Total Capital Requirement	973.8	1663.0
O&M Cost (M$/yr)		
In-Furnace NOx Control	0.28	0.28
Post Combustion NOx Control	3.58	3.58
TSP Control	3.53	3.53
SO2 Control	16.27	16.27
Total Control System	23.65	23.65
Cooling Tower	7.57	7.57
Base Plant	47.21	47.21
CO2 Capture	//	73.65
Total	78.43	131.40
CO2 Section Capital Cost (M$)		
Membrane Module	//	113.20
Membrane Frame Structure	//	23.38
Vacuum Pump	//	37.30
CO2 Cryogenic Purification Unit	//	81.68
CO2 Section Capital O&M Cost (M$/yr)		
Membrane Replacement	//	5.79
Electricity	//	23.73
CO2 Transport	//	5.86
CO2 Storage	//	14.27
Total Variable Cost	//	49.64
Total Fixed Cost	//	24.01
Total O&M Cost	//	73.65
Total Levelized Annual Cost (M$/yr)	222.00	376.30
Cost of Electricity ($/MWh)	58.4	127.0
Cost of Electricity, excl, T&S ($/MWh)	58.4	120.2
Cost of CO2 Avoided ($/tonne)	//	87.90
Cost of CO2 Captured ($/tonne)	//	63.54

Table B.5: Techno-Analysis with Pebax/PEG-MEA, 2-step Air Sweep

Technical Parameters	Reference	w/PEG-MEA
Gross Electrical Output (MW)	600	600
Net Electrical Output (MW)	548.4	447.7
Annual Operating Hours (hours)	6574	6574
Net Plant Efficiency. HHV (%)	34.15	27.92
Base Plant Use (MW)	26.10	26.10
Hot-Side SCR Use (MW)	3.57	4.93
Cold-Side ESP Use (MW)	1.77	2.29
WET FGD Use (MW)	11.67	15.85
CO2 Capture System Use (MW)	//	84.31
Cooling Tower Use (MW)	8.46	18.84
CO2 Product (tonn/year)	//	2.9e6
Vacuum Pump Power Use (MW)	//	29.310
CO2 Purification Use (MW)	//	55.00
CO2 Emitted (kg/kWh)	0.960	0.191
CO2 Captured (kg/kWh)	//	0.986

Table B.6: Economic-Analysis with Pebax/PEG-MEA, 2-step Air Sweep

Economic Parameters	Reference	w/PEG-MEA
Capital Cost (M$)		
In-Furnace NOx Control	13.71	13.71
Post Combustion NOx Control	20.36	24.61
TSP Control	27.12	35.00
SO2 Control	82.92	93.92
Total Control System	144.11	167.24
Cooling Tower	33.55	44.66
Base Plant	529.4	529.4
CO2 Capture	//	253.60
Total	707	995
Total Capital Requirement	973.8	1662.0
O&M Cost (M$/yr)		
In-Furnace NOx Control	0.28	0.28
Post Combustion NOx Control	3.58	3.58
TSP Control	3.53	3.53
SO2 Control	16.27	16.27
Total Control System	23.65	23.65
Cooling Tower	7.57	7.57
Base Plant	47.21	47.21
CO2 Capture	//	74.18
Total	78.43	131.30
CO2 Section Capital Cost (M$)		
Membrane Module	//	110.90
Membrane Frame Structure	//	23.04
Vacuum Pump	//	38.52
CO2 Cryogenic Purification Unit	//	81.15
CO2 Section Capital O&M Cost (M$/yr)		
Membrane Replacement	//	5.67
Electricity	//	24.53
CO2 Transport	//	5.86
CO2 Storage	//	14.29
Total Variable Cost	//	50.34
Total Fixed Cost	//	23.84
Total O&M Cost	//	74.18
Total Levelized Annual Cost (M$/yr)	222.00	376.60
Cost of Electricity ($/MWh)	58.4	127.8
Cost of Electricity, excl, T&S ($/MWh)	58.4	121.0
Cost of CO2 Avoided ($/tonne)	//	90.28
Cost of CO2 Captured ($/tonne)	//	63.49

Table B.7: Techno-Analysis with commercial Pebax, 2-stage Cascade

Technical Parameters	Reference	w/Pebax
Gross Electrical Output (MW)	600	600
Net Electrical Output (MW)	548.4	346.7
Annual Operating Hours (hours)	6574	6574
Net Plant Efficiency. HHV (%)	34.15	21.59
Base Plant Use (MW)	26.10	26.10
Hot-Side SCR Use (MW)	3.57	3.57
Cold-Side ESP Use (MW)	1.77	1.77
WET FGD Use (MW)	11.67	11.67
CO2 Capture System Use (MW)	//	191.3
Cooling Tower Use (MW)	8.46	18.84
CO2 Product (tonn/year)	//	3.12e6
Vacuum Pump Power Use (MW)	//	85.29
CO2 Purification Use (MW)	//	41.02
Feed Compressor Use (MW)	//	109.20
Expander Use (MW)	//	44.22
CO2 Emitted (kg/kWh)	0.960	0.152
CO2 Captured (kg/kWh)	//	1.368

Table B.8: Economic-Analysis with commercial Pebax, 2-stage cascade

Economic Parameters	Reference	w/Pebax
Capital Cost (M$)		
In-Furnace NOx Control	13.71	13.71
Post Combustion NOx Control	20.36	20.36
TSP Control	27.12	27.12
SO2 Control	82.92	82.92
Total Control System	144.11	144.11
Cooling Tower	33.55	46.65
Base Plant	529.4	529.4
CO2 Capture	//	370.0
Total	707	1090
Total Capital Requirement	973.8	1763.0
O&M Cost (M$/yr)		
In-Furnace NOx Control	0.28	0.28
Post Combustion NOx Control	3.58	3.58
TSP Control	3.53	3.53
SO2 Control	16.27	16.27
Total Control System	23.65	23.65
Cooling Tower	7.57	7.57
Base Plant	47.21	47.21
CO2 Capture	//	106.50
Total	78.43	133.90
CO2 Section Capital Cost (M$)		
Membrane Module	//	73.60
Membrane Frame Structure	//	24.03
Feed Compressor	//	71.78
Expander	//	39.03
Heat Exchanger	//	13.16
Vacuum Pump	//	112.10
CO2 Cryogenic Purification Unit	//	36.28
CO2 Section Capital O&M Cost (M$/yr)		
Membrane Replacement	//	4.02
Electricity	//	53.09
CO2 Transport	//	5.48
CO2 Storage	//	14.77
Total Variable Cost	//	79.08
Total Fixed Cost	//	27.44
Total O&M Cost	//	106.50
Total Levelized Annual Cost (M$/yr)	222.00	393.80
Cost of Electricity ($/MWh)	58.4	172.70
Cost of Electricity, excl, T&S ($/MWh)	58.4	163.90
Cost of CO2 Avoided ($/tonne)	//	140.00
Cost of CO2 Captured ($/tonne)	//	76.03

Table B.9: Techno-Analysis with Pebax/COF-5, 2-stage Cascade

Technical Parameters	Reference	w/COF-5
Gross Electrical Output (MW)	600	600
Net Electrical Output (MW)	548.4	361.0
Annual Operating Hours (hours)	6574	6574
Net Plant Efficiency. HHV (%)	34.15	22.48
Base Plant Use (MW)	26.10	26.10
Hot-Side SCR Use (MW)	3.57	3.57
Cold-Side ESP Use (MW)	1.77	1.77
WET FGD Use (MW)	11.67	11.67
CO2 Capture System Use (MW)	//	177.0
Cooling Tower Use (MW)	8.46	18.84
CO2 Product (tonn/year)	//	3.12e6
Vacuum Pump Power Use (MW)	//	87.94
CO2 Purification Use (MW)	//	41.02
Feed Compressor Use (MW)	//	83.60
Expander Use (MW)	//	35.34
CO2 Emitted (kg/kWh)	0.960	0.146
CO2 Captured (kg/kWh)	//	1.314

Table B.10: Economic-Analysis with Pebax/COF-5, 2-stage cascade

Economic Parameters	Reference	w/COF-5
Capital Cost (M$)		
In-Furnace NOx Control	13.71	13.71
Post Combustion NOx Control	20.36	20.36
TSP Control	27.12	27.12
SO2 Control	82.92	82.92
Total Control System	144.11	144.11
Cooling Tower	33.55	46.86
Base Plant	529.4	529.4
CO2 Capture	//	302.1
Total	707	1022
Total Capital Requirement	973.8	1622.0
O&M Cost (M$/yr)		
In-Furnace NOx Control	0.28	0.28
Post Combustion NOx Control	3.58	3.58
TSP Control	3.53	3.53
SO2 Control	16.27	16.27
Total Control System	23.65	23.65
Cooling Tower	7.57	7.57
Base Plant	47.21	47.21
CO2 Capture	//	95.64
Total	78.43	127.10
CO2 Section Capital Cost (M$)		
Membrane Module	//	34.74
Membrane Frame Structure	//	14.21
Feed Compressor	//	54.93
Expander	//	31.36
Heat Exchanger	//	14.99
Vacuum Pump	//	115.60
CO2 Cryogenic Purification Unit	//	36.28
CO2 Section Capital O&M Cost (M$/yr)		
Membrane Replacement	//	1.90
Electricity	//	49.12
CO2 Transport	//	5.48
CO2 Storage	//	14.77
Total Variable Cost	//	72.99
Total Fixed Cost	//	22.65
Total O&M Cost	//	95.64
Total Levelized Annual Cost (M$/yr)	222.00	366.10
Cost of Electricity ($/MWh)	58.4	154.30
Cost of Electricity, excl, T&S ($/MWh)	58.4	145.70
Cost of CO2 Avoided ($/tonne)	//	116.10
Cost of CO2 Captured ($/tonne)	//	65.28

Table B.11: Techno-Analysis with Pebax/PEG-MEA, 2-stage Cascade

Technical Parameters	Reference	w/PEG-MEA
Gross Electrical Output (MW)	600	600
Net Electrical Output (MW)	548.4	346.7
Annual Operating Hours (hours)	6574	6574
Net Plant Efficiency. HHV (%)	34.15	21.59
Base Plant Use (MW)	26.10	26.10
Hot-Side SCR Use (MW)	3.57	3.57
Cold-Side ESP Use (MW)	1.77	1.77
WET FGD Use (MW)	11.67	11.67
CO2 Capture System Use (MW)	//	191.3
Cooling Tower Use (MW)	8.46	18.84
CO2 Product (tonn/year)	//	3.12e6
Vacuum Pump Power Use (MW)	//	85.29
CO2 Purification Use (MW)	//	41.02
Feed Compressor Use (MW)	//	109.20
Expander Use (MW)	//	33.22
CO2 Emitted (kg/kWh)	0.960	0.152
CO2 Captured (kg/kWh)	//	1.368

Table B.12: Economic-Analysis with Pebax/PEG-MEA, 2-stage cascade

Economic Parameters	Reference	w/PEG-MEA
Capital Cost (M$)		
In-Furnace NOx Control	13.71	13.71
Post Combustion NOx Control	20.36	20.36
TSP Control	27.12	27.12
SO2 Control	82.92	82.92
Total Control System	144.11	144.11
Cooling Tower	33.55	46.65
Base Plant	529.4	529.4
CO2 Capture	//	302.0
Total	707	1022
Total Capital Requirement	973.8	1622.0
O&M Cost (M$/yr)		
In-Furnace NOx Control	0.28	0.28
Post Combustion NOx Control	3.58	3.58
TSP Control	3.53	3.53
SO2 Control	16.27	16.27
Total Control System	23.65	23.65
Cooling Tower	7.57	7.57
Base Plant	47.21	47.21
CO2 Capture	//	98.80
Total	78.43	126.20
CO2 Section Capital Cost (M$)		
Membrane Module	//	20.0
Membrane Frame Structure	//	9.65
Feed Compressor	//	71.78
Expander	//	39.03
Heat Exchanger	//	13.16
Vacuum Pump	//	112.10
CO2 Cryogenic Purification Unit	//	36.28
CO2 Section Capital O&M Cost (M$/yr)		
Membrane Replacement	//	1.09
Electricity	//	53.09
CO2 Transport	//	5.48
CO2 Storage	//	14.77
Total Variable Cost	//	76.15
Total Fixed Cost	//	22.15
Total O&M Cost	//	98.80
Total Levelized Annual Cost (M$/yr)	222.00	365.20
Cost of Electricity ($/MWh)	58.4	160.20
Cost of Electricity, excl, T&S ($/MWh)	58.4	151.30
Cost of CO2 Avoided ($/tonne)	//	124.50
Cost of CO2 Captured ($/tonne)	//	66.87

List of Figures

Bibliography

[1] “IEA (2020), World Energy Balances: Overview, IEA, Paris”. In: (2020). URL: `https://www.iea.org/reports/world-energy-balances-overview`.

[2] Hannah Ritchie. “Sector by sector: where do global greenhouse gas emissions come from?” In: (2020). URL: `https://ourworldindata.org`.

[3] “IPCC 2014 - AR5 Climate Change 2014: Mitigation of Climate Change, https://www.ipcc.ch/report/ar5/wg3/”. In: (). URL: `https://www.ipcc.ch/report/ar5/wg3/`.

[4] “C. D. Keeling, S. C. Piper, R. B. Bacastow, M. Wahlen, T. P. Whorf, M. Heimann, and H. A. Meijer, Exchanges of atmospheric CO2 and 13CO2 with the terrestrial biosphere and oceans from 1978 to 2000. I. Global aspects, SIO Reference Series, No. 01-06, Scripps Institution of Oceanography, San Diego, 88 pages, 2001”. In: (2001). DOI: `http://doi.org/10.6075/J08W3BHW`.

[5] Vanessa J. Schweizer et al. “Integrated Climate-Change Assessment Scenarios and Carbon Dioxide Removal”. In: *One Earth* 3.2 (2020), pp. 166–172. ISSN: 2590-3322. DOI: `https://doi.org/10.1016/j.oneear.2020.08.001`.

[6] Yuan Wang et al. “A Review of Post-combustion CO2 Capture Technologies from Coal-fired Power Plants”. In: *Energy Procedia* 114 (2017). 13th International Conference on Greenhouse Gas Control Technologies, GHGT-13, 14-18 November 2016, Lausanne, Switzerland, pp. 650–665. ISSN: 1876-6102. DOI: `https://doi.org/10.1016/j.egypro.2017.03.1209`.

[7] Mai Bui et al. “Carbon capture and storage (CCS): the way forward”. In: *Energy Environ. Sci.* 11 (5 2018), pp. 1062–1176. DOI: `10.1039/C7EE02342A`.

[8] Niklas Hedin et al. "Adsorbents for the post-combustion capture of CO2 using rapid temperature swing or vacuum swing adsorption". In: *Applied Energy* 104 (2013), pp. 418–433. ISSN: 0306-2619. DOI: `https://doi.org/10.1016/j.apenergy.2012.11.034`. URL: `http://www.sciencedirect.com/science/article/pii/S0306261912008276`.

[9] Lalit A Darunte et al. "CO2 capture via adsorption in amine functionalized sorbents". In: *Current Opinion in Chemical Engineering* 12 (2016). Nanotechnology / Separation Engineering, pp. 82–90. ISSN: 2211-3398. DOI: `https://doi.org/10.1016/j.coche.2016.03.002`.

[10] T. Shimizu et al. "A Twin Fluid-Bed Reactor for Removal of CO2 from Combustion Processes". In: *Chemical Engineering Research and Design* 77.1 (1999), pp. 62–68. ISSN: 0263-8762. DOI: `https://doi.org/10.1205/026387699525882`.

[11] Colin A. Scholes et al. "CO2 capture from pre-combustion processes, Strategies for membrane gas separation". In: *International Journal of Greenhouse Gas Control* 4.5 (2010), pp. 739–755. ISSN: 1750-5836. DOI: `https://doi.org/10.1016/j.ijggc.2010.04.001`.

[12] Ioannis Hadjipaschalis, George Kourtis, and Andreas Poullikkas. "Assessment of oxyfuel power generation technologies". In: *Renewable and Sustainable Energy Reviews* 13.9 (2009), pp. 2637–2644. ISSN: 1364-0321. DOI: `https://doi.org/10.1016/j.rser.2009.07.001`.

[13] Matthew E. Boot-Handford et al. "Carbon capture and storage update". In: *Energy Environ. Sci.* 7 (1 2014), pp. 130–189. DOI: `10.1039/C3EE42350F`.

[14] Siddig Abuelgasim, Wenju Wang, and Atif Abdalazeez. "A brief review for chemical looping combustion as a promising CO2 capture technology: Fundamentals and progress". In: *Science of The Total Environment* (2020), p. 142892. ISSN: 0048-9697. DOI: `https://doi.org/10.1016/j.scitotenv.2020.142892`.

[15] Salvatore F. Cannone, Andrea Lanzini, and Massimo Santarelli. "A Review on CO2 Capture Technologies with Focus on CO2-Enhanced Methane Recovery from Hydrates". In: *Energies* 14.2 (2021). ISSN: 1996-1073. DOI: `10.3390/en14020387`. URL: `https://www.mdpi.com/1996-1073/14/2/387`.

[16] "Carbon capture and storage (CCS): the way forward". In: (). DOI: `10.1039/c7ee02342a`.

[17] Paul Breeze. "Chapter 3 - Coal-Fired Power Plants". In: *Power Generation Technologies (Third Edition)*. Ed. by Paul Breeze. Third Edition. Newnes, 2019, pp. 33–70. ISBN: 978-0-08-102631-1. DOI: `https://doi.org/10.1016/B978-0-08-102631-1.00003-1`. URL: `https://www.sciencedirect.com/science/article/pii/B9780081026311000031`.

[18] Miguel Angel Gonzalez-Salazar, Trevor Kirsten, and Lubos Prchlik. "Review of the operational flexibility and emissions of gas- and coal-fired power plants in a future with growing renewables". In: *Renewable and Sustainable Energy Reviews* 82 (2018), pp. 1497–1513. ISSN: 1364-0321. DOI: `https://doi.org/10.1016/j.rser.2017.05.278`. URL: `https://www.sciencedirect.com/science/article/pii/S1364032117309206`.

[19] "ASTM D1434: Standard Test Method for Determining Gas Permeability Characteristics of Plastic Film and Sheeting". In: ().

[20] "INTESI, CARATTERIZZAZIONE E PROVA DI MEMBRANE PER LA SEPARAZIONE DELLA CO2 E LA PURIFICAZIONE DEL SYNTHETIC NATURAL GAS (SNG)". In: (2015).

[21] Cuihua Ma et al. "Recent progress on thin film composite membranes for CO2 separation". In: *Journal of CO2 Utilization* 42 (2020), p. 101296. ISSN: 2212-9820. DOI: `https://doi.org/10.1016/j.jcou.2020.101296`.

[22] Yang Han and W.S. Winston Ho. "Recent advances in polymeric membranes for CO2 capture". In: *Chinese Journal of Chemical Engineering* 26.11 (2018). Carbon Capture Utilisation and Storage Special Issue, pp. 2238–2254. ISSN: 1004-9541. DOI: `https://doi.org/10.1016/j.cjche.2018.07.010`.

[23] M. Waqas Anjum et al. "MIL-125(Ti) based mixed matrix membranes for CO2 separation from CH4 and N2". In: *Journal of Membrane Science* 502 (2016), pp. 21–28. ISSN: 0376-7388. DOI: `https://doi.org/10.1016/j.memsci.2015.12.022`.

[24] Zhongde Dai et al. "Facile fabrication of CO2 separation membranes by cross-linking of poly(ethylene glycol) diglycidyl ether with a diamine and a polyamine-based ionic liquid". In: *Journal of Membrane Science* 523 (2017), pp. 551–560. ISSN: 0376-7388. DOI: `https://doi.org/10.1016/j.memsci.2016.10.026`.

[25] Shadi Meshkat, Serge Kaliaguine, and Denis Rodrigue. "Enhancing CO2 separation performance of Pebax® MH-1657 with aromatic carboxylic acids". In: *Separation and Purification Technology* 212 (2019), pp. 901–912. ISSN: 1383-5866. DOI: `https://doi.org/10.1016/j.seppur.2018.12.008`.

[26] Marzieh Shirinia, Mahdi Abdollahi, and Mohammadreza Omidkhah. "Simultaneous enhancement of CO2 permeability and CO2/CH4 and CO2/N2 selectivity via incorporating dense, rubbery and CO2-philic vinyl acetate- based copolymers into poly(ethylene oxide-b-amide 6) membranes". In: *Reactive and Functional Polymers* 154 (2020), p. 104673. ISSN: 1381-5148. DOI: `https://doi.org/10.1016/j.reactfunctpolym.2020.104673`.

[27] Yang Han, Dongzhu Wu, and W.S. Winston Ho. "Simultaneous effects of temperature and vacuum and feed pressures on facilitated transport membrane for CO2/N2 separation". In: *Journal of Membrane Science* 573 (2019), pp. 476–484. ISSN: 0376-7388. DOI: `https://doi.org/10.1016/j.memsci.2018.12.028`.

[28] Yonghong Wang et al. "Polyvinylamine/amorphous metakaolin mixed-matrix composite membranes with facilitated transport carriers for highly efficient CO2/N2 separation". In: *Journal of Membrane Science* 599 (2020), p. 117828. ISSN: 0376-7388. DOI: `https://doi.org/10.1016/j.memsci.2020.117828`.

[29] Alessio Fuoco et al. "Comparison of pure and mixed gas permeation of the highly fluorinated polymer of intrinsic microporosity PIM-2 under dry and humid conditions: Experiment and modelling". In: *Journal of Membrane Science* 594 (2020), p. 117460. ISSN: 0376-7388. DOI: `https://doi.org/10.1016/j.memsci.2019.117460`.

[30] Ian Rose et al. "Polymer ultrapermeability from the inefficient packing of 2D chains". In: *Nature Materials* 16.9 (Sept. 2017), pp. 932–937. ISSN: 1476-4660. DOI: `10.1038/nmat4939`.

[31] Jongmyeong Lee et al. "Dimensionally-controlled densification in crosslinked thermally rearranged (XTR) hollow fiber membranes for CO2 capture". In: *Journal of Membrane Science* 595 (2020), p. 117535. ISSN: 0376-7388. DOI: `https://doi.org/10.1016/j.memsci.2019.117535`.

[32] Zhihua Qiao et al. "Metal-induced ordered microporous polymers for fabricating large-area gas separation membranes". In: *Nature Materials* 18.2 (Feb. 2019), pp. 163–168. ISSN: 1476-4660. DOI: `10.1038/s41563-018-0221-3`.

[33] I.G.B.N. Makertihartha et al. “Silica supported SAPO-34 membranes for CO2/N2 separation”. In: *Microporous and Mesoporous Materials* 298 (2020), p. 110068. ISSN: 1387-1811. DOI: `https://doi.org/10.1016/j.micromeso.2020.110068`.

[34] Muhammad Tawalbeh et al. “Highly permeable tubular silicalite-1 membranes for CO2 capture”. In: *Science of The Total Environment* 676 (2019), pp. 305–320. ISSN: 0048-9697. DOI: `https://doi.org/10.1016/j.scitotenv.2019.04.290`.

[35] Fanglei Zhou et al. “Ultrathin graphene oxide-based hollow fiber membranes with brush-like CO2-philic agent for highly efficient CO2 capture”. In: *Nature Communications* 8.1 (Dec. 2017), p. 2107. ISSN: 2041-1723. DOI: `10.1038/s41467-017-02318-1`.

[36] Rong Rong et al. “Fabrication of highly CO2/N2 selective polycrystalline UiO-66 membrane with two-dimensional transition metal dichalcogenides as zirconium source via tertiary solvothermal growth”. In: *Journal of Membrane Science* 610 (2020), p. 118275. ISSN: 0376-7388. DOI: `https://doi.org/10.1016/j.memsci.2020.118275`.

[37] Wufeng Wu et al. “Polydopamine-Modified Metal–Organic Framework Membrane with Enhanced Selectivity for Carbon Capture”. In: *Environmental Science & Technology* 53.7 (Apr. 2019), pp. 3764–3772. ISSN: 0013-936X. DOI: `10.1021/acs.est.9b00408`.

[38] Haixiang Sun et al. “Bis(phenyl)fluorene-based polymer of intrinsic microporosity/functionalized multi-walled carbon nanotubes mixed matrix membranes for enhanced CO2 separation performance”. In: *Reactive and Functional Polymers* 147 (2020), p. 104465. ISSN: 1381-5148. DOI: `https://doi.org/10.1016/j.reactfunctpolym.2019.104465`.

[39] Muhammad Rizwan Dilshad et al. “Novel PVA/PEG nano-composite membranes tethered with surface engineered multi-walled carbon nanotubes for carbon dioxide separation”. In: *Microporous and Mesoporous Materials* 308 (2020), p. 110545. ISSN: 1387-1811. DOI: `https://doi.org/10.1016/j.micromeso.2020.110545`.

[40] Mina Kheirtalab, Reza Abedini, and Mohsen Ghorbani. “A novel ternary mixed matrix membrane comprising polyvinyl alcohol (PVA)-modified poly (ether-block-amide)(Pebax®1657)/graphene oxide nanoparticles for CO2 separation”. In: *Process Safety and Environmental Protection* 144 (2020), pp. 208–224. ISSN: 0957-5820. DOI: `https://doi.org/10.1016/j.psep.2020.07.027`.

[41] Wenbo Chen et al. "Metal-organic framework MOF-801/PIM-1 mixed-matrix membranes for enhanced CO2/N2 separation performance". In: *Separation and Purification Technology* 250 (2020), p. 117198. ISSN: 1383-5866. DOI: `https://doi.org/10.1016/j.seppur.2020.117198`.

[42] Rui Ding et al. "Amino-functional ZIF-8 nanocrystals by microemulsion based mixed linker strategy and the enhanced CO2/N2 separation". In: *Separation and Purification Technology* 236 (2020), p. 116209. ISSN: 1383-5866. DOI: `https://doi.org/10.1016/j.seppur.2019.116209`.

[43] Haipeng Zhu et al. "Enhanced CO2/N2 separation performance by using dopamine/polyethyleneimine-grafted TiO2 nanoparticles filled PEBA mixed-matrix membranes". In: *Separation and Purification Technology* 214 (2019). Advanced Separation and Filtration (selected papers presented at the 17th APCChE, held 23-27 August, 2017 in Hong Kong), pp. 78–86. ISSN: 1383-5866. DOI: `https://doi.org/10.1016/j.seppur.2018.02.020`.

[44] Saeed Kalantari et al. "Superior interfacial design in ternary mixed matrix membranes to enhance the CO2 separation performance". In: *Applied Materials Today* 18 (2020), p. 100491. ISSN: 2352-9407. DOI: `https://doi.org/10.1016/j.apmt.2019.100491`.

[45] Jason E. Bara and W. Jeffrey Horne. "Polymeric Membranes". In: *Materials for Carbon Capture*. John Wiley Sons, Ltd, 2020. Chap. 7, pp. 187–214. ISBN: 9781119091219. DOI: `https://doi.org/10.1002/9781119091219.ch7`.

[46] M. Lee, Z. Wu, and K. Li. "2 - Advances in ceramic membranes for water treatment". In: *Advances in Membrane Technologies for Water Treatment*. Ed. by Angelo Basile, Alfredo Cassano, and Navin K. Rastogi. Woodhead Publishing Series in Energy. Oxford: Woodhead Publishing, 2015, pp. 43–82. ISBN: 978-1-78242-121-4. DOI: `https://doi.org/10.1016/B978-1-78242-121-4.00002-2`. URL: `https://www.sciencedirect.com/science/article/pii/B9781782421214000022`.

[47] Z.F. Cui, Y. Jiang, and R.W. Field. "Chapter 1 - Fundamentals of Pressure-Driven Membrane Separation Processes". In: *Membrane Technology*. Ed. by Z.F. Cui and H.S. Muralidhara. Oxford: Butterworth-Heinemann, 2010, pp. 1–18. ISBN: 978-1-85617-632-3. DOI: `https://doi.org/10.1016/B978-1-85617-632-3.00001-X`.

URL: `https://www.sciencedirect.com/science/article/pii/B978185617632300001X`.

[48] Endre Nagy. “Chapter 2 - Membrane Materials, Structures, and Modules”. In: *Basic Equations of Mass Transport Through a Membrane Layer (Second Edition)*. Ed. by Endre Nagy. Second Edition. Elsevier, 2019, pp. 11–19. ISBN: 978-0-12-813722-2. DOI: `https://doi.org/10.1016/B978-0-12-813722-2.00002-9`.

[49] “IECM. (2020). Integrated Environmental Control Model (IECM) Version 11.4 (Carnegie Mellon University).” In: (2020). URL: `https://www.cmu.edu/epp/iecm/index.html`.

[50] “Fayette Power Projects, Communication Sheet”. In: (2016). URL: `https://www.lcra.org/download/fpp-fact-sheet-pdf/?wpdmdl=19884`.

[51] “Electricity Data Browser, CO2”. In: (2020). URL: `https://www.eia.gov/beta/electricity/data/browser/#/plant/6179/?freq=A&pin=`.

[52] “IECM Technical Documentation: Pulverized Coal-Fired Power Plants and Air Pollution Controls”. In: (2019). URL: `www.iecm-online.com`.

[53] I.S. Anufriev. “Review of water/steam addition in liquid-fuel combustion systems for NOx reduction: Waste-to-energy trends”. In: *Renewable and Sustainable Energy Reviews* 138 (2021), p. 110665. ISSN: 1364-0321. DOI: `https://doi.org/10.1016/j.rser.2020.110665`.

[54] Sooraj Mohan, P. Dinesha, and Shiva Kumar. “NOx reduction behaviour in copper zeolite catalysts for ammonia SCR systems: A review”. In: *Chemical Engineering Journal* 384 (2020), p. 123253. ISSN: 1385-8947. DOI: `https://doi.org/10.1016/j.cej.2019.123253`.

[55] Ken Parker. *Electrical operation of electrostatic precipitators*. 41. IET, 2003.

[56] Shahriar Kouravand and Ali M. Kermani. “Clean power production by simultaneous reduction of NOx and SOx contaminants using Mazut Nano-Emulsion and wet flue gas desulfurization”. In: *Journal of Cleaner Production* 201 (2018), pp. 229–235. ISSN: 0959-6526. DOI: `https://doi.org/10.1016/j.jclepro.2018.08.017`.

[57] "IECM Technical Documentation: A Two-Stage Membrane System with Air Sweep for Post-Combustion Carbon Capture and Storage". In: (2019). URL: `www.iecm-online.com`.

[58] Iman Khalilinejad, Hamidreza Sanaeepur, and Ali Kargari. "Preparation of Poly(ether-6-block amide)/PVC Thin Film Composite Membrane for CO2 Separation: Effect of Top Layer Thickness and Operating Parameters". In: *Journal of Membrane Science and Research* 1 (Oct. 2015), pp. 124–129.

[59] Ali Kargari and Sheida Rezaeinia. "State-of-the-art modification of polymeric membranes by PEO and PEG for carbon dioxide separation: A review of the current status and future perspectives". In: *Journal of Industrial and Engineering Chemistry* 84 (2020), pp. 1–22. ISSN: 1226-086X. DOI: `https://doi.org/10.1016/j.jiec.2019.12.020`.

[60] Ke Duan et al. "Covalent organic frameworks (COFs) functionalized mixed matrix membrane for effective CO2/N2 separation". In: *Journal of Membrane Science* 572 (2019), pp. 588–595. ISSN: 0376-7388. DOI: `https://doi.org/10.1016/j.memsci.2018.11.054`.

[61] Jae Eun Shin et al. "Effect of PEG-MEA and graphene oxide additives on the performance of Pebax®1657 mixed matrix membranes for CO2 separation". In: *Journal of Membrane Science* 572 (2019), pp. 300–308. ISSN: 0376-7388. DOI: `https://doi.org/10.1016/j.memsci.2018.11.025`.

[62] "Advanced Membranes and Learning Scale Required for Cost-Effective Post-combustion Carbon Capture,iScience". In: (2019).

[63] "Economic Evaluation of Membrane Systems for Large Scale Capture and Storage of CO2 Mixtures,Engineering Conferences International Year 2004". In: (2004).

[64] "PILOT TESTING OF A MEMBRANE SYSTEM FOR POSTCOMBUSTION CO2 CAPTURE". In: (2016).

[65] "Economic Evaluation of Membrane Systems for Large Scale Capture and Storage of CO2 Mixtures,Engineering Conferences International Year 2004". In: (2004).

[66] Haibo Zhai and Edward S. Rubin. "Techno-Economic Assessment of Polymer Membrane Systems for Postcombustion Carbon Capture at Coal-Fired Power Plants". In: *Environmental Science & Technology* 47.6 (2013). PMID: 23406504, pp. 3006–3014. DOI: `10.1021/es3050604`.

[67] D. T. Coker, B. D. Freeman, and G. K. Fleming. "Modeling multicomponent gas separation using hollow-fiber membrane contactors". In: *AIChE Journal* 44.6 (), pp. 1289–1302. DOI: `https://doi.org/10.1002/aic.690440607`.

[68] "IECM Technical Documentation: Membrane-based CO2 Capture Systems for Coal-fired Power Plants". In: (2012). URL: `www.iecm-online.com,`.